Spring 5-9-2020

The Role of Central ACE2 and Nrf2 in Sympatho-Excitation: Responses to Central Angiotensin II

Anyun Ma
University of Nebraska Medical Center

THE ROLE OF CENTRAL ACE2 AND Nrf2 IN SYMPATHO-EXCITATION: RESPONSES TO CENTRAL ANGIOTENSIN II

By

Anyun Ma

A DISSERTATION

Presented to the Faculty of

the University of Nebraska Graduate College

in Partial Fulfillment of the Requirements

for the Degree of Doctor of Philosophy

Cellular and Integrative Physiology Graduate Program

Under the Supervision of Professor Irving H. Zucker

University of Nebraska Medical Center

Omaha, Nebraska

April, 2020

ACKNOWLEDGEMENTS

I would like to express my sincere gratitude to my advisor, Dr. Irving Zucker, for his extraordinary guidance, help, patience, and support. It is a great honor to be student of an internationally recognized scientist like Dr. Zucker, who also has acted as a role model for me in every way possible. His enthusiasm for science, dedication to work, and leadership have always been a great inspiration, and will continue to influence me in both my life and career. Also I would like to thank my supervisory committee for their guidance, time and constructive comments.

I would like to thank Dr. Lie Gao, for his outstanding help in teaching all animal procedures; Dr. Changhai Tian, for his patient help with molecular techniques; Dr. Hanjun Wang, for all his kind instruction and help during Ph.D. training.

I must also thank our lab manager, Tara Rudebush, for her efficiency and help in managing my transgenic mice and ordering experimental supplies and Ms. Li Yu for helping me to carry out mouse genotyping and western blotting. I thank Ahmed Wafi for all his support and friendship. Finally, I thank all present and past group members for their advice and kind help during this work.

I am also thankful to the staff and fellow graduate students in the Department of Cellular and Integrative Physiology for all their support and help during my Ph.D. training. I would like to acknowledge the animal facility staff who I had the pleasure to work with – Harvey, Renee, Tiffany, for the quality care they provided for my animals.

Lastly, my deepest gratitude goes to my beloved family – my mom, my brother, my lost grandparents…I am blessed to have their endless love in my life.

THE ROLE OF CENTRAL ACE2 AND Nrf2 IN SYMPATHO-EXCITATION: RESPONSES TO CENTRAL ANGIONTENSIN II

Anyun Ma

University of Nebraska, 2020

Advisor: Irving H. Zucker, Ph.D.

Sympatho-excitation is a key characteristic in cardiovascular diseases such as chronic heart failure (CHF) and primary Hypertension (HTN). Evidence suggests that increased sympathetic tone is closely related to activation of the Renin-Angiotensin-Aldosterone system (RAAS) in the central nervous system. An underlying mechanism for sympatho-excitation is thought to be oxidative stress resulting from Angiotensin II (AngII) type 1 receptor (AT1R) activation. Over the past several decades, pharmacological targeting of components of the RAAS have been used as standard therapy in CHF and HTN. However, additional therapeutic strategies are necessary to control these diseases. Oxidative stress is regulated, in part, by the balance between components of the RAAS and the ability of the system to scavenge oxygen radicals. Over the past decade, Nuclear factor E2-related factor 2 (Nrf2) has emerged as an important transcriptional regulator that maintains redox homeostasis by governing a broad array of antioxidant genes in response to oxidant stress. Central Nrf2 dysregulation has been found in animals with CHF and HTN. To determine if Nrf2 contributes to decreased antioxidant defense and increased sympathetic nerve activity (SNA) in CHF, we upregulated Nrf2 in the rostral ventrolateral medulla (RVLM) in C57BL/6 mice and evaluated their hemodynamic and sympathetic function in the CHF state. We found that (1) Nrf2 and two target proteins, NAD(P)H dehydrogenase [quinone]

1 (NQO1) and Heme oxygenase (HO-1) in the RVLM were significantly lower in CHF compared to Sham mice; (2) Urinary norepinephrine (NE) excretion in CHF mice was markedly reduced following Nrf2 upregulation; (3) CHF mice overexpressing Nrf2 exhibited an enhancement in spontaneous baroreflex gain and a decrease in basal renal SNA. In an attempt to understand the antioxidant function of the RAAS we examined the role of Angiotensin converting enzyme 2 (ACE2) in a model of central AngII-induced HTN. Despite its direct enzymatic effect on AngII, ACE2 has been shown to reduce oxidative stress and to be sympatho-inhibitory. It has been demonstrated that animals with CHF exhibit increased Angiotensin converting enzyme (ACE) and decreased ACE2 in the RVLM. We hypothesized that overexpression of ACE2 in the brain reduces the sympathetic and blood pressure (BP) responses to central AngII by activation of Nrf2 and enhancing antioxidant enzyme expression. To illuminate the role of Nrf2 in the central regulation of SNA in response to central AngII, we assessed Nrf2 changes in the RVLM in SynhACE2 mice treated with ICV AngII infusion. Mice with central overexpression of ACE2 inhibited the pressor and sympathetic responses to central AngII. We found that Nrf2 was upregulated in the RVLM in SynhACE2 mice, and that pharmacological upregulation of central Nrf2 had a significant impact on BP in response to central AngII. Overall, the experiments described in this dissertation showed that selectively upregulating Nrf2 in the RVLM attenuates sympatho-excitation in CHF mice. We also describe a novel role of interplay between central AngII, ACE2 and Nrf2 in the regulation of sympatho-excitation in central HTN. While not definitive, these studies suggest a role for ACE2 and Nrf2 as targets for therapy in CHF and HTN.

Table of Contents

ACKNOWLEDGEMENTS 1

Table of Contents 4

List of Figures and Tables 9

Chapter I. Introduction 16

Neural control of the cardiovascular system 17

Chronic heart failure 21

Primary (Essential) HTN 22

Sympathetic overactivity 23

Central RAAS Activation 24

Systemic vs Local RAAS 24

Central RAAS and HTN 26

ACE/AngII/AT1R and ACE2/Angiotensin 1-7 (Ang1-7)/MasR 27

Oxidative Stress 29

Oxidative Stress and its role in Cardiovascular Disease 29

Relation between Oxidative Stress, Sympathoactivation, and RAAS 31

Nrf2 34

Overall hypotheses 35

Chapter II. Experimental Objectives 37

General Goals 38

Objective 1 (Chapter IV) 38

Objective 2 (Chapter V) 38

Objective 3 (Chapter VI) 38

Chapter III. Materials and Methods 39

Animals 40

Radiotelemetry implantation 41

Hemodynamic recordings 43

Chronic heart failure model 43

Echocardiography 45

Microinjection of lentiviral vector into the RVLM 45

ICV infusion and implantation of osmotic minipump 46

Renal Sympathetic Nerve Activity (RSNA) recordings 48

BRS Analysis 48

Metabolic cage study 49

Norepinephrine measurement 49

Cell culture 50

Western blot analysis 50

Immunofluorescence and laser confocal microscopy 51

Statistics 52

Chapter IV. Effects of Nrf2 Over-expression in the RVLM on SNA in Mice with CHF 53

Introduction 54

Experimental Protocol 55

Results 60

Evaluation of CHF model 60

RVLM Nrf2 over-expression in CHF 63

Effects of RVLM Nrf2 knock-in on BP, HR, and SNA 67

Effects of Keap1 knock-out in RVLM on RSNA 71

Discussion 73

Introduction 78

Experimental Protocol 80

Results 83

Central SynhACE2 attenuates ICV AngII - induced HTN 83

SynhACE2 attenuates central AngII induced polydipsia 88

SynhACE2 attenuates central AngII-induced sympathetic overactivity 90

SynhACE2 attenuates central AngII-induced oxidative stress 92

Discussion 94

Chapter VI. Potential Interaction between Central RAAS and Nrf2 97

Introduction 98

Experimental Protocol 99

Results 102

AngII induces Nrf2 nuclear translocation 102

Effect of ACE2 on intracellular Nrf2 in response to AngII 104

Nrf2 and NQO-1 are upregulated in the RVLM of SynhACE2$^{+/+}$ mice 106

Selective knockdown of Nrf2 in the RVLM enhances the pressor effect induced by central infusion of AngII 108

Effects of Nrf2 deletion in the RVLM on water intake and urine output in response to icv AngII 111

ICV-infusion of sulforaphane attenuates the pressor effect induced by central infusion of AngII 111

Effects of sulforaphane on AngII-induced polydipsia 115

Discussion 116

Chapter VII. Perspectives and Potential for Therapy 119

..... 122

Chapter VIII. Summary 123

List of Figures and Tables

Figure 1. 1 Schematic diagram of important central nuclei involved in cardiovascular control and baroreflex loop. 19

Figure 1. 2 Shematic diagram of ACE2 and Nrf2 signaling in RVLM neurons. 36

Figure 3. 1Radio telemetry (left) and schematic of telemetry catheterization into mouse right common carotid artery. 42

Figure 3. 2 Diagrams showing ligation of the left anterior descending coronary artery.. 44

Figure 3. 3 Osmotic minipump implantation. 47

Figure 4. 1 Schematic of animal study design 57

Figure 4. 2 Generation of Keap1 knockout mice. 58

Figure 4. 3 Representative tracing of RSNA recording..... 59

Figure 4. 4 Assessment of CHF model. 61

Figure 4. 5 Expression of Nrf2 and two target proteins in the RVLM of Sham and CHF mice transfected with GFP or Nrf2 viruses. 64

Figure 4. 6 Nrf2, Keap1, NQO1, and HO-1 expression in the RVLM of Keap1f/f mice following Lenti-GFP-Cre virus transfection. 66

Figure 4. 7 Sympathetic outflow and cardiovascular regulation in conscious mice. 68

Figure 4. 8 Renal sympathetic nerve activity and baroreflex sensitivity under 70

Figure 4. 9 Basal RSNA and plasma NE concentration in CHF-Keap1f/f-GFP mice. ... 72

Figure 5. 1 Experimental design 82

Figure 5. 2 Central SynhACE2 overexpression attenuates ICV-AngII induced BP increase 85

Figure 5. 3 Day-night circadian MAP before and after ICV infusion 87

Figure 5. 4 ACE2 over-expression attenuates the enhancement of central AngII..... 89

Figure 5. 5 SynhACE2+/+ attenuates central AngII- induced sympathetic hyperactivity. 91

Figure 5. 6 SynhACE2+/+ mice exhibit anti-oxidative stress property in response to central AngII..... 93

Figure 6. 1 Animal experimental design. 101

Figure 6. 2 Representative immunoblot for Nrf2 translocation in N2A..... 103

Figure 6. 3 Representative immunoblot for whole cell Nrf2 in Ad-hACE2-eGFP transfected N2A cells. 105

Figure 6. 4 Representative immunoblot of Nrf2 and NQO-1 in the brain of synhACE2+/+ with chronic central AngII infusion 107

Figure 6. 5 Representative immunofluorescence staining of Nrf2 knockdown in the RVLM..... 109

Figure 6. 6 Effect of RVLM Nrf2 knock down on central AngII-induced polydipsia and polyuria in Nrf2-floxed mice. 110

Figure 6. 7 Immunoblot of Nrf2 and NQO-1 in RVLM after chronic ICV infusion of AngII, SFN, or AngII+SFN..... 113

Figure 6. 8 ICV-SFN attenuates the pressor responses ad SNA to central AngII. 114

Figure 6. 9 Effects of ICV-SFN on central AngII- induced polydipsia and polyuria..... 115

Figure 7. 1 Overview of the mechanisms and potential involvement of ACE2 and Nrf2 in the regulation of sympathetic outflow in neurons from the RVLM in the setting of CHF and HTN in response to increased central AngII. 122

Table 4. 1 Anatomic, hemodynamic, and echocardiographic measurements associated with failing hearts. 62

Table 5.1 Baseline and post-infusion day-night hemodynamics..... 86

Abbreviations

ACE	angiotensin-converting enzyme
ACE2	angiotensin-converting enzyme 2
ACEIs	ACE inhibitors
Ach	acetylcholine
AHA	American Heart Association
AngI	angiotensin I
AngII	angiotensin II
Ang 1-7	angiotensin 1-7
ANOVA	analysis of variance
AP	arterial pressure
ARB	AT_1R blockers
AT_1R	angiotensin II type 1 receptor
AV	atrioventricular
AV3V	anteroventral third ventricle
BBB	blood-brain barrier
BP	BP
BRS	baroreceptor sensitivity
BSA	bovine serum albumin
CAT	catalase
CHF	chronic heart failure
CMV	cytomegalovirus
CNS	central nervous system
CSAR	cardiac sympathetic afferent reflex

CVD	cardiovascular disease
CVLM	caudal ventrolateral medulla
DAPI	4',6-diamidino-2-phenylindole
DBP	diastolic BP
DMH	dorsomedial hypothalamus
DMV	dorsal motor nucleus of the vagus
EF	ejection fraction
ELISA	Enzyme-Linked Immunosorbant Assay
ERK	extracellular regulated kinase
FS	fractional shortening
HTN	hypertension
HF	high-frequency
HFpEF	heart failure with preserved ejection fraction
HO-1	Heme oxygenase-1
HR	heart rate
HRV	Heart rate variability
IABS-A	Induced Baroreflex Sensitivity under Anesthesia
IBRS-C	Induced Baroreflex Sensitivity in the conscious state
ICV	intracerebroventricular
Keap1	Kelch-like ECH-associated protein 1
LAD	left anterior descending
LF	low-frequency
LTRs	long terminal repeats
LVEDP	left ventricular end-diastolic pressure

MAP mean arterial pressure

MasR mas receptor

MI myocardial infarction

MnPO median preoptic nucleus

mPFC medial prefrontal cortex

NA nucleus ambiguous

NE norepinephrine

Nrf2 Nuclear factor erythroid 2-related factor 2

NO Nitric oxide

NOX NADPH oxidase

NQO1 NAD(P)H dehydrogenase [quinone] 1

NTS nucleus tractus solitarius

OVLT organum vasculosum lamina terminalis

PaO_2 pressure of oxygen

$PaCO_2$ carbon dioxide

PAG periaqueductal gray

PBS phosphate-buffered saline PE phenylephrine

PE phenylephrine

PNMT phenylethanolamine N-methyltransferase

PSD power spectral density

PVN paraventricular nucleus

RAAS renin-angiotensin-aldosterone system

RIPA Radioimmunoprecipitation Assay

ROS reactive oxygen species

RPG respiratory pattern generator

RTN	retrotrapezoid nucleus
RSNA	renal sympathetic activity
RVLM	rostral ventrolateral medulla
SA	sinoatrial
SBP	systolic BP
SBRS	spontaneous baroreflex sensitivity
SDRR	standard deviation of HR
SHRSP	spontaneously hypertensive stroke-prone
SFO	subfornical organ
SNA	sympathetic nerve activity
SNP	sodium nitroprusside
SON	superoptic nucleus
TAC	transverse aortic constriction
tBHQ	tert-butylhydroquinone
VSMC	vascular smooth muscle cell
8-OHdG	8-hydroxy-deoxyguanosine

Chapter I. Introduction

Neural control of the cardiovascular system

It was not until the 1940s that the central “vasomotor” center was discovered[2]. The central cardiovascular pathways are regulated by two general mechanisms: feed forward central command and reflex effects[3]. Mechanisms involved in feed forward control include neurons residing in the forebrain and midbrain, such as dorsomedial hypothalamus (DMH), the paraventricular nuclei (PVN), medial prefrontal cortex (mPFC), insular cortex, and midbrain periaqueductal gray (PAG) [4]. Neurons from these areas project to lower level nuclei in the baroreflex circuitry. These pathways modulate the baroreceptor reflex and sympathetic function thus impacting the short term control of arterial pressure (AP) [4].

Nuclei that are within the baroreflex circuitry on the other hand, include the nucleus tractus solitarius (NTS) in the dorsomedial medulla, cardiac vagal motoneurons in the nucleus ambiguous(NA), caudal ventrolateral medulla (CVLM), and the RVLM [4]. The RVLM contains epinephrine synthesizing C1 neurons and glutamatergic neurons which receive and integrate a variety of inputs from the brainstem and forebrain in regulating BP and mediating multiple reflexes. The A1 noradrenergic neurons, located in the general ventrolateral medulla, are thought to be involved in natriuretic responses through activating vasopressin-secreting neurons in the PVN [5, 6]. RVLM may also contain pH-sensitive neurons that receive excitatory synaptic inputs from the retrotrapezoid nucleus (RTN) chemoreceptors. These chemoreceptors activate the respiratory pattern generator (RPG) which eventually excites the sympathoexcitatory neurons of the RVLM [7, 8].

In addition to these classical neurons involved in the circuitry mediating baroreflex regulation, neurons from other important areas are indirectly related to BP control via changes in osmolality and involvement of the central RAAS [4, 9, 10]. These nuclei

originate from the organum vasculosum lamina terminalis (OVLT) in the anterior wall of the third ventricle, PVN, subfornical organ (SFO), median preoptic nucleus (MnPO), and supraoptic nucleus (SON) of the hypothalamus. These regions are involved in multiple autonomic and behavioral control including the regulation of vasopressin release and drinking behavior, and the maintenance of salt and water balance[11, 12]. The most thoroughly studied central cardiopulmonary regions and a simplified schematic of the baroreflex loop are depicted in Fig 1.1.

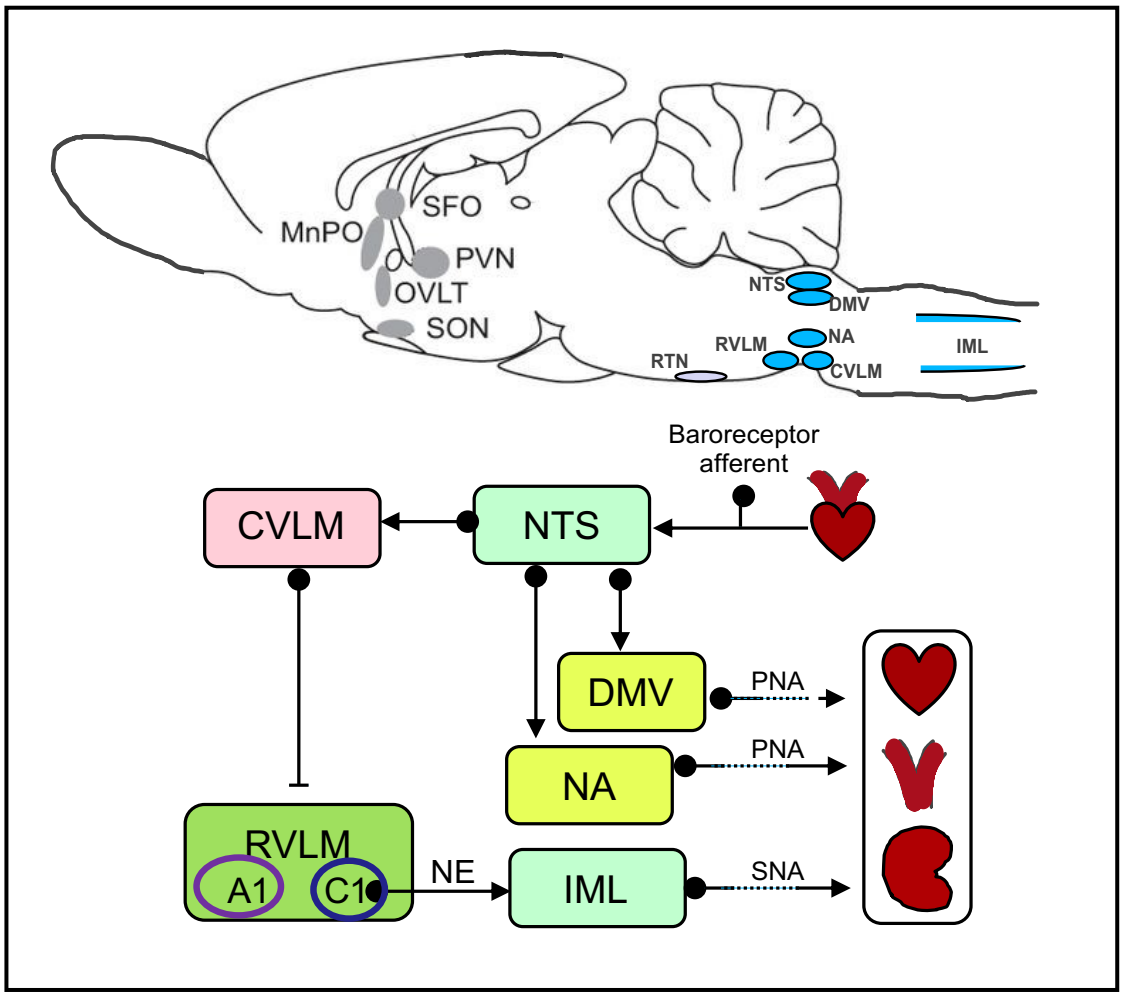

Figure 1.1 Schematic diagram of important central nuclei involved in cardiovascular control and baroreflex loop.

Upper: Blue areas are brainstem autonomic control centers: NTS, nucleus tractus solitarius; DMV, dorsal motor nucleus of the vagus; NA, nucleus ambiguous; RVLM, rostral ventrolateral medulla; CVLM, caudal ventrolateral medulla; IML, intermediolateral nucleus; RTN, retrotrapezoid nucleus. Areas in grey shows circumventricular organs that involve various neuroendocrine functions: SFO, subfornical organ; PVN, paraventricular nuclei; OVLT, organum vasculosum lamina terminalis; MnPO, median preoptic nucleus; SON, supraoptic nucleus.

Lower: Pathways in the baroreceptor reflex control of the sympathetic outflow. The continuous arrow and the dashed arrows indicate a stimulatory synapse and bar-headed lines an inhibitory synapse, respectively. The solid lines indicate the major connections which are well established by studies.

Peripheral reflex mechanisms play a critical role in mediating and interacting between the SNA and the extracellular environment. Several pathways not only form their own feedback loop but also communicate with each other to control BP, fluid volume, oxygen tension and body temperature.

The arterial baroreflex relies on BP sensing elements (mechanoreceptors) in the carotid sinus and aortic arch, that transduce arterial BP fluctuations into neural signals (sensory action potentials). Afferent signals travel in the glossopharyngeal and vagal nerves to the NTS. Neural signals from the NTS project to the CVLM which inhibits the RVLM[4, 13], provoking changes in the sympathetic outflow and vasopressin release. Signals from the NTS also project to the parasympathetic neurons in the dorsal motor nucleus of the vagus (DMV) and the NA, thus completing a negative feedback loop to maintain BP by regulating cardiac output and vascular resistance.

The cardiopulmonary baroreflex is initiated from primary neurons whose cell bodies reside in the nodose ganglia, with the nerve endings distributed in the heart, vena cava and pulmonary vasculature. They sense changes in central blood volume, send afferent signals to central nuclei in a similar pattern as the arterial baroreflex. The efferent effects are similar except that the cardiopulmonary baroreflex mainly adjusts orthostatic BP in response to blood volume changes, due to the high compliance of the areas where the sensory endings are embedded. This reflex has little effect on heart rate (HR), especially in humans [13].

Sympatho-excitation is primarily transduced at the tissue level by adrenergic receptors that are widely expressed in most organs, while parasympathetic innervation is mainly distributed to the heart, bronchi and gastrointestinal tract. Both sympathetic and

parasympathetic outflow can affect the sinoatrial (SA), atrioventricular (AV) nodes, and cardiomyocyte contraction, reciprocally determining HR and contractility.

The arterial chemoreflex is initiated by chemoreceptors located in the carotid sinus (carotid body) and aortic arch. These sensors detect changes in arterial pH, partial pressure of oxygen (PaO_2) and carbon dioxide ($PaCO_2$). In addition to their primary role in regulating ventilation, chemoreflex afferent activity also mediates an increase in sympathetic tone during hypoxia[13].

Chronic heart failure

According to the American Heart Association (AHA) 2017 Heart Disease and Stroke Statistics, approximately 41.5 percent, or 102.7 million people in the US suffered from at least one form of cardiovascular disease (CVD) in 2015 [14]. Globally, CVD has long been the number one cause of death, accounting for an estimated 31.5% of all global deaths [14, 15]. CVD not only exerts a heavy toll on people's health, but also accounts for a tremendous economic burden to society.

The termCHF and congestive heart failure may be used interchangeably although they are not necessarily the same concept. Congestive heart failure is a syndrome characterized by fluid accumulation in the lungs or peripheral circulation, often the result of systolic heart failure where there is a reduced ejection fraction (EF), also known as HFrEF. Opposed to HFrEF, there is heart failure with preserved EF, so called HFpEF, which results from diastolic dysfunction. Both conditions can progress to a chronic stage, thus the term CHF[16].

CHF is usually the end result of CVD and afflicts around 5.8 million Americans and over 23 million people worldwide as of 2015 [17, 18]. Although the incidence of CHF may have been decreased over time due to improved medical care, the absolute number of more than 550,000 newly diagnosed cases each year still reflects persisting difficulties in managing CHF [17].

Symptoms and signs of CHF include dyspnea on exertion, orthopnea, exercise intolerance, refractory volume overload and fatigue [19]. Etiologies of CHF include ischemic heart disease, valvular disease, cardiomyopathy, HTN, diabetes mellitus and other idiopathic conditions. Current management for CHF depends on both causes and stage of the problem. Over the past decades, numerous medications have been used in the management of CHF, including diuretics, β1-adrenergic receptor blockers, calcium channel blockers, digoxin, ACE inhibitors (ACEIs) / AT1R blockers (ARBs). Yet, the only ones that have been shown to be unequivocally beneficial in improving survival rate are ACEIs and ARBs [20, 21]. Although these approaches have made significant progress in symptom control, the incident of CHF is still unacceptably high. Therefore, the quest for exploring new therapeutic targets in CHF is of paramount importance.

Primary (Essential) HTN

HTN is by far the most common primary diagnosis in office visits in the United States, and one of the top causes of morbidity worldwide [22]. According to the World Health Organization, there were an estimated 1.13 billion people worldwide with HTN in 2015. In the US, approximately 75 million American adults have HTN, yet only about half are under control [23].

The ACC/AHA 2017 updated guidelines redefined HTN as office systolic BP (SBP) values ≥130 mmHg and/or diastolic BP (DBP) values ≥80 mmHg, further extending the prevalence of HTN in US adult population to approximately 46 percent [15,19]. Not only does HTN itself exert a huge economic burden, the overall negative consequences of HTN being a contributing factor to a variety of CVD such as stroke and heart failure puts an even larger burden on public health worldwide [24].

95 percent of all HTN cases are primary, or essential HTN, which is high BP without a known cause [25]. Therefore, current management of HTN mainly focuses on symptom control. Pharmacologic therapy for HTN include the use of thiazide diuretics, calcium channel blockers, ACEIs and ARBs [26]. However, despite multiple management, around 30 percent of all uncontrolled patients fall into the category of apparent treatment-resistant HTN in the United States [27]. Thus identifying new insights and targets for HTN treatment is still a high priority.

Sympathetic overactivity

In chronic HFrEF, impaired left ventricular systolic function results in an inadequate cardiac output, which initially unloads peripheral baroreceptors thus increasing sympathetic flow in a negative-feedback manner in an attempt to restore cardiac output [28]. Although being compensatory at first, these responses eventually enter a vicious cycle that lead to further disease progression. In chronic HFpEF, in spite of the fact that some current reviews confirm a correlation between sympathoexciation and HFpEF, evidence on potential neurohormonal mechanisms in this syndrome are scarce[29, 30].

Hypotheses for the central mechanisms relating to deteriorating cardiac function in CHF include both neural and humoral disturbances[31]. First is the altered set point theory,

stating that alterations in baroreflex gain increases the set point for sympathetic outflow (i.e. less sympatho-inhibition). This has been demonstrated in the paced-canine model in our lab, which showed increased baroreceptor stimulation elicits a drop in plasma NE concentration in normal dogs whereas baroreceptor denervation had no effects on NE concentration in CHF [32]. Another important mechanism is an enhanced central AngII / AT1R system acting as a positive feedback cycle and exciting SNA, in part, through increased oxidative stress[33]. It has been shown that AT1R protein and mRNA were upregulated in the RVLM and the NTS in rabbits and rats with heart failure [34, 35].

Given the fact that most heart failure develops from coronary artery disease that is exacerbated by chronic HTN and obesity, it is plausible to speculate that generalized sympathoexcitation in primary HTN may also play a causative role in disease progression. It has been widely agreed that in both human and animal models HTN altered autonomic balance leads to hemodynamic dysregulation [36]. Evidence to support this include findings of enhanced NE spillover from sympathetic nerve terminals in HTN patients and in normotensive individuals with a family history of HTN [37, 38]. In normotensive offspring of HTN subjects, people with a family history of HTN have lower parasympathetic modulation than those with a negative history [39]. Therefore, it is reasonable to believe that central sympathetic overdrive may act as the initial pathogenesis of primary HTN under the background of genetic predisposition and environmental stimuli.

Central RAAS Activation

Systemic vs Local RAAS

In addition to the autonomic reflex control of the circulation, BP and fluid homeostasis are closely regulated by the RAAS. Decreases in renal perfusion pressure are “sensed” by the juxtaglomerular (JG) cells in the kidney and renin is secreted and released into

circulation. Under the catalysis of plasma renin, angiotensinogen produced by the liver is converted into Angiotensin I (AngI), which is subsequently converted to AngII by ACE. ACE is predominantly produced in the lungs [40]. AngII has multiple functions in restoring BP and fluid volume: 1) it is a potent vasoconstrictor activating the AT1R on the blood vessels; 2) AngII acts in the adrenal cortex and stimulates secretion of aldosterone, which in turn increases sodium and water reabsorption in the distal nephron; 3) AngII is capable of directly enhancing activity of the epithelial Na+ channel (ENaC) in the distal nephron thus stimulating sodium and water reabsorption. 4) AngII also causes the release of vasopressin, or anti-diuretic hormone (ADH), from the pituitary gland and evokes thirst, and increased drinking behavior [40].

In addition to the conventional concept of a circulating RAAS, there is a wealth of evidence indicating the existence of local RAAS in various organs including the heart, vasculature, kidney and brain [41]. In CHF patients, local cardiac AngII concentration is increased as well as its gradient across the heart [42]. Using angiotensinogen overexpression transgenic mice, Mazzolal et al. demonstrated that increased AngII synthesis in the myocardium triggered cardiac hypertrophy[43]. Local cardiac intracellular renin expression was found to be enhanced after myocardial infarction and was related to impairment of cell communication through enhancing gap junction permeability [44, 45]. In hypertensive animals, increased cardiac AngII is associated with enhanced inflammation, oxidative stress and cell death [41]. In vascular muscle cells, synthesis of all major components including angiotensinogen, ACE, AngII and renin have been shown [46]. Furthermore, De Mello et al. found that intracellular AngII in resistance vessels counteracts the vasoconstrictive effects of extracellular AngII, thus playing an important role in regulating vascular tone[47]. In the kidney, the intrarenal RAAS was assessed and was found that stimulation of local AT1Rs enhanced sodium reabsorption [48]. So far it

has been widely acknowledged that along with systemic RAAS, local RAAS plays a fundamental role in the pathogenesis of CVD. This has opened a window for target-specific therapeutics aiming locally at individual components of the RAAS system.

Central RAAS and HTN

In 1961, Bickerton and Buckley demonstrated specific central RAAS actions in the dog[49]. In 1971, Jacques Genest's laboratory discovered renin synthesis in dog brain[50]. Numerous studies in animal models have now identified all components of the RAAS in the CNS. The role of the RAAS in the brain has been examined extensively in transgenic animals and by using pharmacological approaches. The central RAAS is related to a variety of mechanisms that mediate multiple actions including cognition, neurodegeneration and most importantly, BP regulation[51]. Intracerebroventricular (ICV) infusion of AngII into rat lateral ventricle has been shown to significantly increase BP, vasopressin release, drinking response (polydipsia) and sympathetic outflow[52]. Injection of AngII into the rat NTS suppressed the baroreflex, which was reversed by the AT1R antagonist losartan[53]. Double transgenic mice expressing both human renin and angiotensinogen generated by Sigmund's laboratory exhibited increased salt intake and arterial BP, which was blunted by ICV, but not intravenous (IV) losartan treatment[54]. These studies indicate that the RAAS in the brain affects BP control and electrolyte balance possibly through different neural pathways.

An integrative review of the central mechanisms underlying HTN included a possible course in the pathogenesis of HTN[55]. In order to maintain a relatively stable BP, there needs to be both a control center that determines a set point and a center that helps stabilize BP around this set point[56]. The former is thought to be in the hypothalamus, especially the PVN and SON; the latter occurs in the medulla oblongata[56]. Systemically

administered ACE inhibitors normalize the set point and baroreceptor sensitivity (BRS). The BRS remains in the normal range even when BP is increased by phenylephrine infusion[57]. Although when ACE inhibitors are given peripherally, it is possible to act in the CNS as well through sites without an intact brain-blood barrier. These findings indicate that AngII may play an essential role in determining the BP set point. What activates the central RAAS is proposed to be increased salt intake which is prevalent in the modern diet. Increased vasopressin stimulated sympathetic outflow and oxidative stress triggered by central AngII, all lead to primary HTN [55].

ACE/AngII/AT1R and ACE2/Angiotensin 1-7 (Ang1-7)/MasR

Within the RAAS system there exist two major counteracting arms – the "ACE/AngII/AT1R" arm and the "ACE2/Ang1-7/Mas receptor (MasR)" arm. ACE, or kininase II, was first isolated in 1956 and found to be the enzyme converting AngI to AngII, and degrading the vasodilator bradykinin[58]. ACE exists in two forms – membrane-bound form as ectoenzymes conventionally found in pulmonary vascular endothelium and testicular epithelial cells, and shed soluble form that is derived from the membrane-bound form present in serum and other body fluids[59, 60]. The current consensus now indicate that ACE is expressed in virtually all endothelial cell types as well as in neurons, smooth muscle cells, adipocytes and immunocytes[61]. For decades, ACE inhibitors have been the first line therapy for many major cardiovascular diseases including HTN, myocardial infarction, and heart failure and have been shown to improve survival in these patients [62].

ACE2 on the other hand, is a more recently discovered carboxypeptidase and is a homolog of ACE[63]. ACE2 was first reported to cleave AngI to Ang 1-9, but later studies found that ACE2 has a much higher efficiency in the hydrolysis of AngII to Ang 1-7[64],

which turned out to play a fundamental role in counteracting AngII effects in many cardiovascular diseases. Thus this so-called “good arm of the RAAS”, ACE2/Ang1-7/ MasR axis, has since been extensively studied[65]. Quantitative PCR analysis has shown that the ACE2 gene is widely expressed in most human organs including the heart, kidney, intestines and brain[66]. Xia et al. reported that ACE2 is widespread throughout the mouse brain cardiovascular control centers such as PVN, NTS, and RVLM[67].

In both CHF and HTN, these two axes of the RAAS have been shown to play pivotal roles in modulating sympathoexcitatory and sympathoinhibitory reflexes. In previous work from our laboratory we have shown that rabbits with CHF exhibit increased ACE, AT1 receptor and decreased ACE2 expression in several central nuclei including the RVLM, the PVN and the NTS [61]. We also demonstrated that SNA was significantly reduced in CHF mice that overexpress ACE2 in the brain[68]. However, the mechanisms by which central ACE2 reduces sympathetic outflow are not clear.

Although it is plausible to presume the anti-sympathetic effects of ACE2 is the result of either AngII consumption or Ang 1-7 production, the exact action of the latter on SNA remains controversial. Potts et al. reported that microinjection of Ang 1-7 into the RVLM exhibited sympatho-excitatory effects in anesthetized rabbits [69]. This was later supported by Frontes et al. by bilateral microinjection of the MasR antagonist A-779 into the RVLM, which produced a significant fall in mean arterial pressure (MAP) and HR [70]. In another study, Silva et al. demonstrated that bilateral microinjections of A-779 into the PVN resulted in a significant decrease in RSNA [71]. However, the sympatho-inhibitory effect of Ang 1-7 has also been shown in several other studies. Gironacci et al. found that minced hypothalami from spontaneous hypertensive rat (SHR) incubated with Ang 1-7 showed significantly attenuated NE release[72]. Similar results were obtained by Mirnela

et al. *in vitro* where Ang 1-7 inhibited the nerve stimulation-induced release of norepinephrine and neuropeptide Y from the mesenteric arterial bed [73].

In the case of HTN, Sriramula et al.[74] showed attenuation of the pressor response to peripheral infusion of AngII in mice that overexpress ACE2 in the brain. The same group also showed that peripheral AngII infusion increased oxidative stress in the PVN and RVLM significantly more in ACE2 knockout mice compared to their non-transgenic littermates[75]. Using transgenic mice overexpressing ACE2 in the SFO, Feng et al. demonstrated that ACE2 prevents the AngII-mediated pressor and drinking responses through AT1 receptor downregulation [76].

Oxidative Stress

Oxidative Stress and its role in Cardiovascular Disease

In 1954, Dr. Denham Harman from University of Nebraska Medical Center first proposed the 'free radical theory of ageing', hypothesizing "free radicals" as the cause of macromolecular degenerative process of aging[77]. Then the concept of "oxidative stress" was introduced into research and clinical field by Helmut Sies in 1985[78]. Oxidative stress was later defined as "an imbalance between oxidants and antioxidants in favor of the oxidants, leading to a disruption of redox signaling and control and/or molecular damage"[79]. Over the past three decades, multiple studies on oxidative stress in a variety of diseases have been carried out. The most widely studied abnormalities include neurocognitive impairment, CVD, kidney dysfunction, and endocrine abnormalities[80].

Reactive oxygen species (ROS) contribute in a major way to cellular and tissue oxidative stress. Major exogenous sources of ROS include environemental chemical exposures, UV light, ionizing radiation, organic solvents, etc. The main source of endogenous ROS have

been identified as mitochondria, peroxisomes, plasma membrane, and intra/extracellular spaces[81]. Important ROS such as superoxide anion radical ($O_2^{\bullet -}$) and hydroxyl radical (HO•) exert their destructive effects through DNA and RNA damage, lipid peroxidation, protein damage/modification, and carbohydrate degradation[82]. To combat oxidative stress, living organisms have evolved defense systems which utilize antioxidant enzymes such as superoxide dismutase (SOD), catalase (CAT), HO-1, NQO1, glutathione (GSH), vitamin C and vitamin E. In addition, several metal compounds such as Zn and Se compounds behave as antioxidants [83].

Long lasting oxidative stress has been shown to be closely related to the development and progression of many cardiovascular diseases including HTN, congestive heart failure, atherosclerosis, and cardiomyopathies[79,80]. Common mechanisms of oxidative stress as a causative or promoting factors of these diseases involve the activation in NF-κB pathways and increased inflammation[81,82], modulation of redox sensitive proteins thus altering certain transcriptional activities[84], direct structural damage, and reduction of antioxidant systems efficiency[27].

In CHF, both clinical and experimental studies have discovered evidence of enhanced oxidative stress[85]. In the periphery, increased ROS promotes CHF progression by mechanisms involving cardiac electrophysiological changes, myocardial remodeling and reducing myofilament calcium sensitivity[86]. These processes eventually lead to left ventricular (LV) dilatation and contractile dysfunction. In the CNS, excessive production of local ROS in the brain has been increasingly investigated and is being presumed by many to be a primary culprit in the progression of CHF. Lindley et al. in 2004 demonstrated that ICV injection of an adenoviral vector encoding superoxide dismutase (Ad-Cu/ZnSOD) significantly decreased the number of chronically activated neurons in PVN and SON in

MI-induced HF mice[87]. Previous studies from our lab showed that NADPH-dependent $O_2^{\bullet-}$ production in the RVLM was significantly increased in the CHF state compared with a sham group[88].

In HTN, ROS exert detrimental effects also through both systemic and central mechanisms. Nitric oxide (NO) is generated mainly in the endothelium. Increased local ROS such as $O_2^{\bullet-}$ rapidly degrade NO thereby promoting vasoconstriction[89]. ROS generated by activated nicotinamide adenine dinucleotide phosphate(NADPH) oxidase, (NOX) have been shown to be key factors that mediate AngII-induced HTN, possibly through upregulating intracelluar pro-inflammatory mediators and vascular smooth muscle cell (VSMC) growth[90]. All of these mechanisms may explain why many patients with HTN exhibit an increase in oxidative stress and a decrease in NO bioavailability in many tissues[91]. Experimental mouse models with genetic deficiencies in NOX1 have also shown to have lower BP compared to their wild type counterparts[92].

There is little question that the CNS contributes to CVD. Elevated oxidative stress within certain brain nuclei has been consistently shown in different animal models. For example, Campos et al. showed that the expression of NOX subunits (p47 phox and gp 91 phox) is elevated in the PVN and RVLM in rats with HTN [93]. Hirooka et al. observed that ROS production is markedly increased in the RVLM of HTN rats [94].

Relation between Oxidative Stress, Sympathoactivation, and RAAS

As mentioned above, the pathogenesis and progression of CHF and HTN are closely related to altered SNA, central RAS and oxidative stress. However, the underlying molecular mechanisms and the exact cause-and-effect relationships between these factors are still under investigation. Current evidence largely point towards the hypothesis

that in both situations, an activated RAAS signaling in the brain trigger sympathoexcitation, most likely through ROS mobilization [95-97].

Following a myocardial infarction (MI), there is an increase in plasma AngII and aldosterone[98]. On the one hand, plasma AngII can cause increased BP though promoting renal sodium absorption and its direct vesoconstrictor effect; on the other hand, circulating AngII can enter the CNS via brain areas lacking an intact blood-brain-barrier, such as the SFO, to activate SNA which, in turn, enhances the effects of the circulating RAAS. Although this process may be most prominent during the acute phase post MI, chronically enhanced SNA is thought to result from a aldosterone-triggered neuromodulatory system that involves “endogenous ouabain” release[99]. The direct effect of “ouabain” is inhibition of Na^+/K^+-adenosine triphosphatase (Na^+/K^+-ATPase) in neuronal membranes, which lowers membrane potential thereby enhancing SNA. Elevated circulating aldosterone can also readily cross the blood-brain-barrier to accomplish the above process.

Tan et al. found the binding density of ACE is significantly elevated in the PVN in MI-induced heart failure[100]. Studies from our laboratory have shown elevated ACE protein in several brain regions including RVLM, PVN and NTS in CHF rabbits [101]. Our previous experiments also showed that the cardiac sympathetic afferent reflex (CSAR) sensitivity is enhanced in dogs with pacing-induced CHF and is normalized by ICV administered the AT1R antagonist, losartan[102, 103]. The CSAR is one of the contributing factors for sympathoexcitation in CHF. Therefore, the overall increased in SNA may at least in part, be attributed to increased CSAR sensitivity due to upregulated AT1R expression. This was later by a study where microinjection of AT1R mRNA antisense into the PVN

normalized the CSAR in rats with CHF [104]. Similar increase of AT1R expression was also found in the RVLM in CHF in studies from our laboratory [105].

Oxidative stress as a contributing factor that activates sympathoexcitation has been well accepted based on large amount of evidence. Zanzinger et al. observed that removal of extracellular $O_2^{\bullet-}$ by microinjection of SOD into the RVLM reduced SNA outflow [106]. Furthermore, many studies have indicated that the sympathoexcitation of the RAAS is through its promotion of ROS generation. Gao et al. showed that NADPH-dependent $O_2^{\bullet-}$ production is significantly increased in the RLVM of CHF rabbits compared with that of sham rabbits; and the effect of AngII on RSNA in the two groups is blocked by pretreatment with tempol or apocynin (APO) [88]. Zimmerman et al. showed that the pressor effects of ICV-AngII were abolished by administration of AdMnSOD in the mouse brain[107]. Campese et al. later showed that both SOD mimetics tempol and PEG-SOD effectively abolished the effects of AngII on central and peripheral SNA[108]. It was further demonstrated that the specific mechanism of this AngII-AT1R-ROS signaling on SNA involves inhibition of the delayed rectifier potassium current (IKv)[109] and influx of extracellular Ca2+ in neural cells[110], thus altering neuronal excitability.

The pathogenesis and progression of primary HTN involve similar mechanisms to those of CHF except for some differences in the triggering events. Although the origin of primary HTN is multifactorial including high salt intake, chronic hypoxia, vascular inflammation and so forth, a common pathogenic initiator most always involves sympathetic overdrive[111]. As one of the several most important mechanisms, increased central RAAS activity in primary HTN has been consistently supported by the literature. An innovative study from Reudelhuber's lab demonstrated that restoration of AngII exclusively in the brain of angiotensinogen-deficient mice increases their BP[112]. Morimoto et al. illustrated that

glia- and neuron-specific overexpression of AngII increases BP, polydipsia, and salt preference in mice[113]. These studies combined suggest that centrally derived AngII is a critical determinant in the development of HTN. In humans, an increase in vascular $O_2^{\bullet-}$, H_2O_2 and a decrease in NO synthesis have also been observed in hypertensive individuals [114, 115]. There is increasing evidence supporting that increased ROS in HTN are contributed by both mitochondria nonenzymatic reactions and the increased intracellular NOX stimulated by RAAS activation[116, 117].

Nrf2

Since increased oxidative stress is thought to be a key molecular mechanism that links the RAAS and SNA, living organisms have developed a variety of antioxidant systems to prevent their harmful effects on cells. One of the most important and widely investigated regulators that help maintain redox balance is the Nrf2/ Kelch-like ECH-associated protein 1 (Keap1) system[118]. Keap1 is a natural inhibitor of Nrf2 and normally keeps Nrf2 in the cytosol in the form of the Keap1-Nrf2 complex[119]. When activated by specific ROS or electrophiles, Nrf2 is dissociated from Keap1 and translocates into the nucleus, binding to antioxidant response elements and transactivating the expression of genes of a series of antioxidant enzymes. A previous study from our lab showed that selective Nrf2 gene deletion in the RVLM increases BP and sympathetic outflow in normal mice due to impaired antioxidant mechanisms [120].

While an activated AngII/AT1R pathway is attributed to the upregulation of NOX in the RVLM in CHF[121], the mechanisms underlying downregulation of antioxidant enzymes remain to be elucidated. A key question is whether decreased Nrf2 in the RVLM in CVD characterized by sympatho-excitation is a result of increased RAAS activity. Feng et al reported that selective overexpression of ACE2 in the SFO prevents the pressor and

drinking reponses to ICV-AngII and downregulates AT1R[76]. In our preliminary studies, we measured Nrf2 expression in the RVLM and found Nrf2 to be elevated in transgenic mice overexpressing ACE2 in the brain, compared to their wild type littermates. This observation provided a suggestion for a potential Nrf2-RAAS interaction and serves as part of the rationale for our hypothesis. As shown in Fig 1.2, we propose that Nrf2 is important in maintaining the autonomic balance through its antioxidative property, Nrf2 might also mediate the sympathoinhibitory effect of ACE2 in response to central RAAS activation.

Overall hypotheses

1. The role of RVLM Nrf2 modulation on sympathetic outflow in diseases such as CHF and HTN has not been well characterized. Therefore, we hypothesize that reduced Nrf2 signaling in the RVLM contributes to impaired antioxidant defenses in CHF, leading to enhanced oxidative stress and sympathetic excitation. We further propose that upregulating Nrf2 will restore redox homeostasis in the RVLM in CHF, thus reducing the augmented sympathetic outflow.

2. Given the fact that ROS is closely related to both the maladaptive effects of AngII/AT1R signaling and to the protective properties of ACE2 and Nrf2 in CVD, we explored the potential roles of RAAS-Nrf2 interaction in mediating central sympathetic activity. Therefore we hypothesize that overexpression of ACE2 in the brain reduces sympathetic outflow in response to chronic ICV-AngII infusion by reducing oxidative stress, in part, through Nrf2 activation.

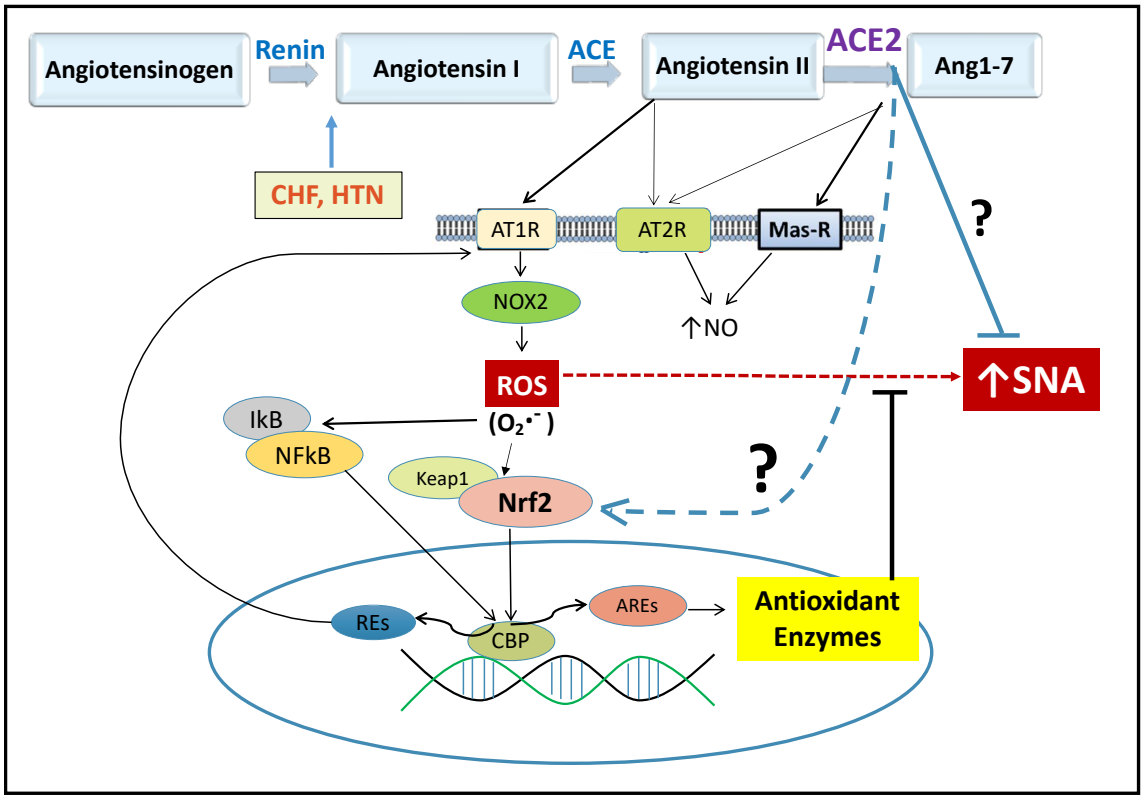

Figure 1. 2 Shematic diagram of ACE2 and Nrf2 signaling in RVLM neurons.

It has been well established that the ACE/AngII/AT1R axis promotes sympathoexcitation in both CHF and HTN, and this axis is also pro-oxidative through activating NOX2. While both ACE2 and Nrf2 have anti-oxidative properties and exibit protective effects in various diseases, it is yet to be identified if this arm of ACE2/Ang 1-7/MasR counteract the sympatho-excitatory effect of central AngII by upregulating Nrf2 and its downstream anti-oxidative defenses.

Chapter II. Experimental Objectives

General Goals

The overall goal of these experiments is to determine the mechanisms by which SNA is increased and antioxidant defenses are impaired in the RVLM in mice with CHF, and to determine the roles of ACE2 and Nrf2 in regulating SNA in HTN. Specifically, the goals of these experiments are defined by 3 objectives:

Objective 1 (Chapter IV)

To determine the effects of Nrf2 overexpression in the RVLM on sympathoexcitation in mice with CHF.

Objective 2 (Chapter V)

To determine the effects of ACE2 overexpression in the brain on pressor and metabolic responses to central AngII infusion.

Objective 3 (Chapter VI)

To determine potential interaction between central RAAS activation and Nrf2 activity.

Chapter III. Materials and Methods

Animals

Experiments were performed on 10- to 12-week-old mice. All the genotypes were on the C57BL/6 background. As described below, some early experiments were carried out in both male and female animals, but the majority were males. Some C57BL/6 mice were purchased from Charles River, Inc. (Wilmington, MA). In Objective 1, the Keap1 floxed ($Keap1^{f/f}$) mice were originally obtained from Johns Hopkins University (laboratory of Dr. Shyam Biswal) and bred at The University of Nebraska Medical Center, Department of Comparative Medicine. $Keap1^{f/f}$ mice contain LoxP sites flanking exons 2 and 3 of the Keap1 gene [12].

In Objective 2, male transgenic mice with ACE2 overexpression in the brain ($SynhACE2^{+/+}$) and their non-transgenic littermates were used. The $SynhACE2^{+/+}$ mice were obtained from laboratory of Dr. Eric Lazartigues. Briefly, SynhACE2 fusion transgene was constructed and was microinjected into fertilized C57BL/6JxSJL/J(B6SJLF2) mouse embryos [122]. PCR genotyping was performed using the three-primer protocol[123]. Mice of genotype $SynhACE2^{+/+}$ were crossed with wild type C57BL/6 mice to get the heterozygous $SynhACE2^{+/-}$, which were further intercrossed to obtain $SynhACE2^{-/-}$ as control group. In Objective 3, the Nrf2 floxed mice ($Nrf2^{f/f}$) were originally obtained from Dr. Shyam Biswal at the Johns Hopkins University [1] and bred in our facility. Selective Nrf2 knockdown was created by microinjection of Lenti-Cre-GFP virus into the RVLM bilaterally.

All the mice were housed in standard polypropylene cages in a facility with a 12:12 hour light-dark cycle (6am – 6pm lights on) and fed with standard mouse chow (Harlan Laboratories, Indianapolis, IN) and allowed water *ad libitum*. All procedures were approved by the Institutional Animal Care and Use Committee at the University of

Nebraska Medical Center. Experiments were carried out consistent with the National Institutes of Health Guide for the Care and Use of Laboratory Animals and conformed with the ARRIVE Guidelines to the extent possible[124].

Radiotelemetry implantation

The mice were implanted with radiotelemetry units (PA-C10, Data Science International, Inc.; St Paul, MN) for BP and HR measurements in the conscious state. Briefly, under 2% isoflurane anesthesia, mice were placed in the supine position. After making a 10-mm incision in the ventral cervical area, the left carotid artery was identified, dissected, and separated from the left vagus nerve at the proximal location near the artery, followed by placing a cotton patch saturated with 2% lidocaine underneath the artery which was fully dilated during the process. The tip of the telemetry catheter (Fig 3.1) was then inserted into the carotid artery and advanced to the level of aortic arch. The transmitter was placed subcutaneously in the right lower abdominal area. Finally, the wound in the neck was closed with absorbable sutures (PERMA-HAND 6-0, Ethicon, Norderstedt, Germany). Animals were left to recover for 1-2 weeks before hemodynamic recordings.

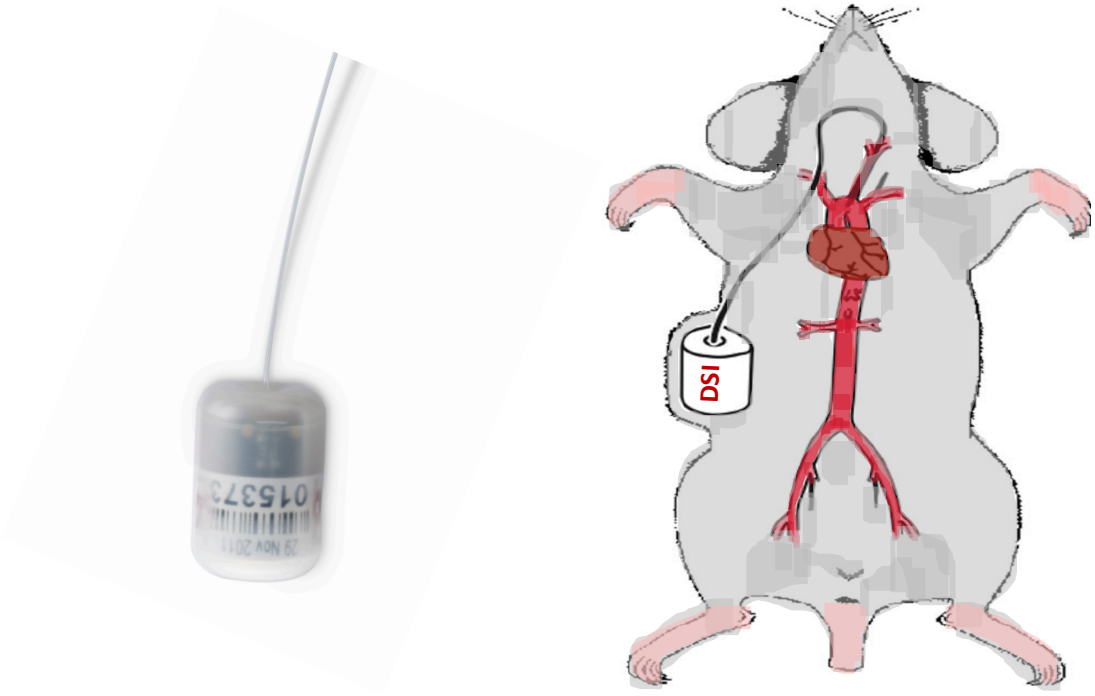

Figure 3. 1 Radio telemetry (left) and schematic of telemetry catheterization into mouse right common carotid artery.

Hemodynamic recordings

BP recording was performed at a sampling rate of 1 KHz using a PowerLab® data acquisition system (model 8S; ADInstruments, Inc.; Colorado Springs, CO). HR was derived from the arterial BP pulse. HR variability (HRV) and power spectral density (PSD) was assessed from the BP and HR using ADI software (Chart 8.0). High and low frequency cutoffs for power spectral analysis were 0.15 Hz to 1.5 Hz for low frequency (LF) and 1.5 Hz to 5 Hz for high frequency (HF) as previously described[125].

Chronic heart failure model

The CHF model was produced by permanent coronary artery ligation, as previously described[126]. Briefly, under anesthesia (~2% isoflurane and 98% O_2), mice were intubated and ventilated with a mouse ventilator (Mouse Ventilator MiniVent model 845, Hugo Sachs Elektronik; tidal volume: 150–250 µL; frequency: 200 breaths/min). The heart was exposed through a left thoracotomy at the fourth intercostal space. The anterior descending branch of the left coronary artery was permanently ligated with a 6-0 suture. Sham mice underwent thoracotomy and manipulation of the heart, but coronary artery ligation was not performed. To reduce acute mortality in the coronary ligated group, in postoperative care the mice were allowed to stay in the housing cage with supplemental 100% oxygen and a heating pad set at 30–32 °C for 3 days or longer as needed. Representative pictures of the model are shown in Fig 3.2.

A. B.

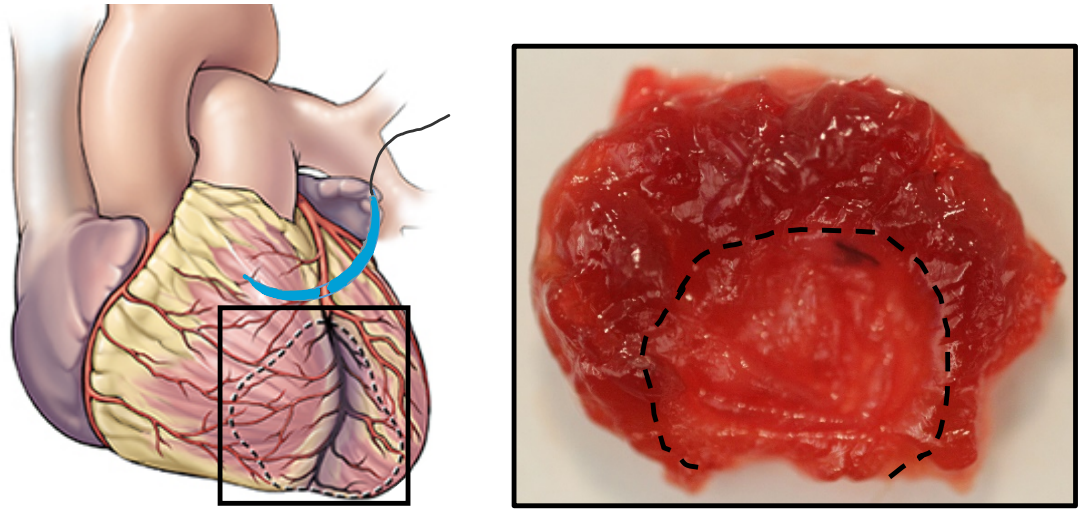

Figure 3. 2 Diagrams showing ligation of the left anterior descending coronary artery.

A) The suture was placed through the myocardium into the anterolateral left ventricle wall underneath the left anterior descending coronary artery, 1-3 mm from tip of the normally positioned left auricle. B) The left ventricle was cut open and spread on a flat plate. A well defined transmural scar was observed in the ischemic area as marked by the dashed line.

Echocardiography

At the fourth week post coronary ligation or sham surgery, mice were echocardiographically imaged on a Visual Sonics Vevo 3100 ultrasound using a 40 MHz probe under light isoflourane anesthesia (0.5–1%). 2D B-mode images were acquired in the long and short parasternal axis. M-Mode images were acquired at the level of the left ventricular papillary muscles. Left ventricular volumes and diameters were measured. Ejection fraction (EF) was calculated by a standard formula EF = [(LVEDV-LVESV)/LVEDV] x 100. Fractional shortening (FS) was calculated as FS = [(LVEDD-LVESD)/LVEDD] x 100. The echocardiographer was blinded as to the origin of the animal groups.

Microinjection of lentiviral vector into the RVLM

CamKIIa promoter (HIV-CamKIIa-GFP-Nrf2) driven Lentivirus encoding the Nrf2 gene was purchased from the Viral Vector Core, University of Iowa, IA. The Cytomegalovirus (CMV) promoter driven Lenti-GFP-Cre virus was purchased from Kerafast, Inc, Boston, MA. Lenti-GFP-Cre contains both 5′ and 3’ lentiviral long terminal repeats (LTRs) and all necessary elements for effective transduction and expression of GFP and Cre genes.

The delivery of viruses into the bilateral RVLM was performed on a mouse stereotaxic apparatus (SR-5M, NARISHIGE, Japan) with the mouse in prone position. The mouse was anesthetized with isoflurane (~2%). Two small holes were made overlying the cerebellum with a sterile 18-gauge needle to locate RVLM according to the following coordinates: 1.2 mm lateral to the midline, 5.3 mm ventral to the dorsal surface of the brain, 1.9 mm caudal to lambda [127]. Viruses were injected bilaterally into the RVLM using a 34-gauge needle attached to a microsyringe (Model 62 RN SYR, Hamilton Company, Reno, NV). Mice were left to recover for 2 weeks before recordings or physiological

experiments. RVLM targeting was confirmed by confocal immunofluorescence of GFP after euthanasia. The brain stem was removed and stored at −80°C for subsequent biochemical measurements.

ICV infusion and implantation of osmotic minipump

The mouse was placed on the stereotaxic apparatus with the skull exposed through a midline scalp incision. Under anesthesia, a small hole was drilled over the right cerebral ventricle using the following coordinates: 1.1 mm lateral from midline, 0.55 mm posterior to the bregma, and approximately 2.5 mm deep from the dorsal surface of the brain (Fig 3.3). Then a small incision was made in the mouse back between the scapulae. Using a hemostat, a small pocket was made by spreading the subcutaneous connective tissues apart. For different experimental purposes, a 14-day or 7-day Alzet osmotic minipump (MODEL 1002, Durect Corporation, Cupertino, CA) was inserted into the pocket. The minipump was attached to a cannula (ALZET Brain Infusion Kit3) for the ICV infusion of artificial CSF (aCSF), AngII (A9525, Sigma-Aldrich), Ang1-7 (A9202, Sigma-Aldrich), or A-779 (SML1370, Sigma-Aldrich) at a rate of 0.25uL/hr (14-day pump) or 0.5uL/hr (7-day pump). The skin incision was eventually closed with a 6-0 suture.

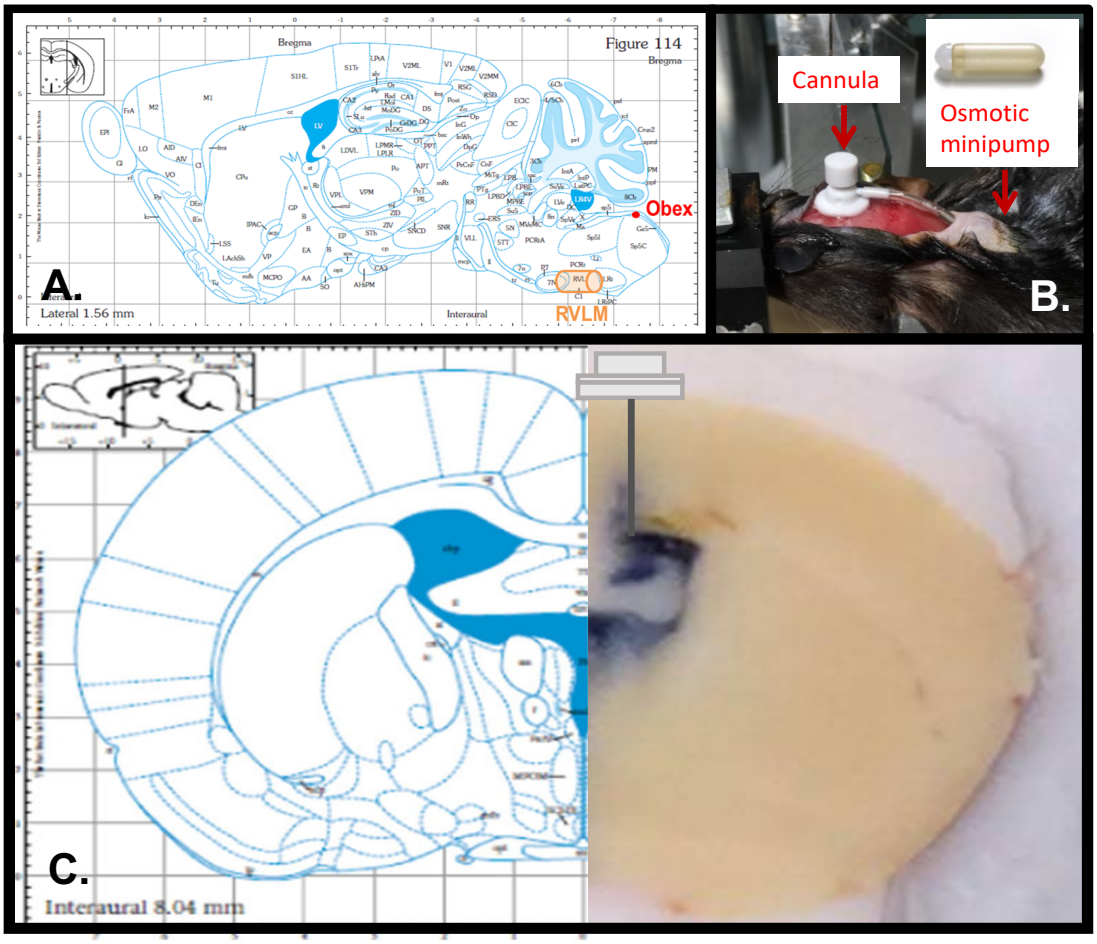

Figure 3. 3 Osmotic minipump implantation.

A. Atlas of mouse brain showing location of the RVLM (orange) in sagittal view. B. Osmotic pump and a cannula set inplanted in a mouse for ICV infusion. C. Methylene blue confirms injection is in lateral ventricle.

Renal Sympathetic Nerve Activity (RSNA) recordings

Mice were anesthetized with isoflurane (2%) and were ventilated with room air after tracheal cannulation (tidal volume: 150 µL, frequency: 200 breaths/min)[128]. The right femoral artery and vein were dissected and separated from the femoral nerve for venous and arterial cannulation (Millar transducer). A bundle of the left renal sympathetic nerves was isolated in the retroperitoneal space through a left flank incision and placed on a pair of platinum-iridium recording electrodes. The nerve-electrode complex was covered with silicone gel (Kwik-Sil, WPI, Sarasota FL). The RSNA signal was amplified (× 1000) and filtered (bandwidth: 30–3000 Hz) using a Grass P55C preamplifier, and input into a PowerLab® data-acquisition system, from which the signal was monitored, recorded, and saved using the LabChart® 7 software (AD Instruments, Inc. Colorado Sprngs, CO).

BRS Analysis

Spontaneous BRS (sBRS) in conscious mice was determined from the pulsatile BP signals based on the sequence technique[129], using HemoLab Software (Version 20.2, courtesy of Dr. Harald M. Stauss, University of Iowa). Individual sequences of increases or decreases in BP in mmHg (x-axis) and pulse interval in msec (y-axis) values were plotted and subjected to linear regression. The average of the slopes of all individual regression lines were then used as an index of baroreceptor-HR reflex sensitivity (ms/mmHg).

Induced Baroreflex Sensitivity in the conscious state (IBRS-C) was evaluated by calculating the percent of the decline in HR from the maximal value within 30 min after intraperitoneal injection of phenylephrine (PE) (10 µg in 50 µl).

Induced Baroreflex Sensitivity under Anesthesia (IABS-A) was analyzed by logistic regression over the entire pressure range after PE administration. The values for BP and RSNA were acquired every 2 s from the threshold to the saturation points. A sigmoid logistic regression curve was fit to the data points using the following equation: RSNA = $\frac{A}{1+\exp\,[B(MAP-C)]} + D,$ where A is the RSNA range, B is the slope coefficient, C is the pressure at the midpoint of the range (BP50), and D is the minimum RSNA. The peak slope (or maximum gain) was determined by taking the first derivative of the baroreflex curve and was calculated with the equation: Gain max = A(1) × A(2) × [1/4], where A(1) is the range and A(2) is the average slope. The mean values for each curve parameter were used to derive composite curves for each experimental group.

Metabolic cage study

In experiments where drinking and urine responses were measured, mice were housed individually in metabolic cages (Harvard Apparatus, Holliston, MA). Food and water were accessible *ad libitum* and all the mice were allowed to adapt to the metabolic cages for 4 days before data collection. 24-hour daily water intake and urine output were recorded and urine samples were collected under a layer of mineral oil for NE analysis.

Norepinephrine measurement

Urinary NE was measured using a Norepinephrine Enzyme-Linked Immunosorbant Assay (ELISA) kit (Labor Diagnostika Nord KG, Nordhorn, Germany). A 50-µl urine sample was diluted with 950 µl double-distilled H_2O to obtain a 20:1 diluted sample, from which 10 µl was used for NE measurements based on the instructions provided by the company. Duplicate measurements were made for each sample. 24-hour NE excretion was calculated from 24-hour urine volume multiplied by NE concentration.

Plasma NE was measured after the blood was collected by cardiac puncture following an acute terminal experiment. Under 2% isoflurane anesthesia, the heart was exposed via a thoracotomy by removing the ventral segment of the 3rd to 6th ribs together with the sternum. A 21G needle connected to 1 mL syringe was inserted into the left ventricle. Blood was withdrawn slowly and transferred into a 1.5 mL Eppendorf tube containing 10% K^+ EDTA (10 µl). Blood was centrifuged at 1000×*g* for 10 min at 4 °C. We were able to reliably obtain ~1 mL blood which resulted in ~500 µL of plasma, from which 300 µL was used to measure the NE concentration using the same ELISA kit as mentioned above.

Cell culture

A mouse neural crest-derived cell line Neuro-2A (N2A) cells (CCL-131, American Type Culture Collection) were cultured in DMEM media supplemented with 10% fetal bovine serum (FBS) and 1% penicillin/streptomycin. Cells were seeded onto 6-well culture plates at a density of 1×10^5 cells/well for western blot studies. N2A cells were kept in a humidified incubator maintained with 5% CO_2 at 37°C. 24 hours after cell seeding, differentiation was induced by starvation with the FBS reduced to 2% in the DMEM. Each set of cell experiments was performed in triplicate.

Western blot analysis

Primary antibodies used were Nrf2 (ab62352, R-IgG, 1/1000), Keap1 (sc-33569, R-IgG, 1/1000), NQO1 (sc-376023, M-IgG, 1/500), HO-1 (sc-10789, R-IgG, 1/200). GAPDH (sc-32233, M-IgG) or β1-actin (ab-8227, M-IgG) was served as internal loading control.

For brain tissue analysis the RVLM was punched under a microscope according to coordinates taken from Paxinos and Franklin's, the Mouse Brain in Stereotaxic Coordinates[130]. For N2A neurons, cells were detached with a cell scraper in 1 mL chilled

PBS for each well and were transferred to an Eppendoff tube. After centrifugation at 3000 rpm for 5 min at 4°C, the supernatant was discarded and the cell pellet was used. Total protein was extracted with Radioimmunoprecipitation Assay (RIPA) buffer (PI89901, Thermo Fisher Scientific) containing 1% protease inhibitor cocktail (ab201119, Abcam). Sample concentrations were measured using a protein assay kit and were adjusted by 4x sodium dodecyl sulfate sample buffer to obtain equal concentrations among samples.

Equal amount of protein samples were loaded into a 8% SDS-PAGE gel (20 μg protein per well). The fractionized protein was then subjected to electrophoresis and electrically transferred to a polyvinyl difluoride membrane. The membrane was blocked in Phosphate-buffered saline (PBS) solution containing 5% non-fat milk powder, then was probed with primary antibodies to the target protein at 4°C overnight. After incubation with primary antibodies, the blot was probed with secondary antibodies at room temperature for 1 hour. After thorough washes with PBS containing 1% Tween 20 (PBST), blot bands were visualized using an enhanced chemiluminescent system (UVP BioChemi). Bands densities were quantified with ImageJ software (NIH). The final data was expressed as band densities of the target protein divided by the loading control protein.

Immunofluorescence and laser confocal microscopy

Lenti-GFP-Cre viral-induced Nrf2 overexpression or knockout in the RVLM was confirmed using immunofluorescence staining. Mice were deeply anesthetized with sodium pentobarbital and perfused transcardially with PBS, followed by 4% paraformaldehyde in PBS. The entire brainstem was removed, mounted on a specimen stage, and sectioned into 40-μm slices in a cryostat. The slices were then washed with PBS three times and permeabilized for 30 min at room temperature with a solution containing 0.3% Triton X-100 dissolved in PBS, followed by blocking with a solution containing 10% normal goat

serum and 0.3% Triton X-100 in PBS at room temperature for 2 hours. The slices were then incubated with Nrf2 antibody (ab31163 R-IgG), in 10% normal goat serum and 0.3% Triton X-100 in PBS at 4 °C overnight. After three washes with PBS, the slices were incubated for 2 hours with secondary fluorescent antibody (Goat anti-Rabbit IgG secondary antibody, Alexa Fluor 546; Invitrogen, A-11010).

For oxidative stress immunofluorescence staining assessment, 20-μm brainstem sections containing the RVLM were cut on a cryostat. The slices were then permeabilized with 2% Triton X-100 at room temperature for 15 minutes. Following blocking with 5% bovine serum albumin (BSA), the slices were incubated with 8 hydroxy D guanosine (8-OHdG) Antibody (sc-393871, Mouse-IgM, Santa Cruz) overnight at 4°C. Slices were then incubated with secondary antibody (ab175472, Donkey-IgG, Alexa Fluor 568; Invitrogen) at room temperature for 2 hours.

Stained sections were mounted with an Aqua-Mount Mounting Medium and visualized under a laser confocal microscope (Leica TSC STED). Staining intensities were quantified with ImageJ software.

Statistics

For cell experiments with one affecting factor, data were analyzed by a one-way ANOVA followed by Tukey's multiple comparisons test. For other data with two affecting factors, a two-way ANOVA followed by Tukey's multiple comparisons test was used to analyze the differences among multiple groups. All data were analyzed using Prism 8 (GraphPad Software, San Diego, CA) and were expressed as mean ± SE. Differences were considered statistically significant at a p value of <0.05.

Chapter IV. Effects of Nrf2 Over-expression in the RVLM on SNA in Mice with CHF

Introduction

As a hallmark of CHF, sympatho-excitation not only exacerbates the failing heart, but also undermines peripheral organ function. Although mainstream therapeutic strategies for this syndrome including β1 adrenergic-blockers, ACEI and ARBs have all been demonstrated to ameliorate symptoms and improve disease prognosis, sympathetic outflow is still increased. Moreover, side effects such as increased risk of withdrawal syndrome with long-term use of β1-blockers or kidney failure with the use of ACEIs are concerned in these medications [131]. Therefore, exploring the central mechanisms of sympatho-excitation appears to be critical to uncover novel therapeutic targets for CHF.

The RVLM functions as a prime SNA outflow center where pre-sympathetic neurons project to the spinal cord. Pathological changes in this area are associated with sympatho-excitation in CHF. Pre-sympathetic neurons arise from the RVLM and send a monosynaptic projection to the IML of the spinal cord [132]. Studies from our laboratory showed that reducing oxidative stress in the RVLM either by oral administration of the 3-Hydroxy-3-methylglutaryl coenzyme A reductase inhibitor, simvastatin [133], or by chronic exercise training[134], could ameliorate sympatho-excitation in CHF in rabbits.

Increased oxidative stress in the RVLM contributes to sympatho-excitation[88]. At the cellular level, oxygen radicals are primarily produced by mitochondria[135] and NOX [136]. These ROS are then scavenged by both enzymatic and non-enzymatic mechanisms[137]. In the RVLM of CHF rabbits, we found that the expression and activity of NOX2 subunits were upregulated[88] whereas SODs, were downregulated[134], suggesting that the increased ROS in the setting of CHF may be a result of enhanced pro-oxidant processes and reduced anti-oxidant defenses. We previously demonstrated the upregulation of NOX in the RVLM of CHF is attributed to enhanced AngII signaling[88]. However, the

mechanisms underlying downregulation of SODs as well as other antioxidant enzymes remain to be elucidated.

As mentioned in the Introduction in Chapter I, the Nrf2/Keap1 complex plays a critical role in the redox-sensitive transcriptional regulatory system. Keap1 functions as a sensor of ROS and electrophiles, whereas Nrf2 serves as an effector for the coordinated activation of cytoprotective genes including a battery of antioxidant enzymes[138]. In the RVLM, this system is an important factor in maintaining normal sympathetic tone and BP in conscious mice[120]. However, the role of RVLM Nrf2 modulation on SNA in CHF has not been elucidated. Therefore, in this Chapter, we tested the hypothesis that overexpression of Nrf2 in the RVLM contributes to reduced oxidative stress, upregulation of anti-oxidant defenses, resulting in a reduction in SNA in the CHF state.

Experimental Protocol

In this experiment, male and female C57BL/6 mice aged between 10 and 12 weeks were used. In the initial (first six animals) experiments, we were not able to observe differences in infarct size or responses to overexpression of Nrf in males and famales, therefore the remainder of the animals were males. In one set of experiments, wild type mice received viral vectors encoding for Nrf2 protein or GFP as a viral control; in another set of experiments, an alterative strategy of upregulating Nrf2 was employed through Keap1 deletion via administering Cre lentivirus in $Keap1^{f/f}$ mice. In these $Keap1^{f/f}$ mice, we assessed their baseline RSNA as well as plasma NE to further address our hypothesis. The general animal study design is shown in Fig 4.1.

Heart failure model was created by permanent left coronary artery ligation, as described above. The sham group underwent a similar procedure without coronary artery ligation. At

the fourth week post surgery, cardiac function was evaluated by echocardiography (Vevo 3100, FUJIFILM VisualSonics). Infarct size was calculated as percentage of LV size using ImageJ softwear. One week after echocardiography, mice underwent procedures where viral-vectors containing either the Nrf2 gene (20 nl HIV-CamKIIa-eGFP-Nrf2 at 1.3×10^8 TU/mL) or Cre recombinase gene (20 nl lentiviral-Cre-GFP at 1×10^8 TU/mL) were delivered into RVLM of wild type or Keap1$^{f/f}$ mice, respectively to upregulate Nrf2. Fig 4.2 illustrates the generation of Keap1 knockout mice. Two weeks after viral injection, the mice were implanted with radiotelemetry units and left to recover for three weeks postoperatively. BP and HR were then recorded for 48 hours continuously. During conscious BP recording, mice were placed in a metabolic cage and a timed urine sample was collected. Spontaneous as well as induced baroreflex sensitivity were evaluated as per the methods above.

Under anesthesia, baseline BP, HR, and renal SNA were recorded and arterial baroreflex sensitivity was analyzed. Mice were then euthanized by 13% KCl and the maximum RSNA was obtained within 1–2 min. Background noise was recorded approximately 15–20 min after death. Baseline RSNA was determined as the percent of maximum RSNA activity after the background noise was subtracted (Fig 4.3)[139].

Blood from Keap1$^{f/f}$ mice was collected following the terminal acute experiment. The urine and plasma were used for NE analysis. For each mouse the brain stem was removed and the RVLM punched for western blot analysis or immunofluorescence staining.

All data are expressed as mean ± SE. A two-way repeated measures ANOVA and the Student-Newman-Keuls test was used for analyzing the differences among the four groups, with the aid of SigmaPlot software. A p value of <0.05 was taken as indicative of statistical significance.

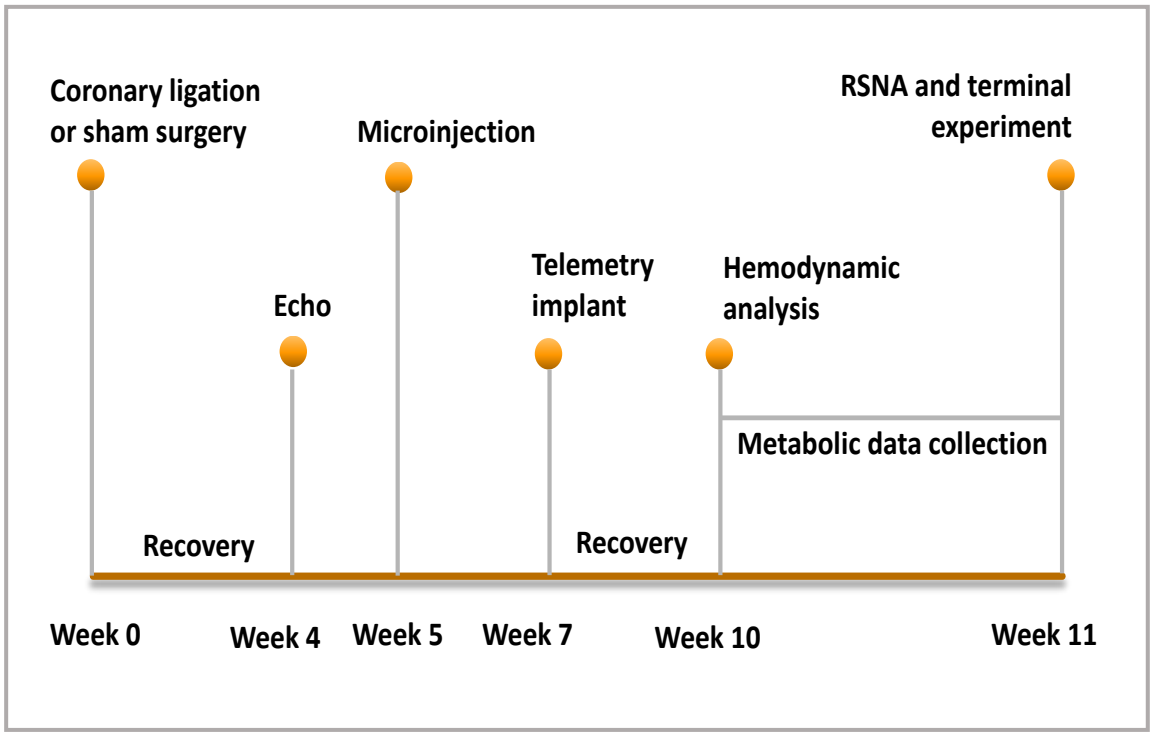

Figure 4. 1 Schematic of animal study design

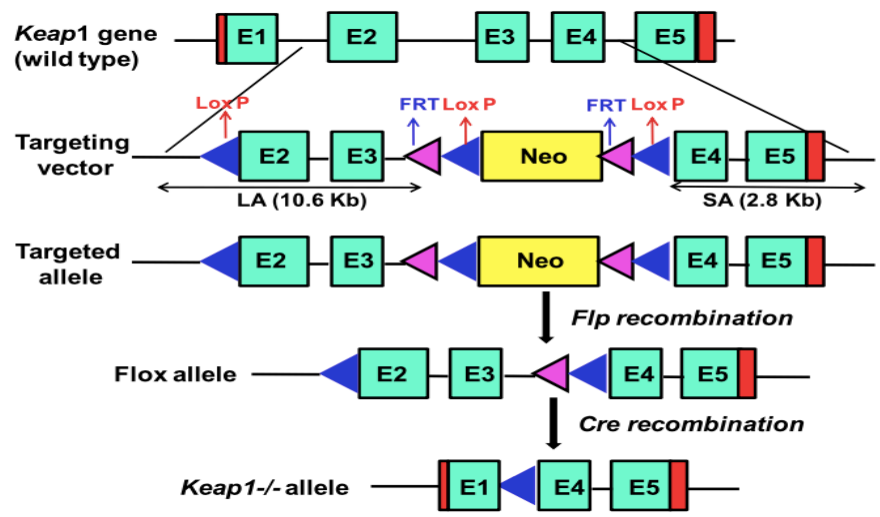

Kong, Thimmulappa, Craciun, et al. from [1]

Figure 4. 2 Generation of Keap1 knockout mice.

Schematic representation of Keap1 gene targeting vector for tissue-specific deletion of Exons 2 and 3 by the insertion of two loxP sites flanking Exons 2 and 3, respectively. LA, long arm; SA, short arm.

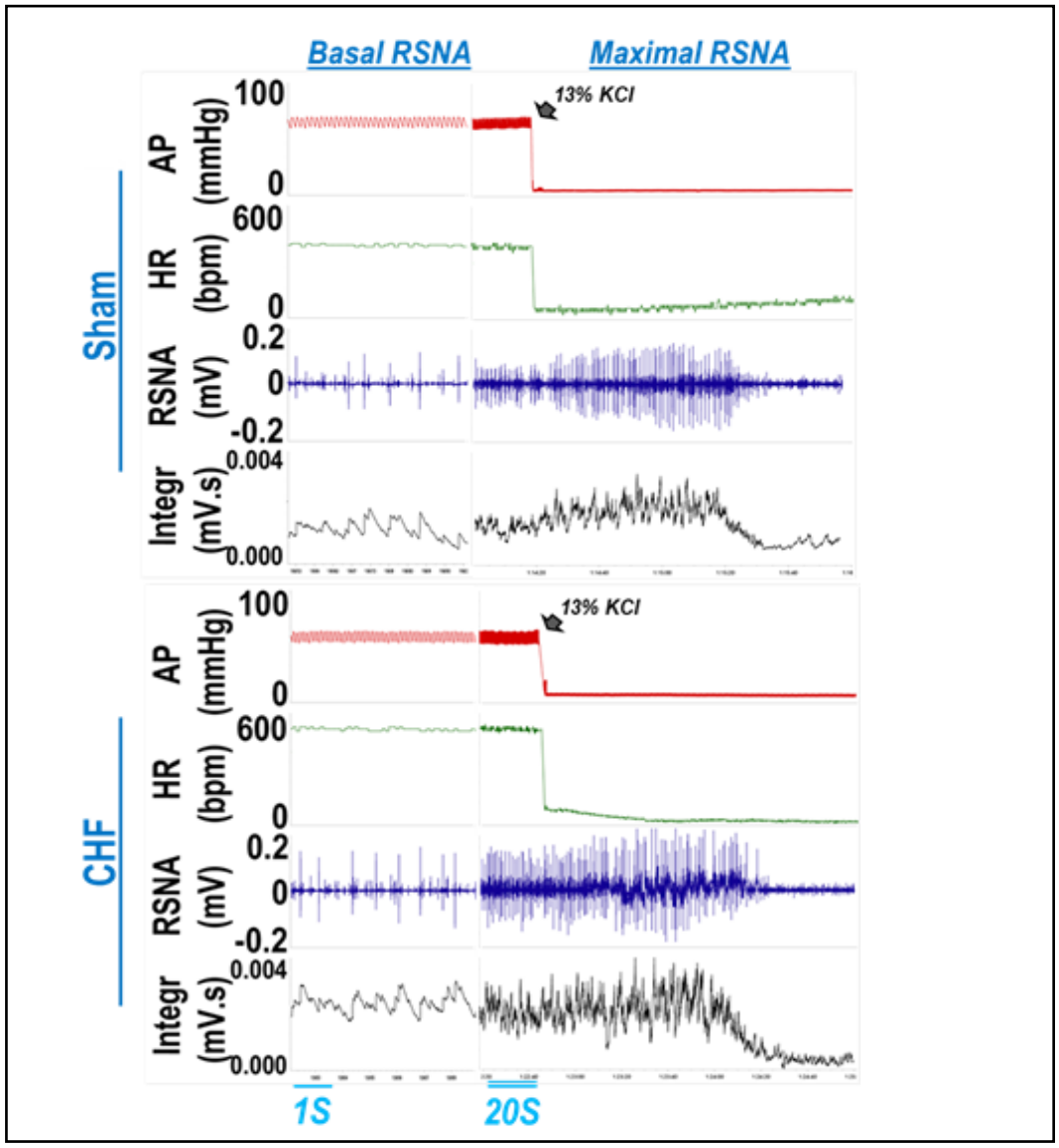

Figure 4. 3 Representative tracing of RSNA recording.

Tracings of AP (red), HR (green), raw RSNA (blue), and integrated RSNA (black). As the final step of the experiment, 13% KCl was given at the break line (black arrow), and the maximal RSNA discharge was recorded about one to two minutes after KCl was given. Nerve activity was expressed as a percent of maximum after subtraction of noise. Top: Sham animal; Bottom: CHF mouse animals.

Results

Evaluation of CHF model

Four weeks after surgery, the CHF mice exhibited severe heart failure with EF approximately 35% as shown in Table 4.1. The weight of infarcted hearts were doubled compared to the sham hearts (CHF-GFP 0.25 ± 0.07 vs. Sham-GFP 0.14 ± 0.01, $p<0.01$). The septal and right ventricular free wall were profoundly thickened, whereas the left ventricular free wall became paper thin and dilated. Fig 4.4B shows the M-mode and long axis 2D echocardiograms, which confirmed the severity of impaired cardiac functions of the infarcted hearts with significantly decreased EF and dp/dtmax. In Table 4.1, grouped data of cardiac function in four groups are shown. No significant differences were found between CHF-Nrf2 and CHF-GFP mice in these parameters.

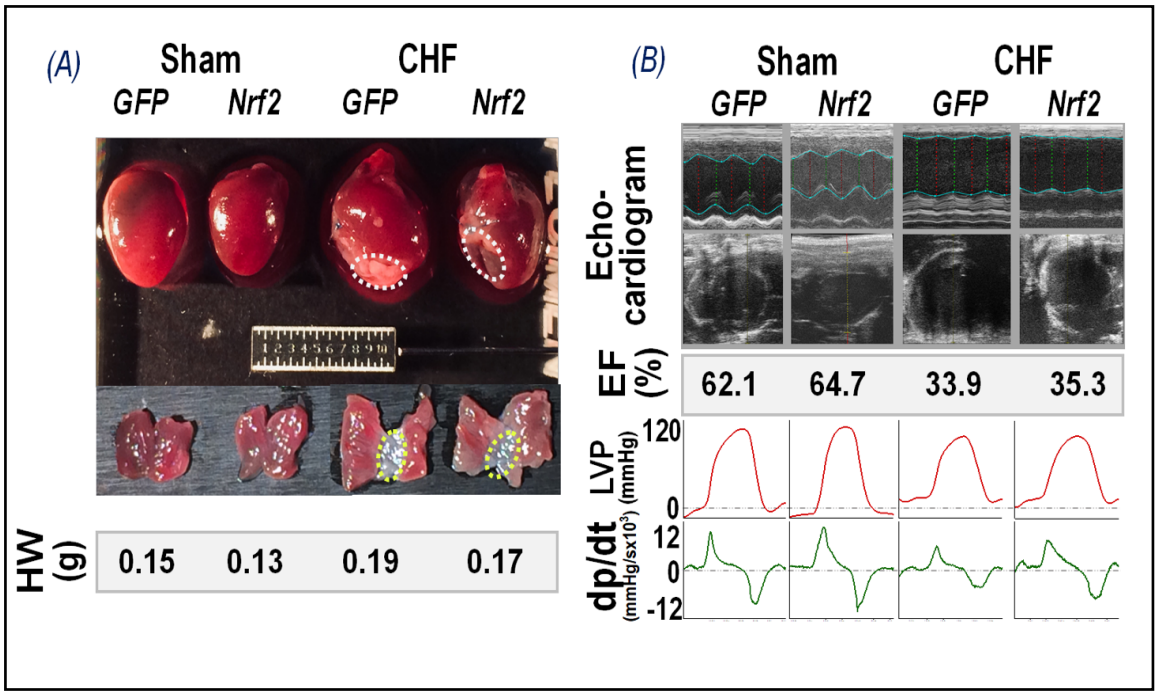

Figure 4. 4 Assessment of CHF model.

A. Appearance of the whole heart and infarcts showing enlarged left ventricle (LV) in CHF-GFP, which seems to be attenuated by Nrf2 overexpression. B. Echocardiograms and hemodynamic measurements in Sham and MI hearts treated with RVLM lenti-GFP or Nrf2. MI: myocardial infarction. HW: heart weight. EF: ejection fraction.

Table 4.1 Anatomic, hemodynamic, and echocardiographic measurements associated with failing hearts.

	Sham-GFP	Sham-Nrf2	CHF-GFP	CHF-Nrf2
Animal No.	13	13	14	14
Heart Weight, g	0.14 ± 0.01	0.16 ± 0.02	0.25 ± 0.07**	0.23 ± 0.06@@
Infarct Size, % of LV	0	0	59.9 ± 12.4**	55.3 ± 15.8@@
Ejection Fraction, %	63.6 ± 7.4	65.1 ± 6.9	34.3 ± 5.1**	37.1 ± 4.3@@
Fractional Shortening, %	30.7 ± 6.2	33.5 ± 5.7	13.5 ± 3.1**	15.3 ± 2.2@@
LVEDP, mmHg	2.2 ± 2.4	1.9 ± 2.5	18.8 ± 9.1**	17.3 ± 8.2@@
dp/dt max, mmHg/s	12463 ± 1020	13724 ± 1052	3154 ± 655**	3298 ± 703@@
dp/dt min, - mmHg/s	13101 ± 1112	14166 ± 1281	3540 ± 721**	3719 ± 772@@

**P < 0.01 vs Sham-GFP, @@P < 0.01 vs Sham-Nrf2.

RVLM Nrf2 over-expression in CHF

Nrf2 over-expression was obtained through two alternative strategies – Nrf2 gene knock-in and Keap1 gene knock-out. For the former, Fig 4.5 shows that there is a significantly lower level of Nrf2 protein in RVLM in CHF group as compared to the Sham. A similar finding was apparent for protein of two Nrf2 target genes, NQO1 and HO-1. Nrf2 gene transfer significantly upregulated Nrf2, NQO1, and HO-1 in the RVLM of CHF mice. While there was an increase in Nrf2 expression in CHF mice, it did not rise to the level of the Sham animals. Nevertheless, it was sufficient to upregulate NQO1 and HO-1 to the Sham counterparts. In the RVLM of sham mice, although Nrf2 protein was significantly upregulated after Nrf2 gene transfer compared to GFP control, the changes in NQO1 and HO-1 did not reach statistical significance.

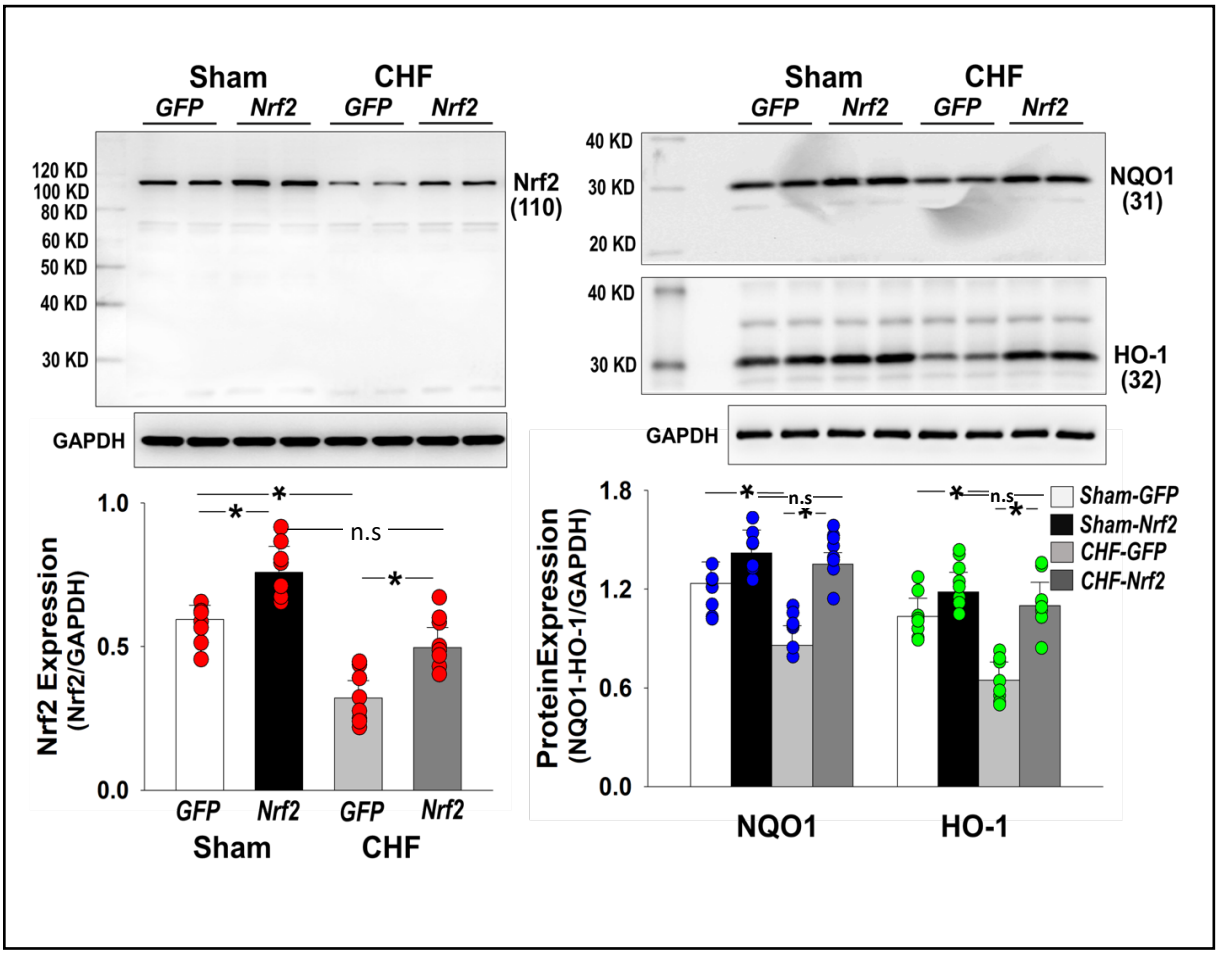

Figure 4. 5 Expression of Nrf2 and two target proteins in the RVLM of Sham and CHF mice transfected with GFP or Nrf2 viruses.

Nrf2 gene transfer significantly upregulated Nrf2 (left), NQO1, and HO-1 (right) in the RVLM of sham and CHF mice. GFP: CamKIIa-GFP-virus; Nrf2: CamKIIa-GFP-Nrf2-virus. (*P < 0.05; n = 7 in Sham-GFP and Sham-Nrf2 groups; n = 8 in CHF-GFP and CHF-Nrf2 groups). There were no differences between protein data comparing sham-Nrf2 with CHF-Nrf2.

In order to document overexpression of Nrf2 in Keap1$^{f/f}$ mice, we used immunofluorescense and western blotting to show protein abundence. Fig 4.6A demonstrates upregulation of Nrf2 confirmed by immunofluorescence, which shows that neurons that are positive for GFP (green) also express strong Nrf2 immunoreactivity (red and in merged image). Western blot for Keap1, Nrf2, NQO1 and HO1 proteins exhibits similar results (Fig 4.6B). In both sham and CHF group, delivery of Lenti-GFP-Cre virus to Keap1$^{f/f}$-*Cre* mouse led to a significantly lower Keap1 and increased Nrf2. NQO1 and HO-1 were increased following Keap1 knock-out in both sham and CHF groups.

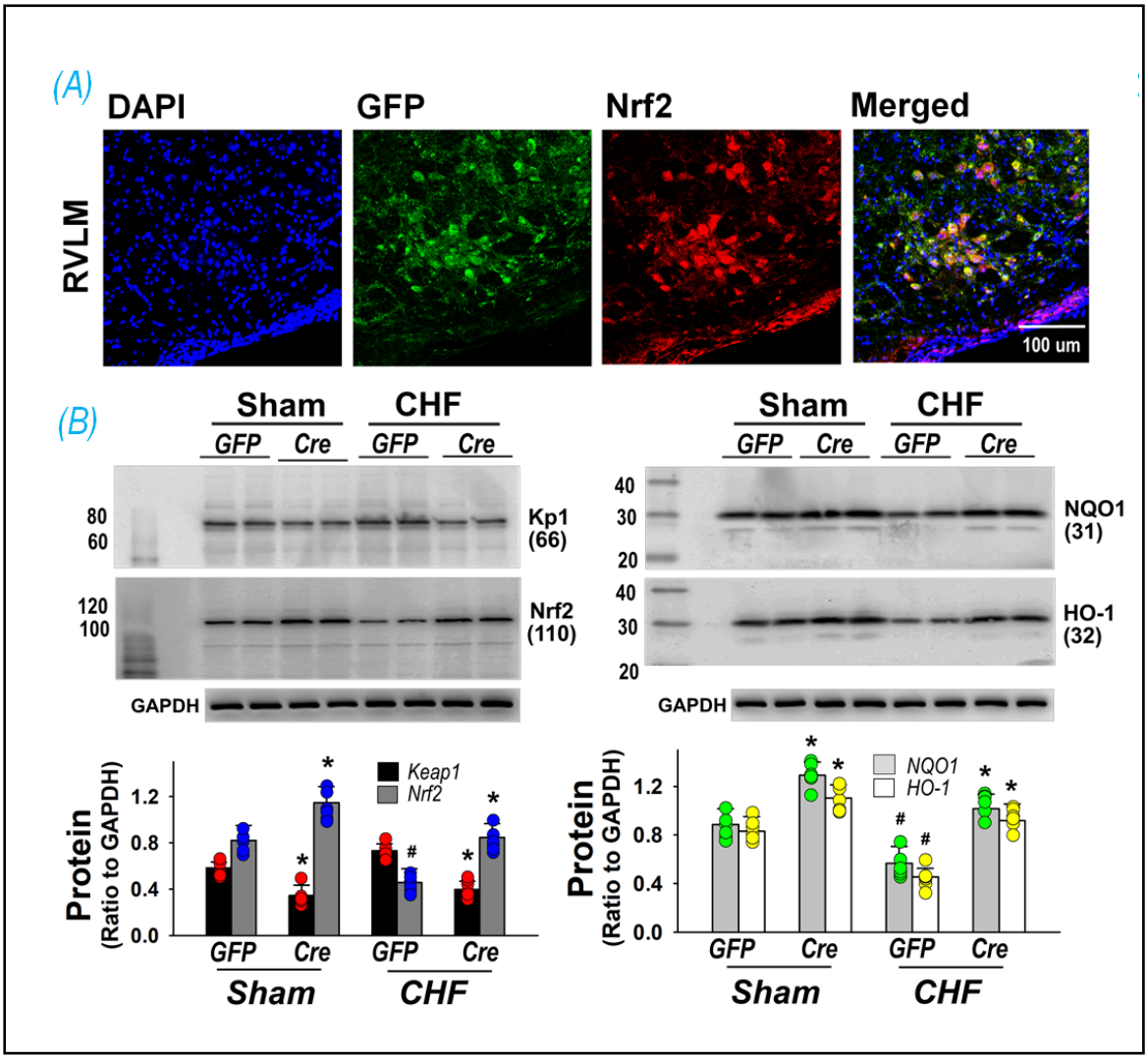

Figure 4. 6 Nrf2, Keap1, NQO1, and HO-1 expression in the RVLM of Keap1$^{f/f}$ mice following Lenti-GFP-Cre virus transfection.

(A) Immunofluorescence images of GFP expression three weeks after virus administration. (B) Western blot data for Keap1, Nrf2, NQO1 and HO1 proteins. These data confirmed effective Nrf2 upregulation by Keap1 knock-out. (*P < 0.05 vs GFP groups; # P< 0.05 vs Sham-GFP group. n= 6/group.)

Effects of RVLM Nrf2 knock-in on BP, HR, and SNA

Urinary NE excretion was assessed as an index of sympatho-excitation in order to determine if over-expression of Nrf2 in the RVLM reduces sympathetic outflow in heart failure. As shown in Fig 4.7A, both NE concentration and excretion were significantly elevated in the CHF-GFP group compared to the Sham-GFP group. Nrf2 over-expression in the CHF group significantly reduced total urinary NE excretion, suggesting that upregulating RVLM Nrf2 suppresses sympathetic outflow in CHF.

For arterial sBRS, data in Fig 4.7B demonstrates that in CHF, both up-sequence gain (1.23 ± 0.20 versus 3.71 ± 0.32 ms/mm Hg, *P < 0.05, n = 8 and 7) and down-sequence gain (0.90 ± 0.21 versus 2.87 ± 0.19 ms/mm Hg, *P < 0.05; n = 8 and 7) were significantly decreased, whereas Nrf2 over-expression restored the BRS (up-sequence gain: 2.45 ± 0.31 ms/mm Hg, down-sequence gain: 2.30 ± 0.32 ms/mm Hg; †P < 0.05 vs CHF-GFP, n = 8 for each group).

We also evaluated the induced BRS by measuring hemodynamic responses to i.p. injection of phenylephrine. Fig 4.7C shows that there were no differences in BP changes among these four groups (upper panel), however, the decline in HR (lower panel) was significantly reduced in the CHF state, reflecting a diminished BRS. Again, an improved BRS was seen in the RVLM Nrf2 over-expression group of CHF mice. Together, these data indicate that RVLM Nrf2 over-expression improves both spontaneous- and induced-BRS in conscious CHF mice.

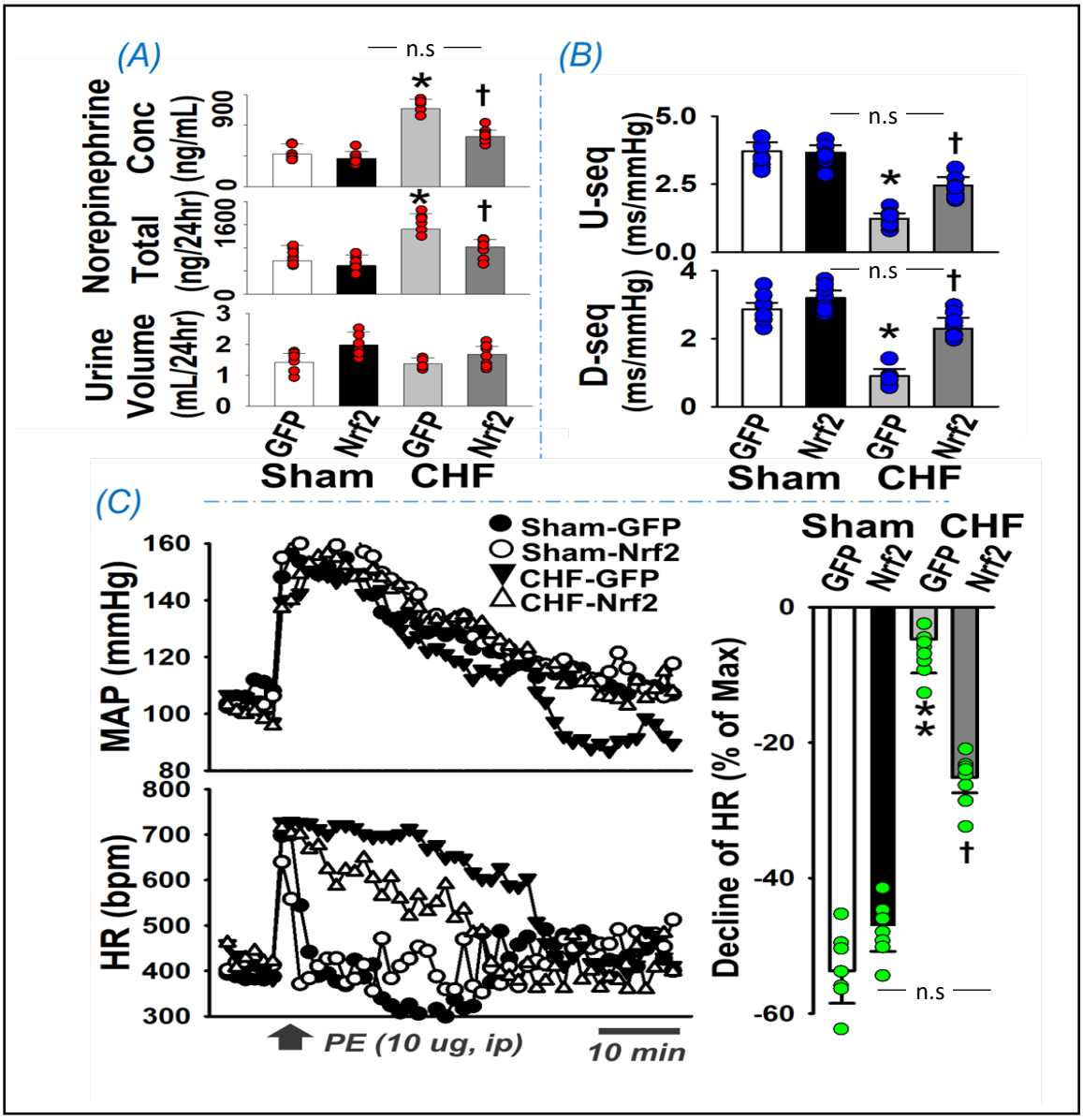

Figure 4. 7 Sympathetic outflow and cardiovascular regulation in conscious mice.

(A) Urinary NE; (B) Spontaneous Baroreflex Sensitivity; (C) Induced Baroreflex Sensitivity. Left panel in (C) is a representative tracing of MAP and HR of one mouse after ip PE; Right panel in (C) is mean data showing the percent decline of HR following PE induced increase in BP. (*P < 0.05 and **P < 0.01 vs Sham-GFP; †P < 0.05 vs CHF-GFP. n = 7, 7, 8, and 8 in Sham-GFP, Sham-Nrf2, CHF-GFP, and CHF-Nrf2 groups.)

Effects of Nrf2 overexpression in RVLM on RSNA and baroreflex in the anesthetized state

Direct measurement of RSNA is difficult to directly record in conscious mice. Therefore, we adopted methods of SNA recording in the anesthesia state. Figure 4.8A shows original tracings of basal RSNA as well as RSNA responses to PE-induced HTN (baroreflex). These recordings demonstrate an increased baseline neural discharge and a blunted sympatho-inhibitory response during HTN in CHF-GFP treated as compared to Sham-GFP treated mice. Mice treated with Nrf2 virus exhibited a restored sympatho-inhibitory response in CHF. Figure 4.8B displays the mean data for basal RSNA frequency, integrated nerve activity, and normalized nerve activity. All three parameters were found to be higher in the CHF-GFP treated group compared to the Sham-GFP group. In CHF mice, these parameters were reduced in the Nrf2 overexpression group. The composite baroreflex curves/gains (Figure 4.8C, top) and four parameters of reflex sensitivity (bottom) are shown. The maximal gain, average slope and range of RSNA response were significantly decreased, whereas the BP50 and minimum RSNA were significantly higher in the CHF-GFP group compared with the Sham-GFP group. Nrf2 over-expression in CHF mice significantly reduced these parameters.

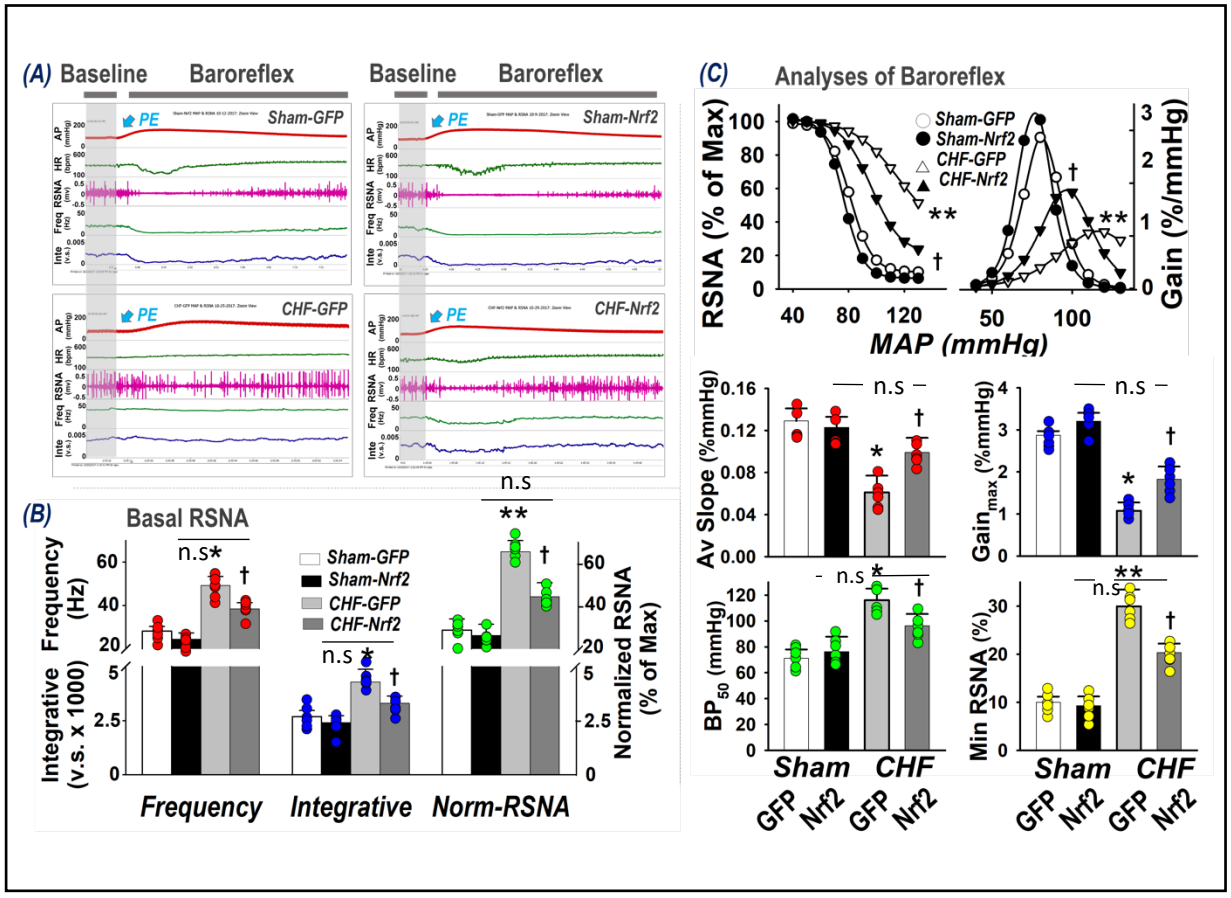

Figure 4. 8 Renal sympathetic nerve activity and baroreflex sensitivity under

(A) Original recording; (B) Analysis of basal sympathetic nerve activity; (C) Baroreflex curves and curve parameters. PE: Phenylephrine. *P < 0.05 and **P < 0.01 vs Sham-GFP; †P < 0.05 vs CHF-GFP. n = 6.

Effects of Keap1 knock-out in RVLM on RSNA

Since the RVLM Keap1 knock-out showed a significant increase in Nrf2, NQO-1, and HO-1 in CHF mice, we determined their basal RSNA and plasma NE to evaluate these physiological effects. As shown in Fig 4.9A, RSNA in CHF-Keap1$^{f/f}$-GFP mice was markedly higher as compared to Sham-Keap1$^{f/f}$-GFP group. Similar to the results seen for direct Nrf2 virus knock-in animals, indirect upregulation of Nrf2 in the CHF-Keap1$^{f/f}$-Cre mice, the basal RSNA in CHF was attenuated compared to CHF-Keap1$^{f/f}$-GFP group. Similar to direct Nrf2 knock-in, Keap1 knock-out did not alter baseline RSNA in sham animals. Similar patterns were observed for plasma NE concentration between each group (Fig 4.9B). Together with the Nrf2 knock-in data above, these results strongly indicate that manipulating Nrf2 has a direct impact on sympatho-excitation in the CHF state.

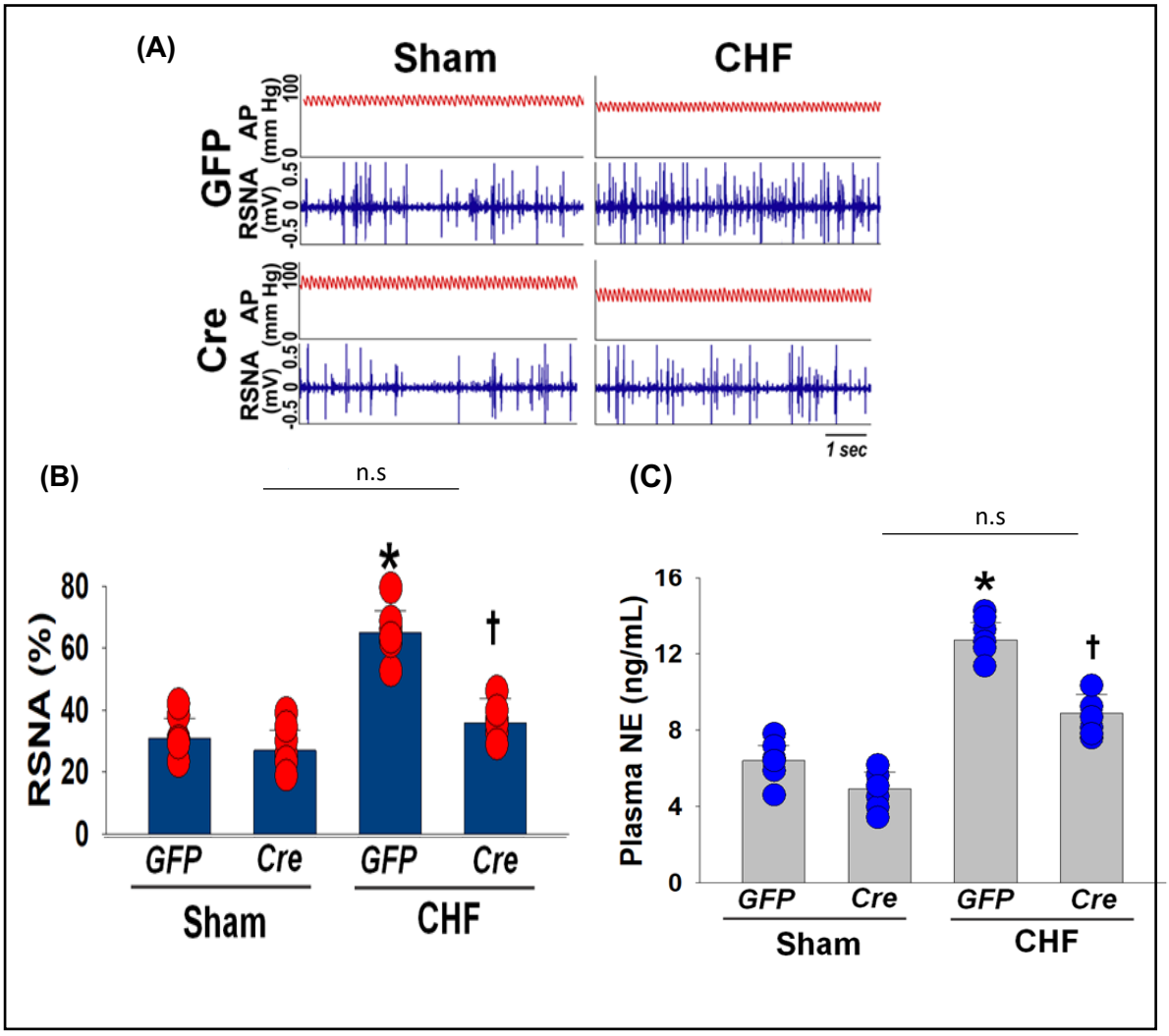

Figure 4. 9 Basal RSNA and plasma NE concentration in CHF-Keap1$^{f/f}$-GFP mice.

(A). RSNA recording (upper) and mean data (lower) show a higher basal RSNA in CHF-Keap1$^{f/f}$-GFP mice as compared with Sham-Keap1$^{f/f}$-GFP; the increased basal RSNA was ameliorated in CHF-Keap1$^{f/f}$-Cre mice. (B). The increased plasma NE concentration in CHF-Keap1$^{f/f}$-GFP mice was restored after Keap1$^{f/f}$-Cre treatment. *P<0.05 vs GFP groups; †P<0.05 vs CHF-GFP. n = 6.

Discussion

CHF are characterized by increased SNA. In early stage CHF, sympatho-excitation is an important compensatory mechanism in maintaining hemodynamic stability in response to impaired cardiac function. However, long-lasting sympatho-excitation eventually leads to a vicious cycle and contributes to the progression of HF. Current therapeutic strategies for CHF including ACEIs and β-adrenergic antagonists mainly focus on the peripheral sympathetic regulation, and their potential adverse effects may contribute to the worsening of this condition. For example, β adrergic-blockade protects myocytes but leaves the α-receptor vulnerable to sympathetic stimulation and may result in vasoconstriction and reduced tissue perfusion. Since the augmented sympathetic tone in the CHF state originates centrally, this study aimed to elucidate one potential mechanism of sympatho-excitation in the CNS in CHF to provide further evidence for a potential novel central therapy, perhaps by targeting central delivery via nanoparticles or exosomes.

In this study, we adopted the widely used method of left anterior descending (LAD) coronary artery ligation to establish CHF model. While there are other methods for small animal HF models such as transverse aortic constriction (TAC), LAD ligation mimics the most severe cause of HF in humans (coronary thrombosis) resulting in MI. This model has been reliably shown to result in neurohumoral activation similar to that is seen in humans with CHF. In addition, the established correlation between infarct size and LV function made LAD ligation model more feasible in quality control [140, 141]. The TAC model on the other hand, results in pressure overload, cardiac hypertrophy and remodeling, but does not result in CHF until very late in the disease (many months)[142].

In the LAD ligation induced CHF model, we found that Nrf2 protein and two of its targets, NQO1 and HO-1, in the RVLM of CHF mice were significantly downregulated compared

to the Sham group. Upregulating Nrf2 by introducing an HIV-CamKIIa-eGFP-Nrf2 virus into the RVLM of C57BL/6, or by introducing lentiviral-Cre-GFP in Keap1$^{f/f}$ mice significantly restored the decreased Nrf2, NQO1, and HO-1 in CHF mice. Upregulation of Nrf2 also improved arterial baroreflex function, lowered plasma and urinary excretion of NE, and reduced RSNA. These data strongly suggest that an impaired antioxidant defense at least partially contributes to sympatho-excitation in CHF, and upregulation of Nrf2 can ameliorate the increased SNA. Therefore, enhancement of antioxidant mechanisms in the RVLM may be a potential strategy in treating or preventing diseases like CHF and HTN.

The relative lack of statistically significant restoration of cardiac function (EF, FS) in the CHF mice after Nrf2 overexpression was not surprising due to the severe and large MI created in this model. In general, mouse MI models result in infarct sizes too large to reverse cardiac dysfunction following most interventions. This is an intrinsic limilation of the mouse MI model. A reduction in RSNA in this model may benefit the peripheral vasculature more than the myocardium. To minimize this limitation, one needs to evaluate modulation of Nrf2 in other models of CHF.

The lack of complete normalization of Nrf2 protein following Keap1 knockdown in CHF animals is not clear. However, this is not surprising given the lower level of Nrf2 expression seen in the CHF group and the likelihood that there are other factors that regulate NQO1 and HO-1 in addition to Nrf2 (e.g. proteosomal degradation).

In a previous study we showed that selective deletion of Nrf2 and the consequent enhancement of oxidative stress in the RVLM lead to sympatho-excitation and HTN [120]. This suggests that redox homeostasis is essential for normal function of sympathetic networks. It has been shown that enhanced oxidative stress and reduced antioxidant

defense in the RVLM are responsible for sympatho-excitation in both CHF [143] and HTN [144]. While we did not exam all antioxidant proteins, NQO1 and HO-1 were markedly downregulated in the RVLM in CHF. The underlying mechanisms for this downregulation are not clear. In this study, we found that Nrf2 expression in the RVLM of CHF mice was significantly lower than that in Sham mice, suggesting that the dysfunctional transcription of antioxidant enzyme genes may be responsible for the impaired antioxidant defense. Using two methods we showed that upregulating RVLM Nrf2 through gene transfer restores impaired baroreflex sensitivity which is characterized by sympatho-excitation. These findings are also consistent with studies from other groups where a downregulation of Nrf2 protein in the PVN in the SHR was observed [145]. In these studies, investigators administered a selective Nrf2 activator, tert-butylhydroquinone (tBHQ), and found that both BP and SNA were significantly reduced.

The cellular mechanisms by which over-expression of Nrf2 alters RVLM neuronal activity in mice with CHF is still unknown. The pre-sympathetic neurons in the RVLM are categorized as C1 or non-C1 groups based on the expression of phenylethanolamine N-methyltransferase (PNMT), and both groups utilize glutamate as the primary excitatory neurotransmitter [146] and can be targeted by a CAMKIIa vector. In a recent study it was reported that in mice, optogenetic activation of C1 cells alone results in a decrease in BP, but when C1 and non-C1 cells were stimulated simultaneously, BP was markedly increased [147], suggesting different functions of C1 and non-C1 cells in the RVLM. In this study because of the use of HIV-CamKIIa-GFP-Nrf2 vector, we were not able to distinguish between these two cell types. We assume that upregulation of Nrf2 in all glutamatergic neurons in the RVLM contributes to the amelioration of sympathetic dysfunction. The findings from the Keap1$^{f/f}$ mouse model indicate that overexpressing Nrf2 in a more widespread manner in the RVLM, including neurons and non-neuronal cells,

also contributes to the suppression of SNA in CHF, suggesting a global oxidative stress in the RVLM. Increased ROS can remarkably impact neurons and glial cells by direct oxidation of lipids, proteins, and DNA as well as the induction of mitochondrial injury [148]. By oxidative modification of potassium channels [149], the excitability of neuronal cells is increased while pro-inflammatory cytokines are released from activated glial cells [150]. In addition, Nrf2 also plays a critical anti-inflammatory role in the cross-talk between Nrf2 and NF-κB, through competing for binding to CBP (CREB-binding protein) thus depriving its interaction with NF-κB thereby decreasing pro-inflammatory activity[118]. All these mechanisms may underly the dysfunction in the RVLM in the CHF state.

It is possible there may have been sex differences in the responses to overexpression of Nrf2 and sympathoinhibition as human studies have shown these gender differences[151]. However, our initial studies did not show major differences in the effect of RVLM Nrf2 on SNA. In addition, our Keap1$^{f/f}$ mouse line produced slightly more males than females, therefore there were more males in this study. For a more thourough exploration of sex differences, future studies need to be done with more female animals included and a separate analysis done.

In summary, data from this study suggest that enhanced oxidative stress in the RVLM in CHF may be attributed to reduced transcriptional regulation of antioxidant genes, thus resulting in sympathetic overactivity. Furthermore, upregulating antioxidant enzyme expression through the Nrf2-Keap1 pathway in the RVLM may be a potential new therapeutic strategy to improve autonomic regulation in CHF. While we investigated the RVLM, our data does not rule out important contributions from other autonomic areas in the medulla and hypothalamus.

Chapter V. Effects of ACE2 over-expression in the Brain on Pressor and Metabolic Responses to Central AngII

Introduction

HTN is one of the most common causes of morbidity and mortality, worldwide. Essential HTN is characterized, in part, by activation of the RAAS and SNA [152]. There is a consensus that much of what is called “essential” HTN has a neurogenic component [153]. The circulating and central RAAS alter autonomic function and it is well accepted that central AngII increases AP by activating SNA and vasopressin secretion indicating the primacy of central alterations in the response to AngII [154]. The areas of the CNS that regulate cardiovascular function and sympathetic function are, to a large degree, centered around the RVLM and integrative areas of the brain stem such as the hypothalamus, the organum vasculosum of the lamina terminalis and the NTS, among others. Alterations in the function of these centers have been shown to play a critical role in CVD [155]. Through activation of AT1R, AngII activates several downstream signals to elicit enhanced sympathetic activation and pressor effects [156].

The ACE homolog ACE2 is a carboxy peptidase that cleaves the terminal phenylalanine from AngII to form Ang1-7. This metabolite is an important component of the RAS system, the so-called “good arm of the RAAS” [65, 157]. In previous work from this laboratory we have shown that rabbits with CHF exhibit increased ACE and decreased ACE2 in several central nuclei including the RVLM, the PVN and the NTS [101]. We also demonstrated that SNA was significantly reduced in CHF mice that overexpress ACE2 in the brain[68]. Similarly, in HTN, Sriramula et al. showed attenuation of the pressor response to peripheral infusion of AngII in mice that overexpress ACE2 in the brain. The same group also showed that peripheral AngII infusion increased oxidative stress in the PVN and RVLM significantly more in ACE2 knockout mice compared to their non-transgenic littermates [75]. By over-expression of ACE2 in the RVLM, Yamazato et al. showed a

significant decrease in BP in the SHR rats [158]. However, the exact mechanisms by which central ACE2 reduces sympathetic outflow in HTN are not quite clear.

Sympatho-excitation is increased by central AngII activity, especially in the autonomic regulating areas mentioned above. Thus, it is rational to speculate that the sympatho-inhibitory effects of ACE2 is the result of decreased AngII due to the conversion to Ang 1-7. However, some studies [159] showed that in global ACE2 knockout (KO) mice, while their systolic BP was comparable to wild type mice, vasodilator function was significantly impaired. ACE2 deficiency - induced vascular dysfunction was improved by Tempol, a superoxide dismutase-mimetic. More importantly, AngII levels were not significantly different between adult ACE2 KO and WT mice. These studies suggest that ACE2 plays an important role in regulation of oxidative stress through an AngII independent pathway. Ang1-7 is the product of AngII being converted by ACE2 and has been show to possess vasodilator activity as an opposing effect to that of AngII [160]. By binding to the MasR, Ang1-7 negatively modulates AngII/AT1R–activated c-Src and its downstream targets ERK1/2 and NOX in endothelial cells[161]. Diz et al. [162] and others have provided evidence that Ang 1-7 enhances baroreflex sensitivity and exerts sympatho-inhibitory effects. Gironacci et al. showed that Ang 1-7 decreased NE release from the hypothalamus of SHR[72]. Therefore, it is plausible to presume that the anti-sympathetic effect of ACE2 may be through increased Ang1-7 converted from AngII. However, the central effect of Ang1-7 still remains controversial in terms of SNA control. Potts et al. showed that Ang 1-7 exhibits a sympatho-excitatory effect when given into the RVLM in anesthetized rabbits [69]. Silva et al. also demonstrated that injection of the MasR antagonist, A-779 in the PVN decreases RSNA in anesthetized rats, indicating a possible sympatho-excitatory quality of Ang1-7 [71]. Based on these studies, there may be another

mechanism that is not directly related to either AngII or Ang1-7 that mediates the anti-sympathetic effects of ACE2.

In order to assess the role and potential mechanism of central ACE2 in regulating BP and sympathetic overactivity, we evaluated responses of ACE2 over-expression in the mouse brain to central AngII- induced HTN.

Experimental Protocol

This experiment was performed on 3-month-old male SynhACE2$^{+/+}$ transgenic mice and their non-transgenic littermates on the C57BL6 background. The experimental design is shown in Fig 5.1 below.

All mice were instrumented with a radio telemetry unit (PA-C10; Data Sciences International Inc., Minneapolis, MN) with the catheter inserted into the left common carotid artery as described in Chapter III. Animals were allowed to recover for 1 week before hemodynamic recording. MAP and HR were measured 2 hours daily from noon to 2:00 PM. A 24-hour recording was attained each week usually on a Saturday or Sunday. Following 3 days of baseline recording, a cannula connected to a 14-day osmotic minipump (Model 1002, Alzet, Inc. Cupertino, CA) was implanted into the right lateral ventricle at a pumping rate of 0.25 ul/hour, to create a hypertensive model by chronic ICV infusion of AngII. The control group received aCSF. In order to avoid acute postoperative stress induced high BP, mice of all groups were equipped with minipumps filled with only aCSF for 1 week before switching to minipumps filled with different drugs. The protocol timeline is demonstrated below. After each group received the assigned treatment with AngII (100 ng/kg/min)[163], Ang1-7 (200 ng/kg/min) or A779 (400 ng/kg/min)[164]. These

doses are based upon previous studies and on the fact that AngII at this dose does not evoke an increase in BP when given peripherally[163].

During hemodynamic recording, mice were placed in a metabolic cage. After a 3-day adaptation, 24-hour urine samples were collected daily and saved for NE analysis. Mice were sacrificed 14 days after ICV infusion of different treatments. Brains were removed after euthanasia, some brainstem RVLM punches were used for western blot analysis, some tissue was used for immunofluorescence staining.

Results were analyzed by 2- way ANOVA for repeated measures followed by Bonferroni correction or Tukey's test for multiple comparisons. All data are expressed as mean ± SE. Statistical analysis were performed using Prism8 (GraphPad Software, Inc. San Diego, CA). Differences were considered statistically significant at a p value of <0.05.

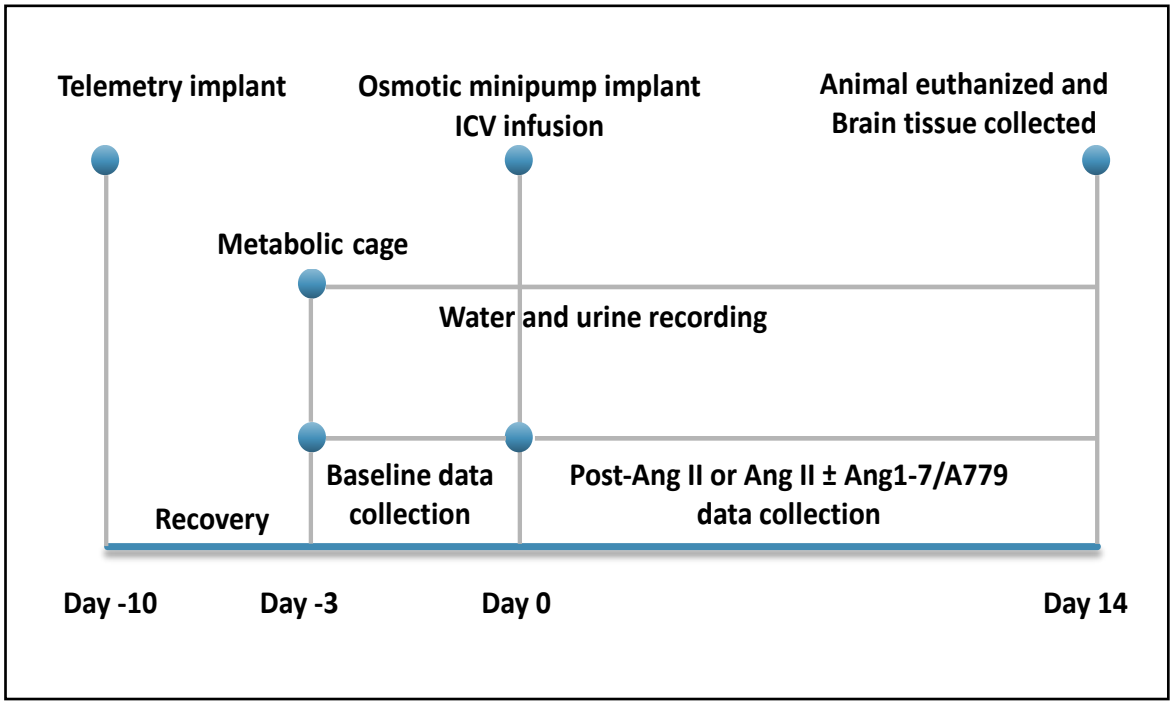

Figure 5. 1 Experimental design

Results

Central SynhACE2 attenuates ICV AngII - induced HTN

To evaluate the effect of SynhACE2 over-expression on hemodynamic changes induced by central AngII, we assessed MAP and HR over 2 weeks of ICV AngII administration in both SynhACE2$^{+/+}$ mice and their control littermates as described above. As shown in Fig 5.2A, in non-transgenic (SynhACE2$^{-/-}$) animals, chronic ICV infusion of AngII significantly increased MAP (AngII [average of post-ICV day 1-9] 126.4±2.0 mmHg vs baseline [average of 3-day recordings] 92.7±1.5 mmHg n=7, $P<0.05$) as well as compared to aCSF infusion controls (AngII [average of post-ICV day 1-9] 126.4±2.0 mmHg n=7, vs. aCSF [average of post-ICV day 1-9] 96.1±0.9 mmHg, n=5 $P<0.05$). The aCSF treated group did not show altered MAP from baseline level after treatment. ACE2 over-expression attenuated AngII-induced HTN to a level that was comparable to the vehicle treated SynhACE2$^{-/-}$ group (MAP [average of post-ICV day 1-9] of AngII/synACE2$^{+/+}$: 101.1±2.1 mmHg, n=5). There were no effects on HR in any of the treatment (Fig 5.2B).

To determine if the inhibition of the hypertensive effect of AngII in SynhACE2$^{+/+}$ animals is mediated through an enhancement of the Ang1-7/MasR pathway, we co-administered MasR blocker, A779 with AngII to SynhACE2$^{+/+}$ mice. As is shown in Fig 5.2A, the attenuated high BP due to AngII was not prevented by co-infusion of A779 in SynhACE2$^{+/+}$ animals (SynhACE2$^{+/+}$/AngII/A779 vs SynhACE2$^{+/+}$/AngII: 97.9±10.6 vs 98.7±14.2mmHg, $p>0.05$). If the conversion of AngII to Ang1-7 by overexpression ACE2 was the mediator of the inhibition of the AngII pressor response, we would assume that Ang1-7 itself would show a similar benefit. Therefore, we co-administered Ang1-7 with AngII to SynhACE2$^{-/-}$ mice failed to blunt the pressor response induced by AngII. These data suggest that MasR activation may not be the primary mechanism of ACE2 attenuating central AngII induced

HTN. We interpret the findings as indicating that the primary mechanism by which ACE2 overexpression reduces the pressor response to central AngII is through degradation of AngII, rather than increased Ang1-7. However, we do not have peptide measurements to confirm this.

The 24-hour hemodynamic data prior to and after AngII treatment are summarized in Table 5.1 and are separated by day and night averages. A circadian variability was clearly visible in both aCSF and AngII infusion groups. Fig 5.3 summarizes the day and night data of MAP and HR before and after ICV infusion. Chronic ICV AngII evoked a pressor response in both the day and night compared to aCSF in SynhACE2$^{-/-}$ mice. However, this change was markedly inhibited in SynhACE2$^{+/+}$ mice. HR also tended to rise with ICV AngII in SynhACE2$^{-/-}$ mice but not in SynhACE2$^{+/+}$ mice.

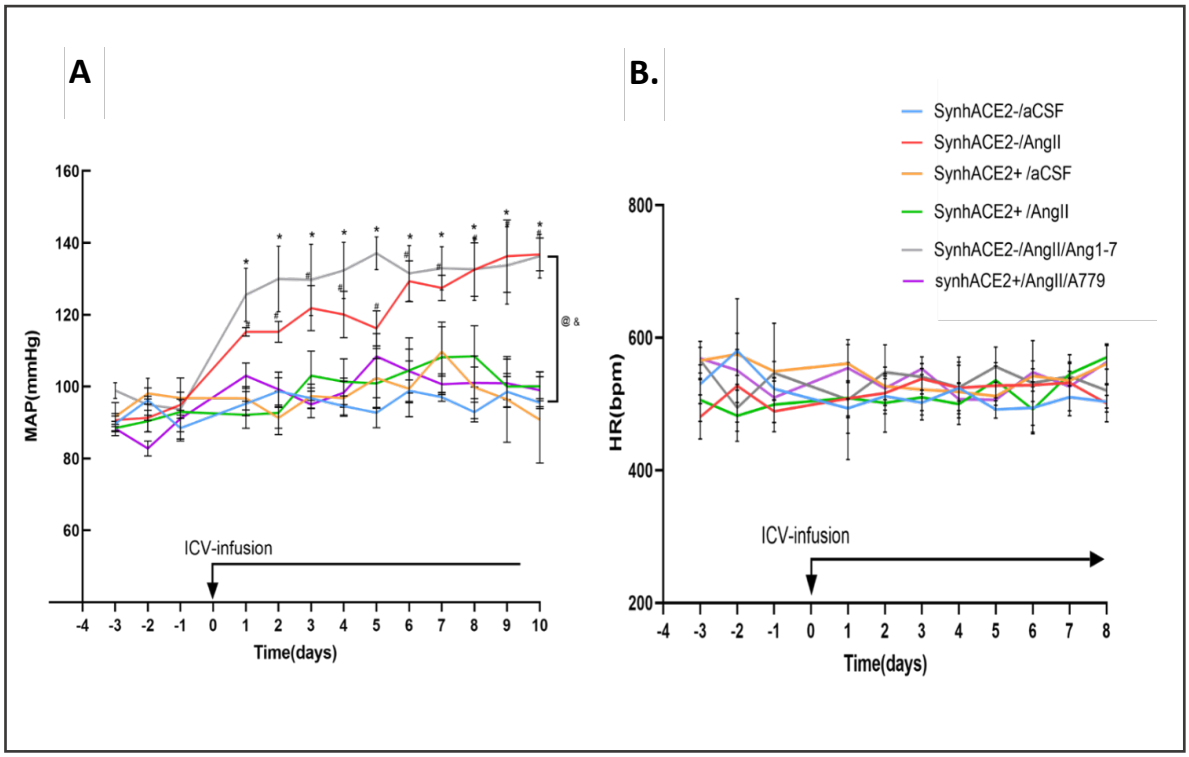

Figure 5. 2 Central SynhACE2 overexpression attenuates ICV-AngII induced BP increase.

A. Chronic ICV AngII infusion induced a progressively increased mean arterial BP in the SynhACE2-/- mice, which was completely blunted in the SynhACE2+/+ mice. Chronic ICV co-administration of AngII and Ang 1–7 in SynhACE2-/- mice did not attenuate the pressor response, nor did co-administration of AngII and Mas receptor blocker A779 in SynhACE2+/+ mice reverse the anti-hypertensive effect. Baseline BP was not altered by ACE2 over-expression. B. HR was not affected by ICV-AngII in any of the genotypes. (n=5-7; #p < 0.01 vs. SynhACE

Table 5.1 Baseline and post-infusion day-night hemodynamics

		synhACE2$^{-/-}$				SynhACE2$^{+/+}$			
		aCSF		AngII		aCSF		AngII	
		Day	Night	Day	Night	Day	Night	Day	Night
Baseline	**MAP(mmHg)**	95.1±4.2	106.6±11.8*	102.1±3.8	112.8±6.9*	91.7±4.2	103.5±2.7*	97.8±3.5	112.0± 7.1*
	HR(BPM)	525.2±99.7	510.1±156.1	474.2±140.4	479.3±159.5	559.1±170.9	578.1±164.2	533.6±101.2	583.9±124.1
Post-icv	**MAP(mmHg)**	93.4±6.8	108.2±11.8*	120.7±9.6**	127.7±12.1**	98.5±6.9	111.1±8.6	100.9±21.7#	115.3±28.1*#
	HR(BPM)	430.3±142.3	490.6±154.7	546.7±37.8	595.4±70.8	464.2±123.3	532.5±188.6	500.3±79.7	573.9±131.6

Each value is the 12 hour average of grouped data based on 24-hour BP and HR recordings. (n=5-7, *p<0.05 night time vs day time-MAP; **p<0.01 vs SynhACE2- Baseline MAP; #p<0.05 vs SynhACE2- Post AngII-infusion MAP)

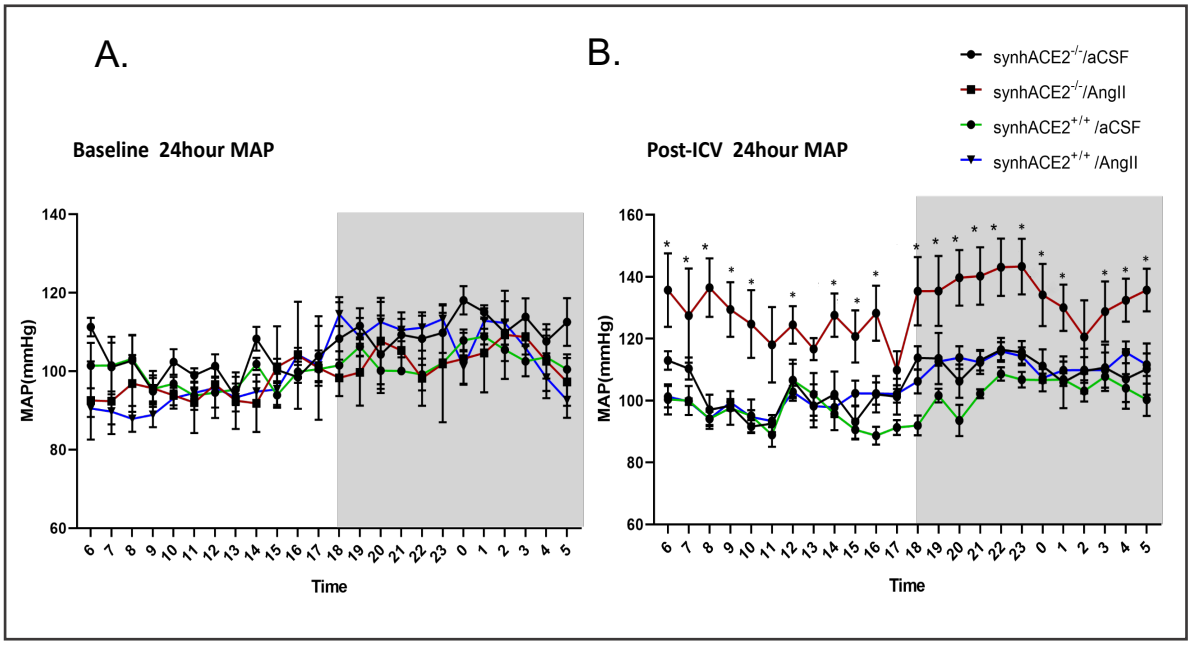

Figure 5. 3 Day-night circadian MAP before and after ICV infusion

24 hour MAP in four groups before (A) and after (B) ICV infusion of AngII or aCSF. No difference were shown between groups in the baseline blood pressure. AngII infusion significantly increased MAP compared to aCSF group. ACE2 overexpression completely blocked the increase of MAP in response to ICV-AngII(n=5, *p<0.05). SynhACE2$^{+/+}$ /aCSF group did not show significant change in MAP compared to SynhACE2$^{-/-}$/ aCSF control.

SynhACE2 attenuates central AngII induced polydipsia

AngII is well known for its ability to trigger thirst and fluid intake [165]. To assess the effect of ACE2 over-expression on central AngII - induced drinking response, we recorded daily water intake and urine output for each group of animals. Baseline daily water intake and urine generation showed no difference between animals of all genotypes. With central AngII treatment, the effect on drinking behavior is shown in Fig 5.4. In SynhACE2$^{-/-}$ animals, the peak values for daily water consumption markedly increased from a baseline of 5.6±0.2ml to 25.9±0.6 ml ($n=5$, $p<0.05$), with a significant increase in 24-hour urine excretion concomitantly from 1.6±0.3 to 13.9±1.5 ml ($n=5$, $p<0.05$). This enhancement of fluid intake started gradually after AngII infusion and was sustained during the infusion. In SynhACE2$^{+/+}$ mice however, the drinking and urine volumes in response to ICV AngII were attenuated (ΔH2O volume=10.5±2.1 ml, Δ Urine volume=6.9±1.7 ml $n=5$, $p<0.05$) compared to their non-transgenic littermates. There were no differences between SynhACE2$^{+/+}$ and SynhACE2$^{-/-}$ mice infused with aCSF infusion (ΔVolume=0.1±2.2ml, $n=5$).

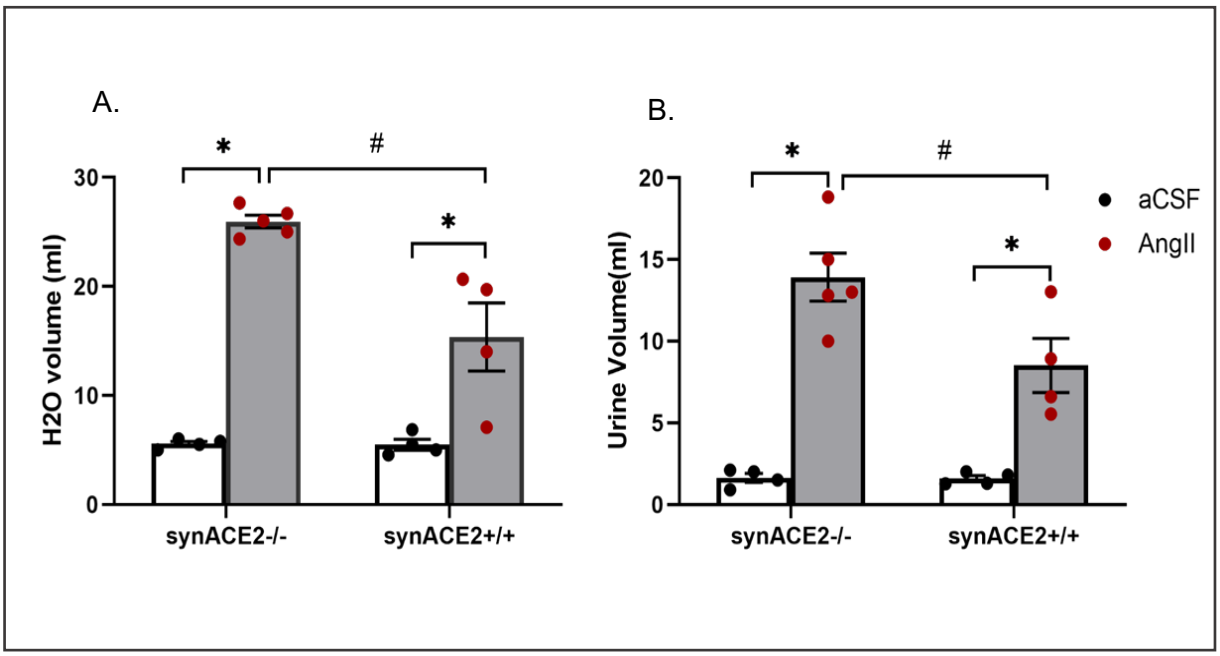

Figure 5. 4 ACE2 over-expression attenuates the enhancement of central AngII

A. Chronic AngII infusion produced an overall increased water intake during the 2-week infusion period, the response was reversed in SynhACE2$^{+/+}$ mice (n=4-5; *p < 0.05). B. The increased urine output due to central AngII was blunted in SynhACE2+/+ mice (*p < 0.05 vs. aCSF; #p < 0.05 vs. SynhACE2$^{-/-}$; n=4-5).

SynhACE2 attenuates central AngII-induced sympathetic overactivity

To determine if the anti-hypertensive ability of SynhACE2$^{+/+}$ mice in response to central AngII is due to a reduction in SNA, we measured 24-hour urinary NE excretion and evaluated HRV as indirect indicators of SNA. HRV was evaluated in the perspectives of both the time-domain, as reflected by the standard deviation of HR (SDRR), and the frequency-domain, as reflected by low-frequency (LF) to high-frequency (HF) power spectral ratio using pulsatile BP data.

Fig 5.5A shows changes of 24-hour NE excretion in each group. While baseline 24-hour NE excretion were similar between all animals, ICV AngII infusion in the SynhACE2- group markedly increased NE excretion compared to their baseline level, as well as to SynhACE2$^{+/+}$ or aCSF mice. This enhancement of NE excretion due to AngII was prevented in animals with ACE2 over-expression. However, NE excretion was not altered in SynhACE2$^{+/+}$ mice after aCSF infusion compared to baseline. Fig 5.5B and 5.5C show a clear decrease in SDRR as well as an increase in LF/HF in the AngII treated SynhACE2$^{-/-}$ group, indicating cardiac autonomic responses was skewed to an increased sympathetic activation. These changes were also normalized in mice overexpressing central ACE2. Taken together, these data suggest that selective over-expression of ACE2 in the brain can prevent the AngII induced disturbance in autonomic nervous activity reflected by increased NE excretion and decreased HRV.

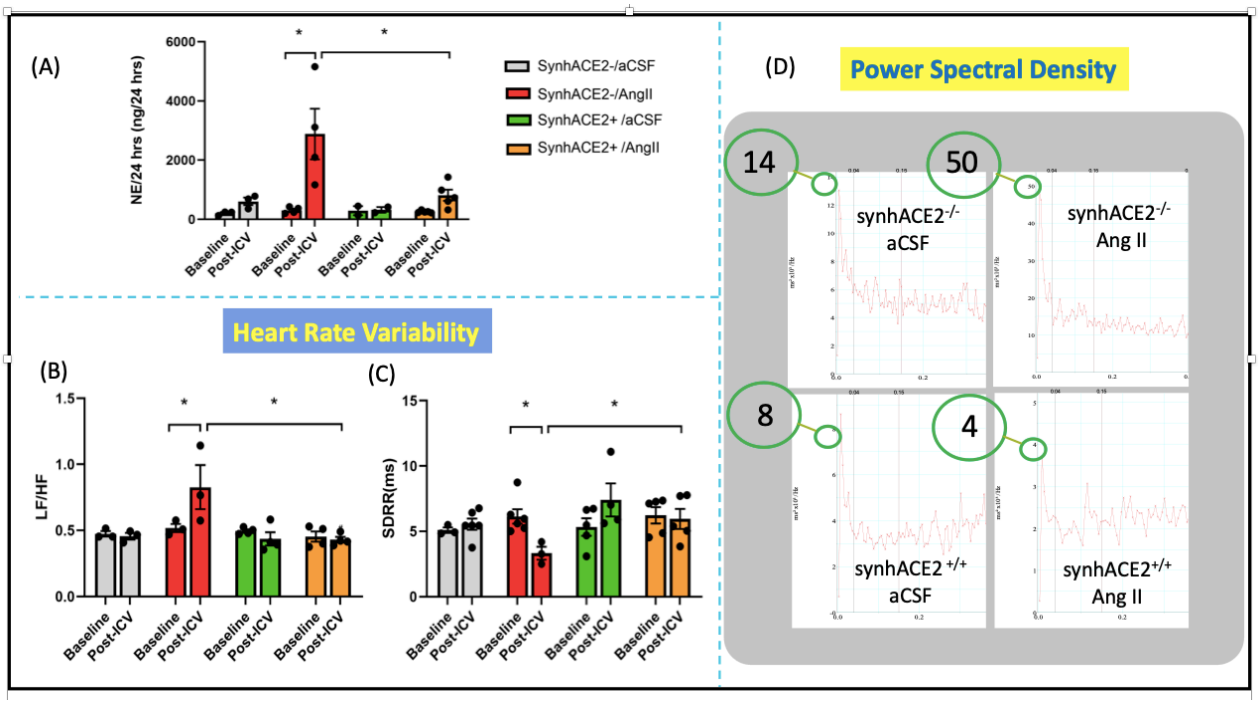

Figure 5. 5 SynhACE2+/+ attenuates central AngII- induced sympathetic hyperactivity.

A. 24h NE excretion was reduced in SynhACE2$^{+/+}$ mice. (n=4; *p < 0.01 compared to synhACE2$^{-/-}$ /aCSF post-ICV; #p < 0.05 compared to SynhACE2$^{-/-}$ /AngII post-ICV.) SDRR (B) and LF/HF (C) during baseline and post-infusion period showed ACE2 overexpression improved AngII induced HR variability impairement. (n=3-4; *p < 0.05 compared to SynhACE2$^{-/-}$ AngII-baseline; #p < 0.05 compared to SynhACE2-/- /AngII-Post-ICV)

SynhACE2 attenuates central AngII-induced oxidative stress

To determine if over-expression of ACE2 could prevent central AngII mediated ROS production, we measured oxidative stress using 8-hydroxydeoxyguanosine (8-OHdG) immunostaining of brainstem slices containing RVLM areas. ROS oxidize lipids, proteins and nucleic acids and cause cellular lesions. Since DNA is prevalent in both nuclei and mitochondria, evaluating DNA damage is widely used to assess cellular oxidative stress. 8-OHdG, is an oxidized nucleoside of DNA frequently used for such assessment. As shown in Fig 5.6, central AngII infusion markedly increased RVLM DNA oxidation in SynhACE2- animals. The enhanced immunostaining intensity was reduced in SynhACE2$^{+/+}$ mice treated with ICV AngII, to the extent comparable to that of the aCSF group. ACE2 over-expression itself did not seem to alter redox state in aCSF treated animals. Taken together, these data confirmed that central SynhACE2 over-expression effectively prevented oxidative stress in RVLM in response to ICV AngII.

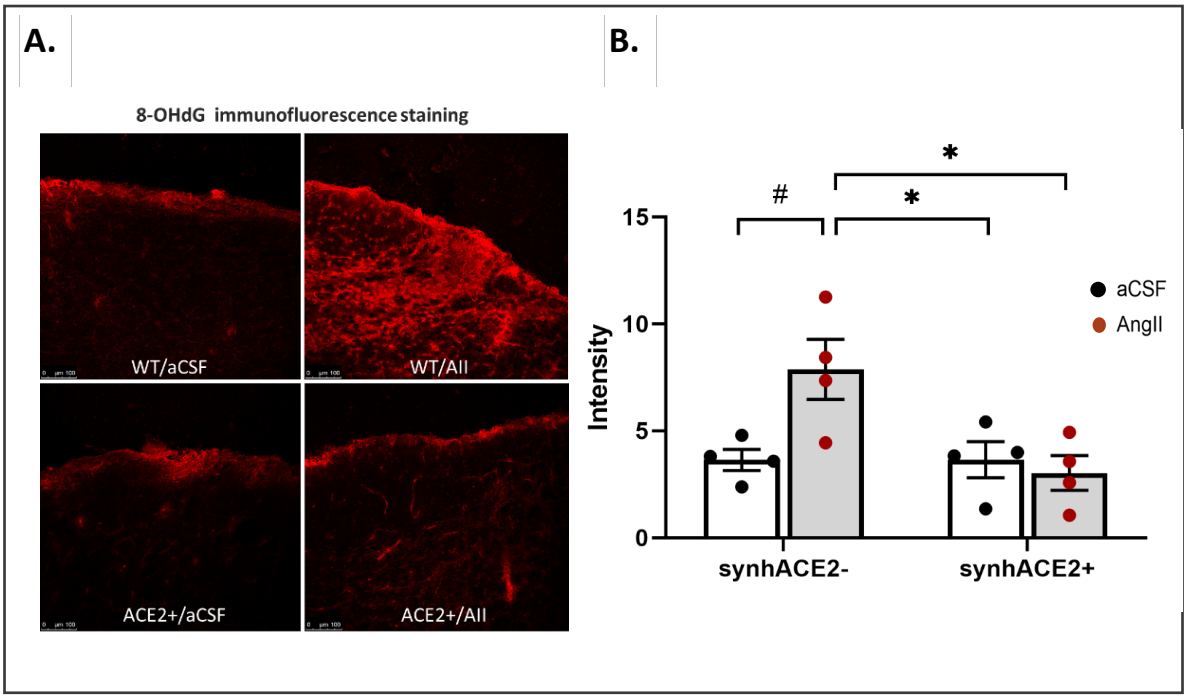

Figure 5. 6 SynhACE2$^{+/+}$ mice exhibit anti-oxidative stress property in response to central AngII.

Representative 8-OHdG immunofluorescence staining in the RVLM (A) and quantified data (B) showed that ICV AngII infusion significantly increased DNA oxidation in the RVLM area of SynhACE2$^{-/-}$ mice, but not in SynhACE2$^{+/+}$ group. ACE2 over-expression did not change ROS production during aCSF treatment. (n=4, *p<0.05 vs. SynhACE2-/AngII; #p<0.05 vs. SynhACE2$^{-/-}$/aCSF).

Discussion

The current study provides evidence that ACE2 upregulation in the brain abolishes the central pressor effect of AngII in conscious mice. Because this effect has been shown to be mediated by a reduction in oxidant stress elicited by AngII [75] we hypothesized ACE2 overexpression in the brain would decrease the sympathetic and ROS responses to central AngII.

It has been shown that increased levels of circulating AngII are present in patients with severe primary HTN [166]. In addition to the vasoconstrictor effects of circulating AngII, HTN can be evoked by the direct effects of AngII on brainstem neurons either through regions lacking a brain blood barrier (BBB), or through impaired BBB due to chronic HTN [167, 168]. Although studies have shown evidence that peripheral AngII can access neurons in the brainstem [169], increased AngII originating from the CNS also contributes to central RAAS over-activation [170]. Therefore, chronic ICV administration of AngII is a plausible approach to create a model for primary HTN.

As indicated above, it is believed that the mechanism of central AngII induced HTN is through generation of ROS which consequently excites sympathetic neurons resulting in increased BP. This concept was confirmed by our data (Fig 5.5 and Fig 5.6). It is reasonable to speculate that targeting either AngII or ROS centrally would attenuate primary HTN. In this study using SynhACE2$^{+/+}$ mice, we were able to target central AngII and ROS to confirm the mechanism for the anti-hypertensive property of central ACE2 over-expression.

Although it has been well accepted that the Ang1-7/MasR axis possesses a variety of protective effects on cardiovascular function, it is still not clear if Ang1-7 is the key mediator

for the anti-pressor effects of ACE2 in response to AngII administration. Due to the complexity of central nuclei and inter-nuclear communication, there may exist many variables that make the same effector exert opposite influences. Fontes et al. showed that microinjection of Ang 1-7 directly into rat RVLM increased MAP at a dose of 25 pmol [70]. Feng et al. showed that chronical subcutaneous (s.c.) infusion of A779 (600 ng/kg/min) reversed the anti-pressor effect of central ACE2 in response to peripherally administered AngII (600 ng/kg/min, s.c.) [122]. Based on these findings it is hard to reach to a firm conclusion in terms of the effect of Ang 1-7 since the results seem to involve several factors including dose, administration route, target location, etc. Feng et al. showed that SFO selective over-expression of ACE2 attenuates the pressor effect of AngII (ICV bolus), which was not reversed by the MasR antagonist, A779 [76]. Wysocki et al. [171] showed that subcutaneous infusion of human recombinant ACE2 prevented the hypertensive effect of AngII (1000 ng/kg per minute, s.c.) and this effect was not blocked by A779 (100 ng/kg/min, s.c.) infusion. In Wistar rats, Campagnole-Santos et al. observed that ICV Ang 1-7 failed to attenuate central AngII induced BP increase, but improved baroreflex sensitivity impairment [172]. Our data are largely consistent with these findings, which seem to indicate there exists discrepancies between central and peripheral, or between different nuclei with regard to responses to RAAS component interactions.

In the current study, inhibition of the pressor response to central AngII in SynhACE2$^{+/+}$ mice was not altered by infusion of MasR antagonist A779. We speculate that AngII degradation may constitute the major mechanism by which central ACE2 over-expression inhibits this response. However, given some evidence that ACE2 can act as an antioxidant [159], other factors such as anti-oxidant defense systems may play an intermediate role.

In this study we used only male mice instead of both genders. Numerous studies have demonstrated the differences in BP between age-matched male and female human beings[173]. In many animal studies, sex differences in local RAAS activities have been indentified in several peripheral organs and in different compenents of RAAS[174]. Although direct evidence of the existence of sexual dimorphism in central ACE2 expression is relatively lacking, and there does exist BP differences to peripheral AngII infusion between genders [174, 175], our initial studies with both genders did not show major difference in the responses to centrally administered AngII. However, in order to apply the conclusions of this study to both genders, further studies need to be done.

In summary, the current study shows that brain selective over-expression of ACE2 profoundly abolished the pressor response to central administration of AngII. The MasR agonist Ang 1-7 and blocker A779 had no effects on BP or drinking responses following central AngII infusion, skewing the underlying mechanism towards an effect of ACE2 on AngII-AT1R signaling. The data suggest that a reduction in central oxidative stress may participate in this response.

Chapter VI. Potential Interaction between Central RAAS and Nrf2

Introduction

Nrf2 plays an important role in the development of primary HTN, based on both direct and indirect evidence [176-178]. In a previous study we demonstrated that selective deletion of Nrf2 in the RVLM in normal mice led to a downregulation of antioxidant enzymes and elevated ROS, resulting in increased SNA and BP [120]. This suggests that central Nrf2 contributes to BP BP regulation via modulation of oxidative stress and SNA. Senanayake et al. found that administration of a dietary phase 2 protein inducer, sulforaphane (SFN), lowered BP in spontaneously hypertensive stroke-prone (SHRSP) rats to a level comparable to normal Sprague Dawley rats [179]. Noyan-Ashraf et al.[180] demonstrated that female SHRSP on a diet high in glucoraphanin exhibited in lower BP due to its metabolite, SFN. Although Nrf2 was not directly messured in their study, the observed effects were potentially due to the upregulation of Nrf2 expression and function induced by SFN. As a master regulator of a variety of antioxidant enzymes, Nrf2 may mediate an important mechanism in the pathogenesis of primary HTN. However, whether Nrf2 deficiency is a cause of the development of HTN, or it is an adaptive mechanism as a result of HTN is not clear.

The potential interaction between central Nrf2 and the RAAS, on the other hand, is an important question to be elucidated. A direct relation between Nrf2 and the RAAS has been indicated in several studies. Chang et al. [181] showed that overexpression of angiotensinogen in mouse renal proximal tubular cells downregulates Nrf2 signaling, thus increasing BP. Zhao et al. [182] found that Nrf2 deficiency upregulates intrarenal ACE2 and Ang1-7 MasR expression and attenuates HTN. Kang et al. showed that AngII suppresses Nrf2 signaling in the renal epithelial cells in a model of renal fibrosis [183]. The studies above suggest that Nrf2 and the RAAS may interact in the regulation of SNA and

BP. However, most of these studies were limited in the kidney. In the CNS, especially in the background of cardiovascular disease like HTN, the interaction between Nrf2 and the RAAS is yet to be defined.

Based on the evidence in the above chapters that both Nrf2 and ACE2 overexpression in the brain attenuates oxidative stress, inhibits sympathoexcitation and prevents BP increases, it is reasonable to speculate that in primary HTN, the central RAAS and Nrf2 may interact in a way that increases SNA. To test the potential interaction and its role in regulating BP and autonomic function in HTN, we evaluated RVLM Nrf2 and oxidative stress in SynhACE2$^{+/+}$ mice treated with chronic ICV-AngII infusion. We also assessed the effect of Nrf2 changes on AngII-induced HTN by either knocking-down Nrf2 in floxed mice or activating Nrf2 with SFN.

Experimental Protocol

Cell experiments were carried out using N2A neuron cells as described in Chapter III. One set of differentiated cells were treated with either the aCSF vehicle, AngII (30 or 100 nM), Ang1-7 (200 nM), the NOX inhibitor, APO, or SFN (10uM) for four hours or overnight. Cells then were subjected to nuclear fractionation to evaluate Nrf2 translocation. Another set of differentiated cells were transfected with hACE2-eGFP adenovirus to assess the effect of ACE2 overexpression on intracellular Nrf2 with or without AngII (100nM) stimulation. Cells were collected for western blot analysis.

In vivo studies were performed on 3-month-old SynhACE2$^{+/+}$, SynhACE2$^{-/-}$, or wild type male mice on the C57BL background. For selective Nrf2 knockout in the RVLM, Nrf2$^{f/f}$ mice were subjected to bilateral microinjection of Lenti-Cre-GFP virus into the RVLM as described in Chapter III. The experimental design is shown in Fig 6.1 below.

All mice were instrumented with a radio telemetry unit (PA-C10; Data Sciences International Inc., Minneapolis, MN) with the catheter inserted into the left common carotid artery as described in Chapter III. Animals were allowed to recover for 1 week before hemodynamic recording. AP and HR were measured 2 hours daily from noon to 2:00 PM. A 24-hour recording was attained each week usually on a Saturday or Sunday. Following 3 days of baseline recording, a cannula connected to a 7-day osmotic minipump (Model 1002, Alzet, Inc. Cupertino, CA) with a pumping rate of 0.5ul/hour, was implanted into the right lateral ventricle to create a hypertensive model by chronic ICV infusion of AngII. The control group received aCSF. In order to avoid acute postoperative stress induced high BP, mice of all groups were equipped with minipumps filled with only aCSF for 1 week before switching to minipumps filled with different drugs. Each group received the assigned treatment with either AngII (100 ng/kg/min) or aCSF. In some experiments mice also received the Nrf2 activator, SFN (500ng/kg/min) to determine if this would abrogate the response to central AngII. SDRR and LF/HF were analyzed based on AP and HR recording data.

During hemodynamic recording, mice were placed in a metabolic cage. After a 3-day adaptation period, 24-hour urine samples were collected daily. Mice were sacrificed 7 days after ICV infusion of different treatments. Brains were removed after euthanasia. Brainstem RVLM punches were used for western blot analysis. Some tissue was used for immunofluorescence staining.

Results were analyzed by one-way or two-way ANOVA for repeated measures followed by Dunnett's correction or Tukey's test for multiple comparisons. All data are expressed as mean ± SE. Statistical analyses were performed using Prism8 (GraphPad Software,

Inc. San Diego, CA). Differences were considered statistically significant at a p value of <0.05.

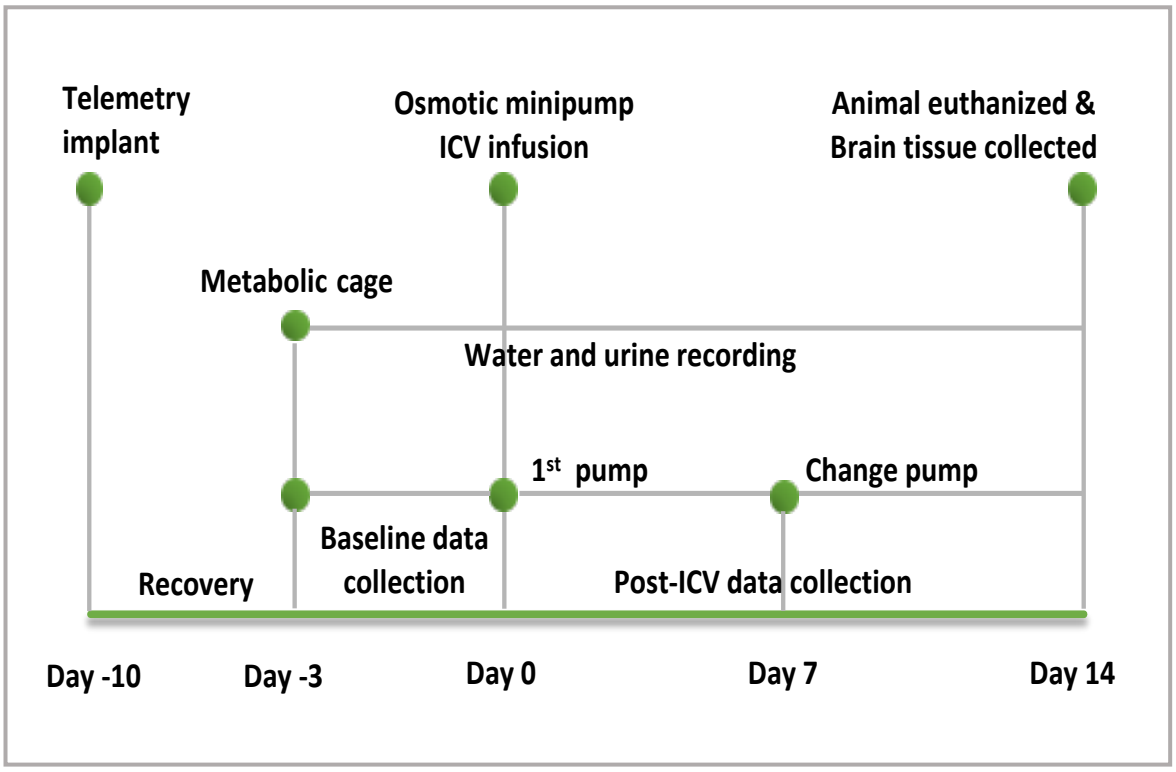

Figure 6. 1 Animal experimental design.

Results

AngII induces Nrf2 nuclear translocation

As a transcription factor, Nrf2 regulates phase 2 anti-oxidant enzyme expression by nuclear translocation when activated by intracellular ROS[184, 185]. However, many redox protective agents, such as β-lactoglobulin peptide (BRP2) or SFN were found to exert their anti-oxidant effects by also promoting Nrf2 nuclear translocation[186]. Therefore in our cell experiments the first question we wanted to clarify was the effect of AngII on Nrf2 behavior. Using N2A cells, we assessed Nrf2 translocation after AngII at different concentrations and different time periods, using SFN treatment as a positive control. Fig 6.2A demonstrates western blot data for Nrf2 in cytoplasmic and nuclear fractions after AngII stimulation. In the cytoplasmic fraction, although there were no statistical differences in Nrf2 between different conditions, in the nuclear fraction however, Nrf2 increased in a dose and time-dependent manner, with a peak level reached at 100nM AngII and 4 hour-treatment. GAPDH and Lamin-B were chosen for cytoplasmic and nuclear loading controls, respectively.

To further investigate if this AngII-induced Nrf2 translocation was a result of oxidative stress, we treated with both Ang 1-7 and the NOX inhibitor, APO with AngII. As is shown in Fig 6.2B, both Ang 1-7 and APO significantly reduced nuclear Nrf2 translocation in response to AngII. Though specific ROS were not measured, these data indirectly suggested that AngII-induced Nrf2 translocation is very likely a cellular protective mechanism in response to oxidative stress due to AngII stimulation.

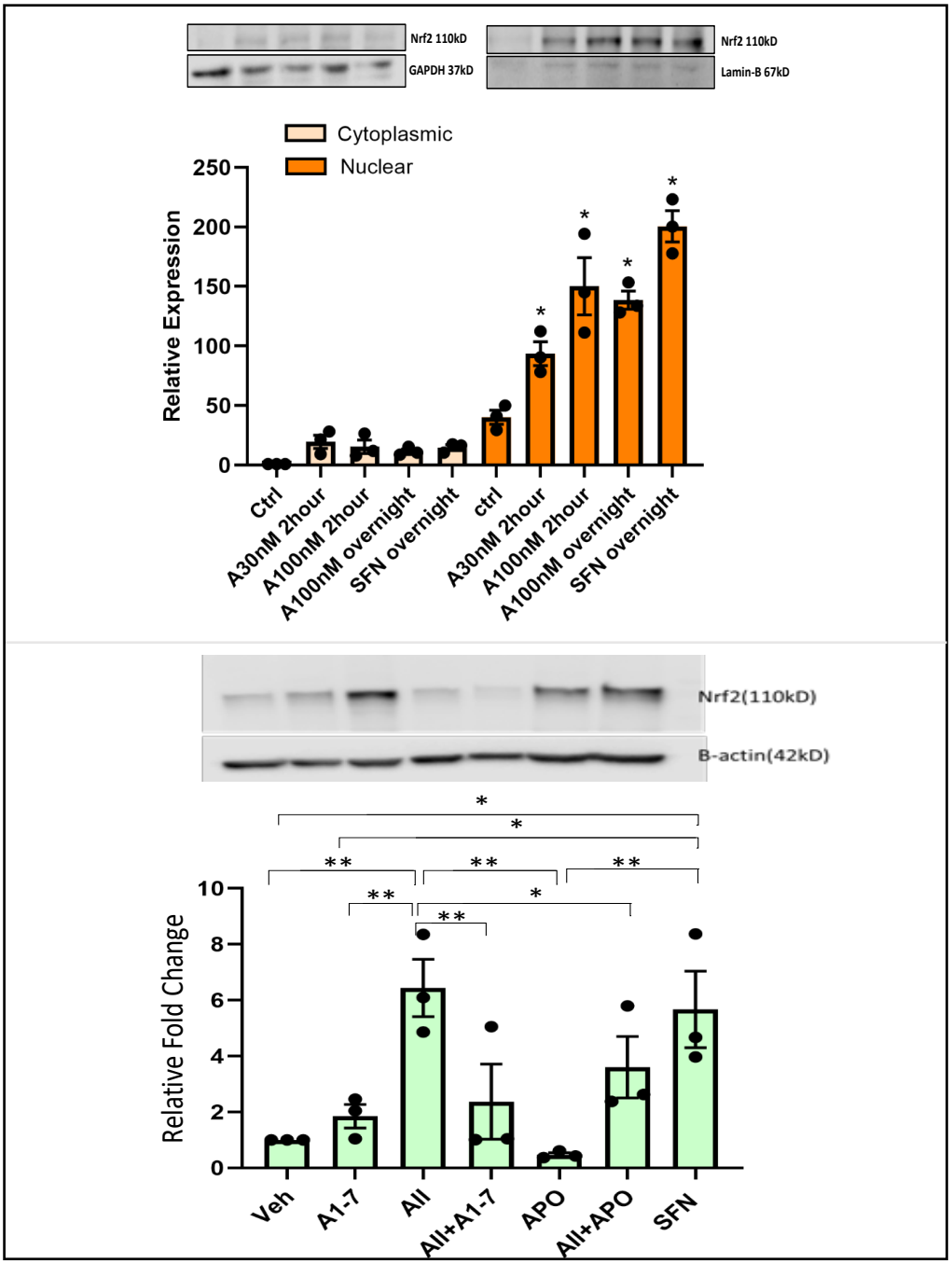

Figure 6. 2 Representative immunoblot for Nrf2 translocation in N2A

A. Cytoplasmic (light orange) and nuclear (dark orange) fractions were prepared from N2A cells treated with either vehichle, AngII(30, 100nM), or SFN (10uM) for either 2 hours or overnight. B. Nrf2 in nuclear fraction after treatment with Ang 1-7, AngII or APO. (n=3, *p<0.05)

Effect of ACE2 on intracellular Nrf2 in response to AngII

As discussed in earlier chapters, ACE2 is the key enzyme that converts AngII into Ang 1-7 and possesses strong antioxidant properties. In order to determine the effect of ACE2 on Nrf2 under AngII stimulation, we transfected N2A cells with hACE2-eGFP adenovirus to overexpress intracellular ACE2 prior to AngII treatment. Firstly, we evaluated ACE2 virus transfection efficiency at different MOI (multiplicity of infection) and different incubation times. Fig 6.3A-B demonstrates ACE2 adenoviral transfection efficiency is positively corelated to viral titer (1-50 MOI) and incubation time (24-96 hour). Furthermore, we found that ACE2 overexpression increases whole cell Nrf2 shown in the western immunoblot (Fig 6.3B). Although the presence of either ACE2 or AngII upregulated Nrf2 in N2A cells, when combined together, Nrf2 increase was attenuated, as is shown in Fig 6.3B. Taken together, these data showed that Nrf2 responds to both AngII and ACE2 in N2A cells separately; co-existence of AngII and ACE2 though does not trigger a synergistic increase of Nrf2.

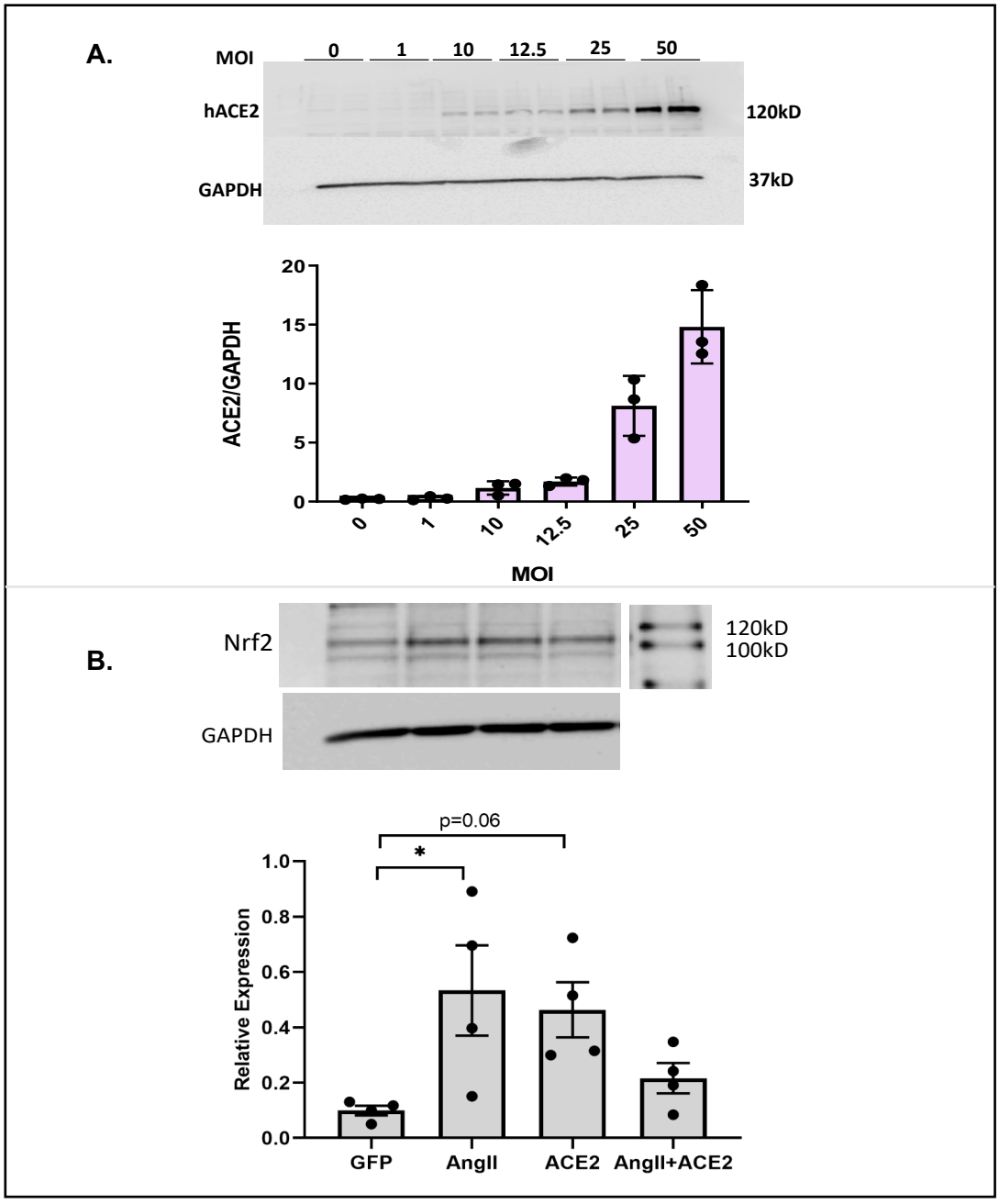

Figure 6. 3 Representative immunoblot for whole cell Nrf2 in Ad-hACE2-eGFP transfected N2A cells.

A. Whole cell ACE2 expression after Ad-hACE2-eGFP viral transfection at different titers. B. Whole cell Nrf2 protein in ACE2 overexpressed-N2A cells treated with or without AngII. Both ACE2 and AngII by themselves increase intracellular Nrf2; when combined together, the overall effect is decreased Nrf2 response compared to either treatment alone. (*p<0.05)

Nrf2 and NQO-1 are upregulated in the RVLM of SynhACE2$^{+/+}$ mice

In previous studies we showed that in animals with heart failure, there was a decreased expression of both ACE2 and Nrf2 in the RVLM [101, 187]. To further determine if there is a correlation between ACE2 and Nrf2, we measured Nrf2 protein in the RVLM of SynhACE2$^{+/+}$ mice and their littermates treated with or without central AngII. We found that ICV AngII evoked an upregulation of Nrf2 in the RVLM compared to ICV aCSF in SynhACE2$^{-/-}$ animals (Fig 6.4A). This upregulation was inhibited by ACE2 overexpression. In order to determine if these changes in Nrf2 are specific to the RVLM, we also assessed tissues from the cerebral cortex and the hypothalamus, where no differences in Nrf2 levels were found. The antioxidant enzyme NQO-1 (Fig 6.4B) exhibited a similar trend as Nrf2.

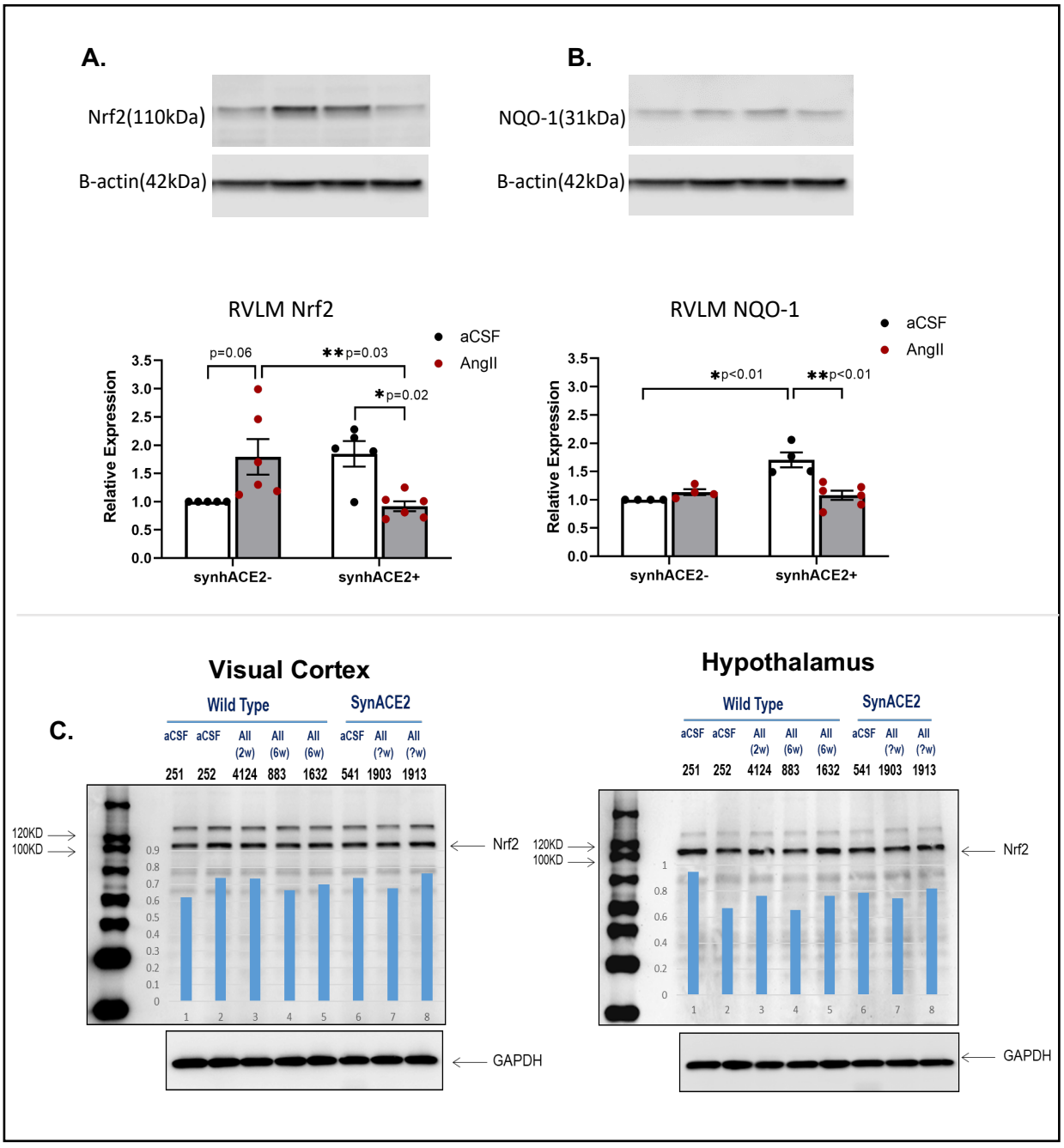

Figure 6. 4 Representative immunoblot of Nrf2 and NQO-1 in the brain of synhACE2$^{+/+}$ with chronic central AngII infusion.

A. Nrf2 from RVLM punches showed an increase in response to ICV-AngII infusion, which was restored by ACE2 overexpression, RVLM NQO-1 was significantly increased by ACE2 overexpression, which was attenuated in the ACE2$^{+/+}$ /AngII group. C. Nrf2 was not different between groups in the visual cortex or hypothalamus (n=4-6, *p<0.05).

Selective knockdown of Nrf2 in the RVLM enhances the pressor effect induced by central infusion of AngII

As discussed in Chapter I, Nrf2 is a critical transcription factor for antioxidant defenses in many diseases [188-190]. In chronic heart failure, activation of Nrf2 decreases AT1R expression in the RVLM and evokes sympatho-excitation[191]. In healthy mice, selective deletion of Nrf2 in the RVLM induced HTN [120]. However, the response to ICV AngII is unknown in the face of Nrf2 deletion. Therefore, using $Nrf2^{f/f}$ mice, we evaluated the impact of central AngII infusion in animals with RVLM Nrf2 deficiency to address the potential role of Nrf2 in AngII-induced neurogenic HTN. We selectively deleted Nrf2 in the RVLM. Immunofluorescence staining confirmed reduced Nrf2 in the RVLM following Cre-GFP injection (Fig 6.5A-B). Figure 6.5C demonstrates micro-punches of RVLM subjected to western blotting which shows a significant reduction in Nrf2 protein ($n=3$, $p<0.05$). In a functional study, we showed that depletion of Nrf2 in the RVLM increased baseline 24 hour day-night BP (mean ΔMAP= 21.0±1.8mmHg, $n=3$, $p<0.05$) (Fig 6.5D), which is consistent with our previous data [120]. In addition, we also found that compared to the $Nrf2^{f/f}$-GFP control group treated with AngII (mean ΔMAP= 9.0±1.7mmHg increase compared to baseline, $n=3$, $p<0.05$), Nrf2 deletion in the RVLM increased the MAP as high as 30.0 mmHg in $Nrf2^{f/f}$-Cre mice, indicating an enhancement of the pressor effect of central AngII infusion (Fig 6.5E).

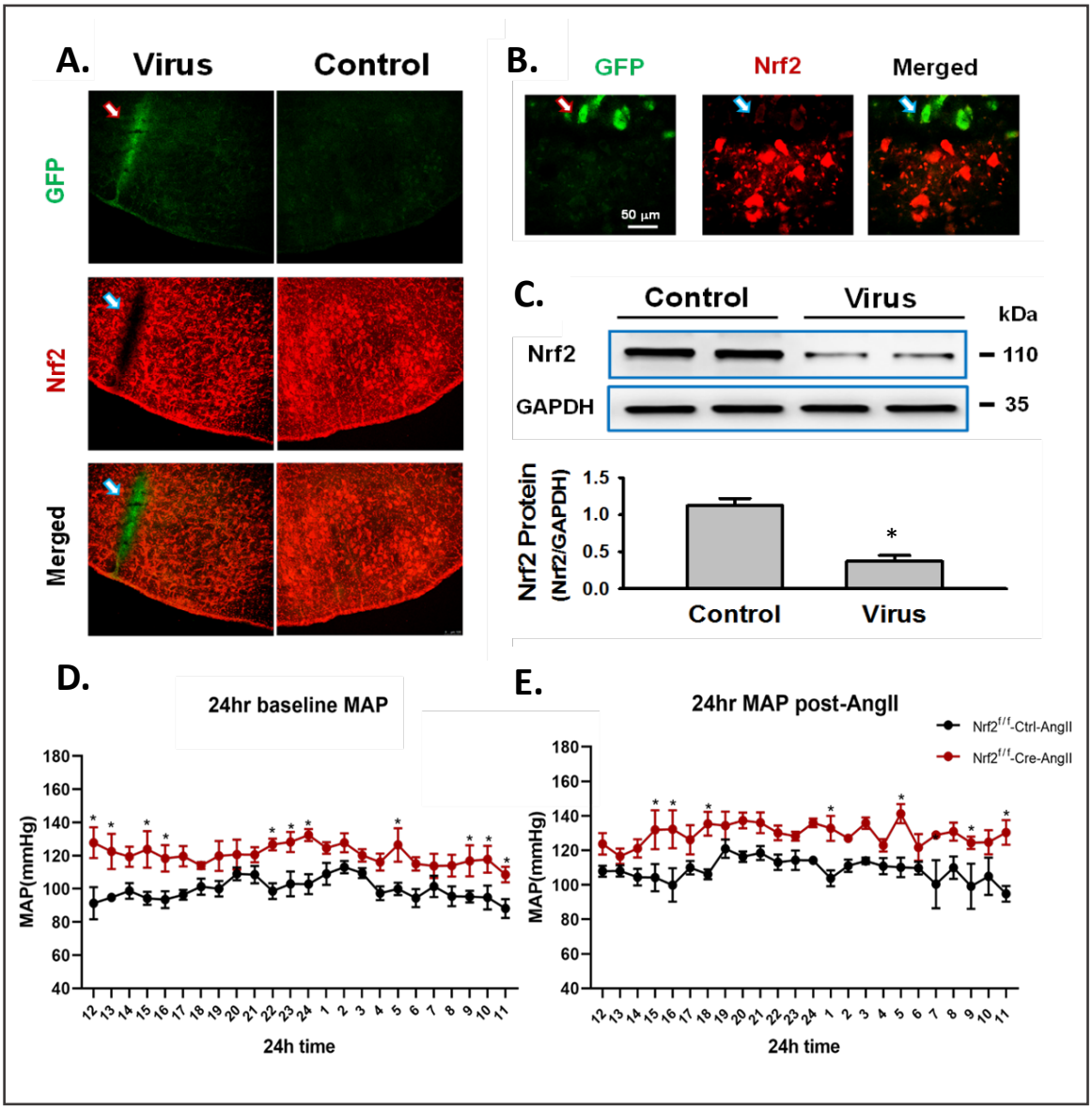

Figure 6. 5 Representative immunofluorescence staining of Nrf2 knockdown in the RVLM

Nrf2 was selectively knocked down in the RVLM (A-B). RVLM Nrf2 protein quantification was validated by western immunoblot(C) (n=3, *p<0.05). 24 hour mean arterial BP at baseline (D) and 24 hour mean arterial BP 7 days post ICV-AngII infusion (E) showed that Nrf2 deletion in the RVLM enhanced central AngII-induced increase in BP (n=3, *p<0.05).

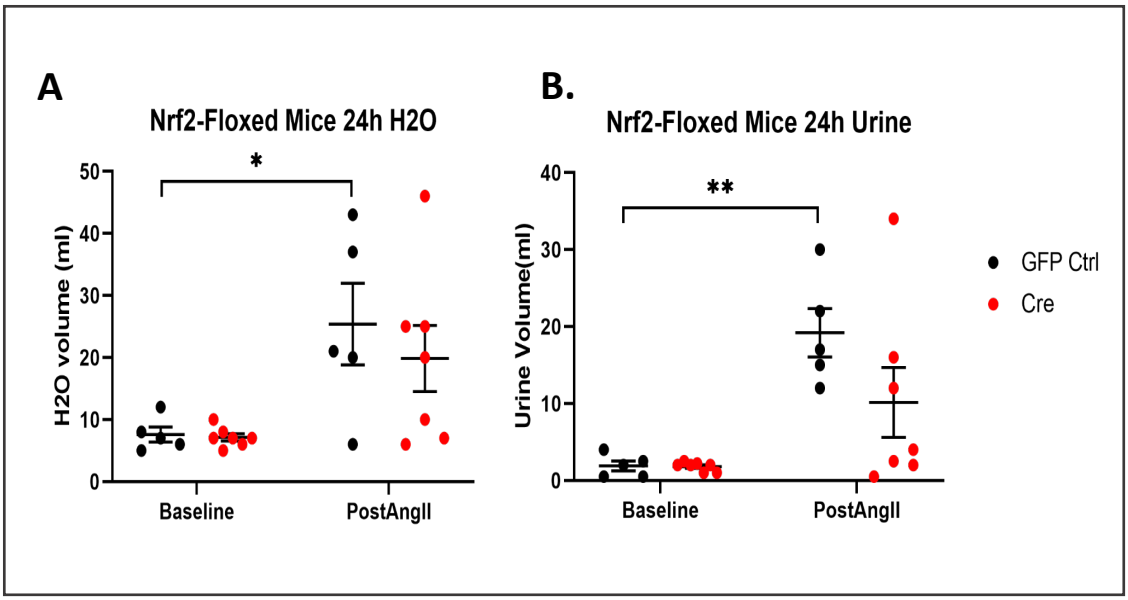

Figure 6. 6 Effect of RVLM Nrf2 knock down on central AngII-induced polydipsia and polyuria in Nrf2-floxed mice.

A. Chronic AngII infusion produced a significant increase in water intake during the 2-week infusion period. This response was not enhanced by Nrf2 knock down using Cre virus delivered to the RVLM in $Nrf2^{f/f}$ mice. B. Chronic AngII infusion produced an increase in urine output during the 2-week infusion period, which was not enhanced by Nrf2 knock down in the RVLM (n=5-7; *$p < 0.05$, **$p<0.01$).

Effects of Nrf2 deletion in the RVLM on water intake and urine output in response to icv AngII

In $Nrf2^{f/f}$ mice that had Nrf2 knocked down in the RVLM we evaluated drinking and urine responses. We measured daily 24-hour water intake and urine volume and averaged the values over 7 consecutive days. In contrast to our expectations, Nrf2 deficiency suppressed the polydipsic and polyuric effect induced by ICV AngII infusion (Fig 6.6, n=5-7). Prior to AngII treatment there was no difference between GFP- and Cre- treated $Nrf2^{f/f}$ groups).

ICV-infusion of sulforaphane attenuates the pressor effect induced by central infusion of AngII

To confirm a role of Nrf2 in mediating BP control in AngII-induced HTN, we upregulated central Nrf2 using icv infusion of SFN, a sulfur-containing compound that has been shown to possess potent antioxidant and anti-inflammatory properties through activation of Nrf2 [192]. In this experiment, we infused AngII ICV with and without SFN to elucidate the protective effect of Nrf2. Nrf2 upregulation was assessed in the terminal experiment with RVLM punches, showing that both AngII and SFN increased Nrf2 individually (although SFN was non-significantly here), co-administration of the two seemed to have a synergistic effect on Nrf2 upregulation (Fig 6.7A). NQO-1 protein followed a similar trend as Nrf2 under corresponding treatment, but did not show statistical significance (Fig 6.7B)

Fig 6.8A demonstrates the functional data. After 3 days of baseline MAP recording, ICV-AngII markedly increased BP in (red line and first half of black line). On day 6 SFN was administered with AngII in some animals that were treated with AngII alone. A significant decrease in BP was observed (second half of black line) ($p<0.05$). The group that was treated with SFN and AngII throughout the process exhibited a reduced increase in MAP

compared to the group treated with AngII alone (red) ($p<0.05$). SFN by itself did not alter BP (green line). Fig 6.8B are the 24 hour BP recording before and after ICV infusion, respectively. Although SFN attenuated the increase in AngII–induced BP most significantly during the day ($p<0.05$, right panel), the attenuation was not consistent throughout the 24-hour day-night cycle.

Fig 6.8 C and D show SDRR and LF/HF calculated based on the MAP and HR recordings. After the first ICV-infusion of AngII, SDRR decreased and LF/HF increased suggesting increased sympathetic tone (red and blue groups in the two panels). SFN plus AngII infusion trended towards a blunting in the decrease in SDRR, however this did not reach statistical significance (blue). For LF/HF however, SFN significantly restored the alteration caused by ICV-AngII (grey and blue). These data suggest that SFN, at least, in part, improves autonomic balance skewed by central AngII infusion.

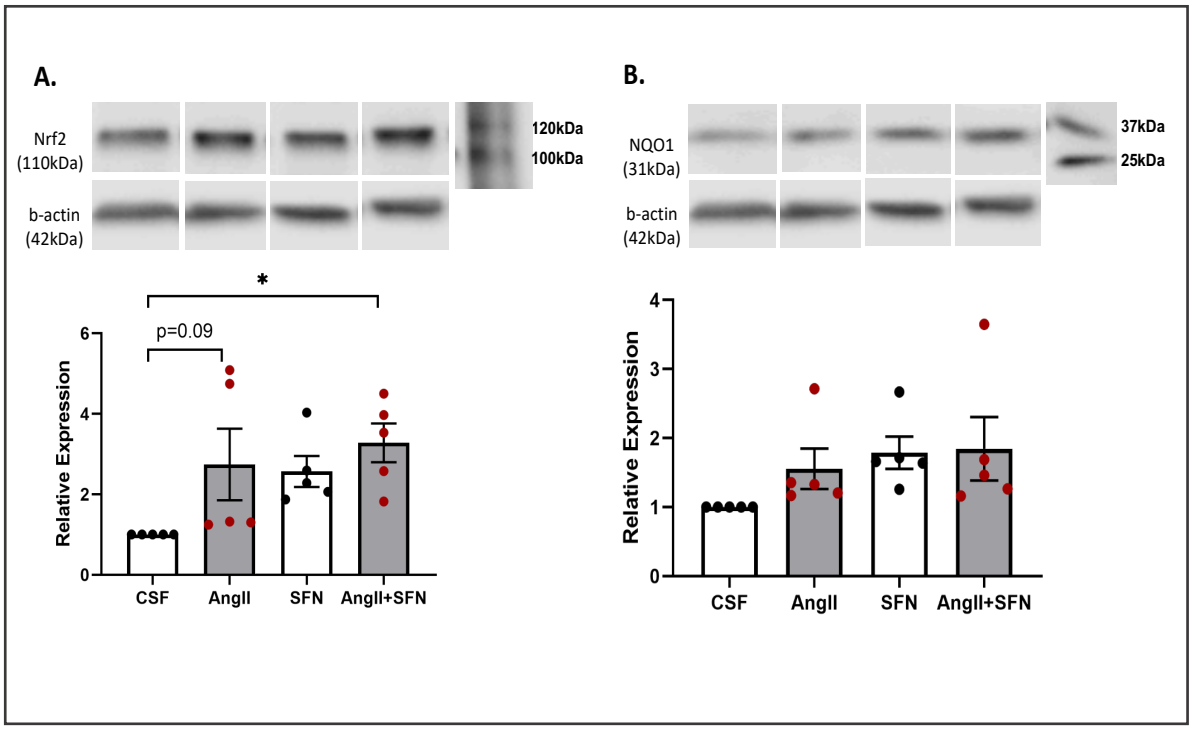

Figure 6. 7 Immunoblot of Nrf2 and NQO-1 in RVLM after chronic ICV infusion of AngII, SFN, or AngII+SFN.

A. Co-administration of AngII and SFN ICV increased Nrf2 protein in RVLM. B. No difference was found in NQO1 after co-administration of AngII and SFN ICV infusion. (n=5, *p<0.05)

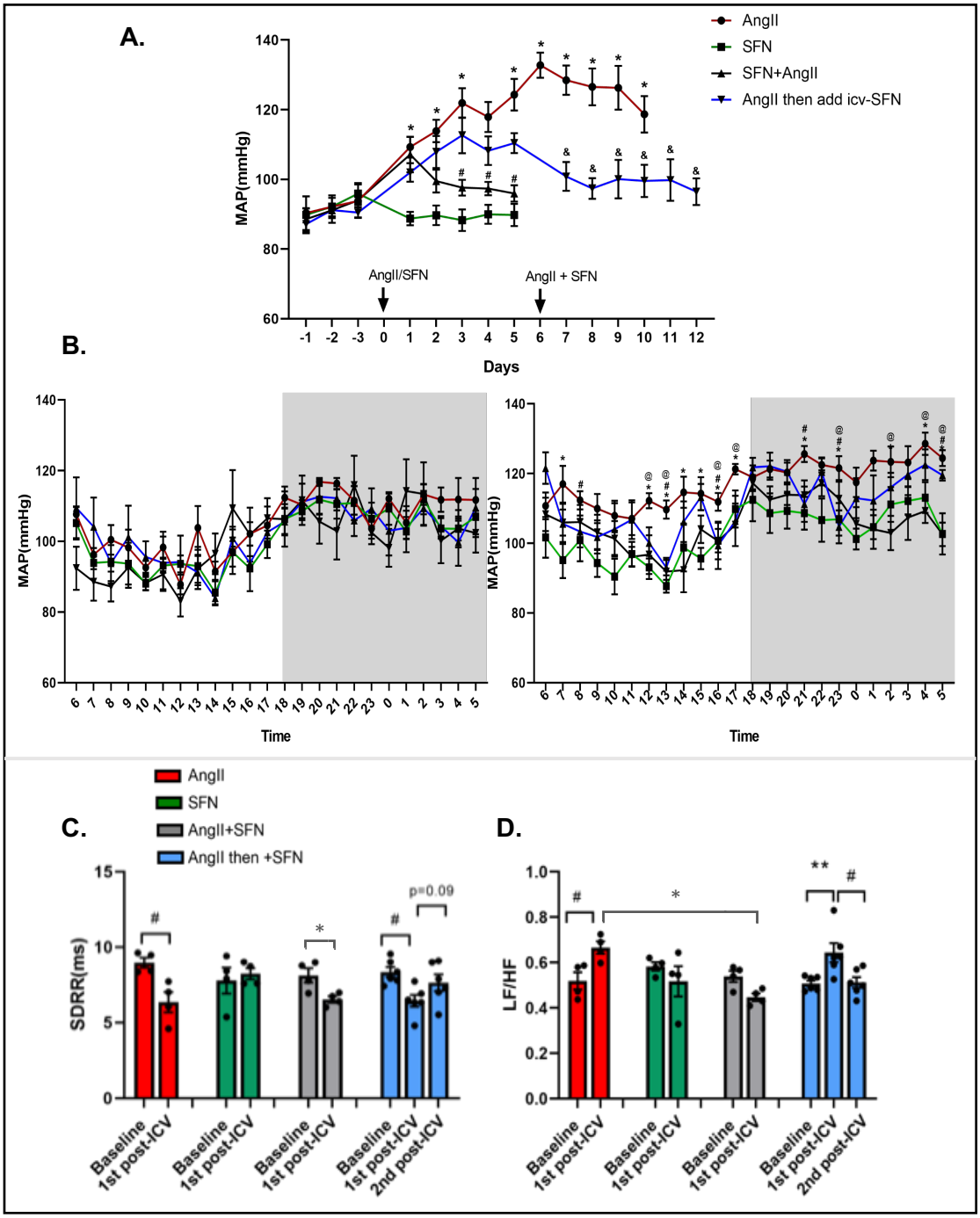

Figure 6. 8 ICV-SFN attenuates the pressor responses and SNA to central AngII.

A. ICV-AngII infusion increases MAP which was attenuated with subsequent infusion of ICV-SFN. SFN alone did not alter BP. MAP was recorded 2 hours around noon every day(n=6, *p<0.05 compared to baseline; #p<0.05, &p<0.05 compared to AngII). B. 24 hour MAP in four groups before (left) and after (right) ICV infusion of the respective treatment (*p<0.05 compared to SFN, #p<0.05 compared to SFN+AngII, @p<0.05 compared to AngII then add ICV-SFN). C. SDRR (left) and LF/HF (right) during baseline and post-ICV infusion period. SFN showed some improvement in AngII induced reduction in HRV. (*p<0.05, #p<0.05, **p<0.01)

Effects of sulforaphane on AngII-induced polydipsia

To determine the effect of ICV-SFN on AngII-induced polydipsia and to also further assess the potential role of Nrf2 in fluid control, we assessed daily water intake and urine output. Fig 6.9 illustrates that ICV AngII increased drinking behavior by approximately 15 mL compared to baseline. Interestingly, although SFN reduced the BP increase by central AngII, it failed to suppress the polydipsia/polyuria effects, regardless of when SFN was administered.

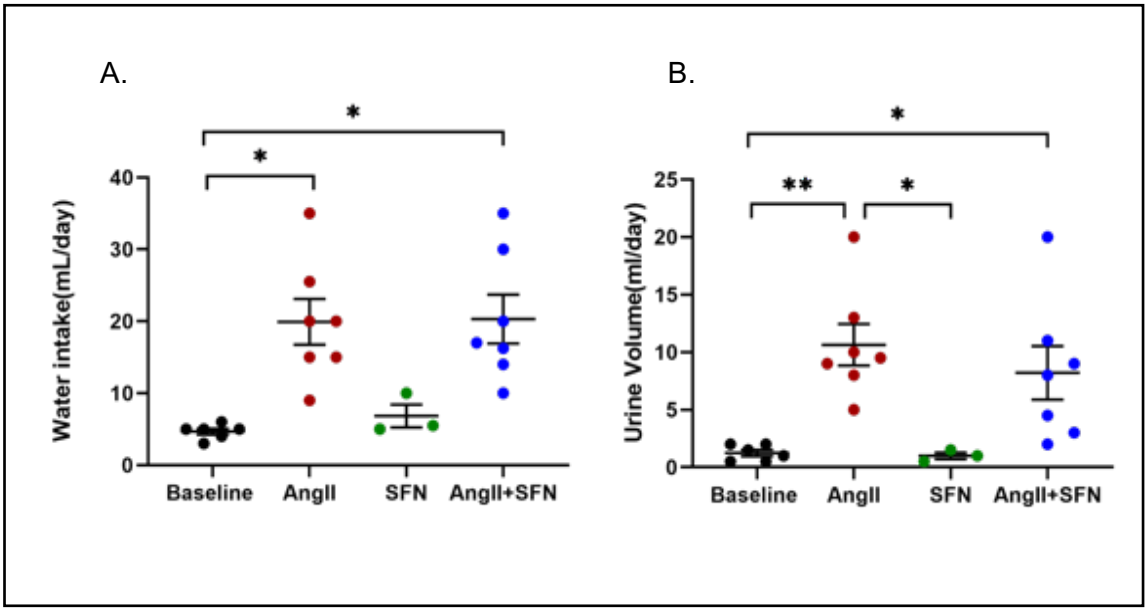

Figure 6. 9 Effects of ICV-SFN on central AngII- induced polydipsia and polyuria.

A. Chronic AngII infusion produced an overall increased water intake during the 1-week infusion period, addition of ICV-SFN showed similar increase in water intake(n=7; *p < 0.05). B. Central AngII significantly increased urine output (**p < 0.01, n=7). Addition of ICV-SFN also has a significantly higher level of urine output compared to baseline (*p < 0.05, n=7). SFN alone-group showed significantly lower daily urine volume but it did not further reduce urination compared to baseline.

Discussion

The study in this chapter explored the interaction between the RAAS and Nrf2. Our data demonstrated nuclear Nrf2 in neuronal N2A cells was increased in response to AngII stimulation in a time- and dose- dependent manner and provided direct evidence that intracellular Nrf2 responds to AngII. 100nM of AngII for 2 hours triggered the maximal increase in nuclear translocation, indicating the response is an acute process in these neuronal cells. In order to further confirm that Nrf2 translocation was a result of increased intracellular oxidative stress, we treated cells with APO to dampen the oxidative stress response to AngII. We found that APO effectively suppressed the Nrf2 response to AngII stimulation. However, Ang 1-7 (also shown to possess antioxidant activity) did not show the same effect as APO. It is possible that $O_2^{\bullet -}$ plays an important role in mediating the AngII-induced Nrf2 translocation process while Ang 1-7 may not work through $O_2^{\bullet -}$ inhibition, or Ang 1-7 being degraded by local enzymes such as neprilysin[193]. Other possibilities include optimal dosage of Ang 1-7 for the expected effect or variations in the expression of endogenous MasR on N2A cells[194].

As a critical connection between AngII and Ang 1-7, ACE2 is a key molecule that is involved in this relationship. Neuro 2A cells overexpressing ACE2 showed that ACE2 by itself upregulated intracellular Nrf2 almost as much as AngII, and when treating the ACE2 overexpressing cells with AngII blocked the Nrf2-inducing effect by AngII. These data were consistent with western blot data from RVLM tissue, which also showed a similar trend of Nrf2 changes in four treatment groups. These data suggest that Nrf2 upregulation is another possible quality of ACE2 that contributes to its anti-AngII effects. However, the exact mechanism by which ACE2 upregulates Nrf2 is not completely clear. In ACE2 viral-transfected cells, AngII failed to trigger an increase in Nrf2. This is difficult to explain since

the Nrf2-upregulating effect of ACE2 should have a “synergistic” effect on Nrf2. It is possible that the consumption of AngII by ACE2 is too rapid to allow the latter to exert its Nrf2-inducing effect; or the degradation of AngII by ACE2 somehow overrides the Nrf2-inducing effects of AngII or ACE2 alone. Importantly, significant differences in Nrf2 protein between the four treatment groups only existed in the RVLM among all the tissues tested, which included the visual cortex and hypothalamus. Taken together, this experiment indicated that both AngII and ACE2 induced an increase in intracellular Nrf2 protein and that ACE2 can inhibit this effect on Nrf2 exerted by AngII.

To further understand the role of the interaction between the central RAAS and Nrf2 in modulating SNA we selectively knocked down Nrf2 in the RVLM using Nrf2 floxed mice and viral Cre delivery to evaluate their BP response prior to and after chronic ICV-AngII infusion. In $Nrf2^{f/f}$ mice treated with Cre virus, the baseline BP was significantly increased compared to mice treated with GFP virus. With AngII treatment, this increase was further enhanced. These results provide at least partial evidence that Nrf2 may attenuate sympathetic outflow. An interesting finding was the unaltered polydipsic and polyuric response by Nrf2 deletion to central AngII. Although Nrf2 has been shown to be a potent antioxidant factor that reduces sympathoexcitation in several studies[120, 195], it failed to exaggerate the drinking and urinary response to AngII. Possible reasons may be that although suppressing SNA, RVLM Nrf2 may not exert a major influence on those neurons projecting to the thirst control centers which are mostly located in forebrain regions.

To further assess the role of central Nrf2 in regulating BP and SNA, we used SFN, a proven potent Nrf2 activator, in the ICV infusion in an attempt to upregulate central Nrf2. SFN is an extensively studied compound in translational medicine and can be found in most cruciferous vegetables[196]. RVLM Nrf2 protein upregulation was tested in terminal

studies by western blot. In SFN treated groups, Nrf2 was, in general, increased. Hemodynamic studies confirmed our hypothesis that ICV-SFN infusion blocked the pressor effects of central AngII reflected through both BP maintenance and HRV parameters. For BP assessment, not only did co-administration of SFN and AngII suppress the hypertensive response but adding ICV-SFN infusion after one-week of ICV-AngII also significantly reversed the BP increase. Again, in accordance with our data from Nrf2 knockout mice, SFN did not affect the polydipsia or polyuria responses by AngII. We conclude that Nrf2 deletion has a major effect on BP and SNA but little influence on drinking behavior and therefore urine flow.

In summary, in this study we showed that selective deletion of Nrf2 in the RVLM of mice resulted in an enhanced BP increase in response to central AngII infusion, and upregulation of Nrf2 by ICV-SFN resulted in attenuation of the pressor response to central AngII. These results provide evidence that central Nrf2 may possess anti-hypertensive properties, and this property may be at least one signaling pathway mediating the protective effect of ACE2 overexpression in response to chronic central AngII infusion.

Chapter VII. Perspectives and Potential for Therapy

Therapy for cardiovascular disease, especially CHF and HTN has been relatively static for the past two decades. The use of agents that target the RAAS, β1-1 adrenergic blockers, diuretics and in some cases vasodilators are the primary pharmacological agents that are used to treat these disorders. While effectively lowering morbidity and mortality the degree of CHF and HTN are still unacceptably high. There is a desperate need to develop novel therapies that target unexplored mechanisms for CHF and HTN. While centrally acting drugs such as clonidine and moxonidine have been used they are associated with negative side effects and are difficult to regulate their dose – response relationships[197]. Because both disorders are associated with oxidative stress and increases in sympathetic outflow it is reasonable to evaluate therapies that have been shown to affect both mechanisms.

The two agents studied in this dissertation have been shown to reduce oxidative stress in both CHF and HTN [74, 120, 185, 198]. ACE2 or ACE2 activation and Ang 1-7 have been used to treat HTN in animal models[171, 199-201]. The mechanism for the protective effects of these therapies has been assumed to be a reduction in AngII peptide and both a vasodilator and sympatho-inhibitory effect of Ang 1-7 mediated, in part, through a reduction in oxidative stress [202, 203] primarily in the peripheral circulation. According to ClinicalTrials.gov there are 13 clinical trials where modulation of ACE2 is or has recently been investigated for the treatment of HTN, stroke, and the metabolic syndrome. Similarly there are 56 trials where Nrf2 activation is being used to treat a variety of diseases including cardiovascular disease. None of these trials specifically target the central nervous system although areas of the CNS may be involved in the positive actions of ACE2 and Nrf2 activation.

The results presented here suggest that activation or overexpression of both ACE2 and Nrf2 reduce sympathetic outflow in HTN and CHF when the RVLM is targeted. What is less clear from this work is how this could be used in a translational way for human disease. Systemic administration of ACE2 or Nrf2 activators will, of course, target all tissues. It is highly likely that small molecule activators such as diminazene aceturate (DIZE; [204]), sulforaphane[205] and dimethyl fumarate[206] are likely to gain entry through the blood brain barrier or via areas with no blood brain barrier such as the circumventricular organs[207]. Therefore, systemic administration may also target the CNS and potentially the sympatho-regulatory areas in the brain. In addition, new modalities of drug delivery have been developed using a variety of nanoparticles and extracellular vesicles for antioxidant therapy [208-212]. While animal studies have been positive, it is not clear how to specifically target these particles to the CNS in humans.

While targeting each of these molecules individually may have beneficial effects the studies described in this dissertation do not allow us to define the role of ACE2 in Nrf2 – mediated reduction in ROS in CHF or HTN. Figure 7.1 provides an overview of the potential interactions between these pathways. We suggest that any intervention that augments ACE2 and Nrf2 will have a beneficial effect in the settings of CHF and HTN. This work provides supportive evidence for focusing on ACE2 and Nrf2 in modulating the sympathetic nervous system in disease.

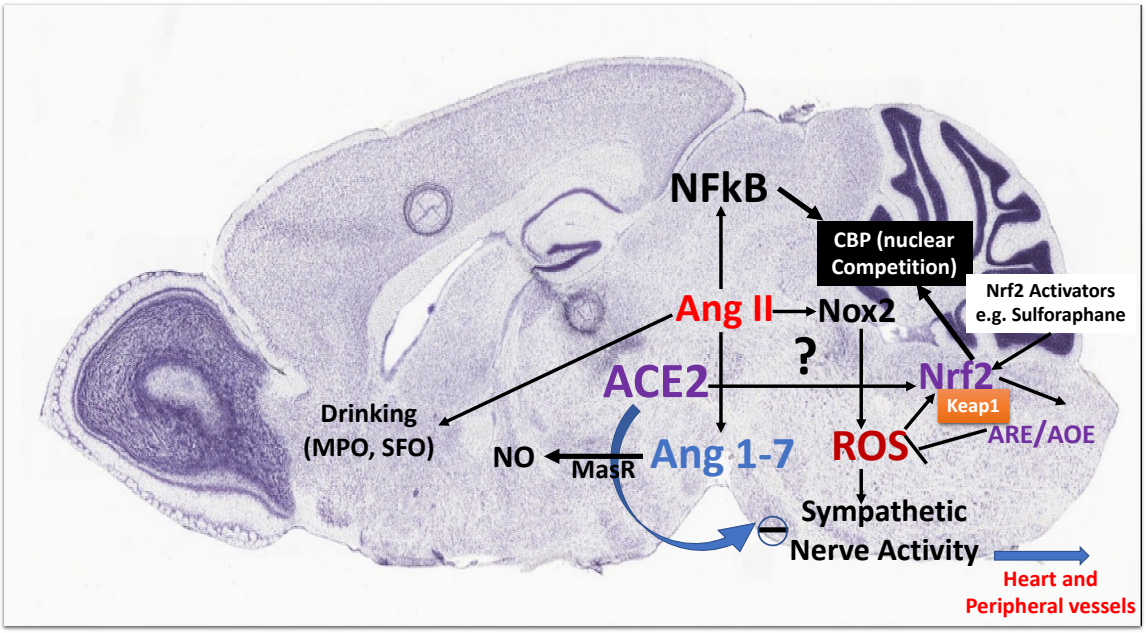

Figure 7.1 Overview of the mechanisms and potential involvement of ACE2 and Nrf2 in the regulation of sympathetic outflow in neurons from the RVLM in the setting of CHF and HTN in response to increased central AngII.

The diagram is based on data demonstrated in part from this thesis. AngII is a known pro-oxidant and pro-inflammatory peptide that is rapidly converted to Ang 1-7 by the action of ACE2. Through the AT1R it activates Nox2 which results in increased levels of superoxide in the cytosol. AngII, through increased levels of ROS, activates both Nrf2 and NFkB (not studied in this thesis). Both transcription factors are released from their protein inhibitors in the cytosol and translocate to the nucleus where they compete for binding to the creb binding protein (CBP). Increased inflammation in response to high levels of AngII may result in reduced Nrf2 levels. In addition, increased ubiquitination of Nrf2 in heart failure and in inflammatory states contributes to the reduced Nrf2 in CHF and HTN. Overexpression of ACE2 reduces the levels of AngII, thus decreasing ROS generation and sympatho-excitation. Decreases in AngII mediated inflammation may also result in augmented Nrf2 levels and thus increases in antioxidant enzyme transcription. Other potential mechanisms not studied here are the role of nitric oxide (NO) in scavenging ROS due to increased Ang 1-7. It does not appear that overexpression of ACE2 in the brain reduces AngII induced HTN by augmenting levels of Ang 1-7 but more likely by reducing central AngII levels. There remains a question as to a direct effect of ACE2 overexpression on Nrf2 in these cardiovascular diseases.

Chapter VIII. Summary

The present thesis examined the putative sympatho-inhibitory properties of Nrf2 and ACE2 in the CNS and potential interplay between the RAAS and Nrf2 in regulating BP. The findings in this work suggest:

1). Nrf2 expression in the RVLM of mice with coronary artery ligation-induced CHF was significantly lower compared to sham mice. Overexpression of Nrf2 in the RVLM significantly reduced SNA and improved arterial baroreflex function in CHF mice;

2). Central ACE2 possesses anti-hypertensive, antioxidative, and sympatho-inhibitory effects and modifies the response to chronic central AngII infusion. The data suggest that the anti-hypertensive effects of ACE2 overexpression are most likely through an Ang 1-7 independent mechanism;

3). Nrf2 may at least partially mediate the sympatho-inhibitory effect of ACE2 in response to central AngII induced HTN.

Although we have made every effort to take a comprehensive approach in these studies, we acknowledge that there are limitations. In our HTN model, despite the fact that chronic ICV-AngII infusion evoked a sustained increase in AP it is not clear where AngII is working since the AT1R is expressed throughout the brain. The non-specificity in targeting specific regions of autonomic control is a major limitation. Even though we focused on an important sympatho-regulatory nucleus (the RVLM), other nuclei in the brainstem and hypothalamus need to be considered in future studies, given the complexity of projections between each area.

In a previous study, CHF animals exhibited a downregulation of Nrf2 in the RVLM and increased sympathoexcitation [213, 214]. Therefore, it is natural to assume that chronic RAAS activation in the CNS, which is also correlated with sympathoexcitation, would be

associated with downregulation of Nrf2 as well. However, in our model of central AngII induced HTN, we found that after two weeks of HTN, Nrf2 in the RVLM was markedly increased compared to their control littermates. One possible reason for this finding could be differences in acute-versus-chronic phases in terms of Nrf2 activation. In the case of CHF, it usually takes 4 to 6 weeks to develop a chronic state of heart failure. In response to AngII infusion however, Nrf2 was mobilized as an acute defense mechanism in response to AngII-induced oxidative stress, which was what we observed after 2 weeks of ICV AngII infusion. It may be possible that with longer central AngII infusion, Nrf2 protein may be reduced as is seen in CHF. Therefore, further studies of the time course of Nrf2 changes in the RVLM during AngII infusion is important for a thorough understanding of these phenomena.

Further questions worth discussion is whether the changes of Nrf2 under circumstances in the above chapters are the direct result of Nrf2 translocation, expression, or both. Nrf2 exists in the cytoplasm in a sequestered form before it is activated and translocates to the nucleus. Despite Keap1 dependent regulation, there are multiple Keap1 independent modifications that affect Nrf2 protein and activation, including phosphorylation, acetylation, and epigenetic alteration in order to “fine tune” the Nrf2 signaling pathways [215]. In our N2A cell study, we demonstrated that nuclear Nrf2 increases in response to AngII stimulation in a dose-dependent manner. In our molecular studies using RVLM punches we only exmined the protein changes for Nrf2. However, to determine if there are changes in Nrf2 expression or degradation, further evaluation at the message level and ubiquitination should be carried out in the future.

In terms of the drinking and urine flow findings, we did not see a significant impact of Nrf2 on AngII induced polydipsia and polyuria. Fluid retention is found in a large proportion of

CHF and HTN patients[216, 217], and is thought to be commonly attributed to disease exacerbation and therapy resistance. The periventricular anteroventral third ventricle (AV3V) region, containing the MnPO, OVLT, and AV3V in the brain is critically involved in the maintenance of normal body fluid balance and distribution. Buggy et al. demonstrated that ablation of AV3V region in rats abolished the drinking responses elicited by ICV injections of AngII [218]. In the current study, we showed that chronic ICV infusion of AngII markedly increased drinking behavior as expected. Although manipulating Nrf2, either by viral injection in the RVLM or by SFN infusion, significantly affected BP changes caused by AngII, the drinking and urine responses were not altered. On one hand, the MnPO of the hypothalamus could respond to AngII infusion as a thirst-generating stimulus [219], and this response may be minimally affected by oxidative stress. Alternatively, deletion of Nrf2 in the RVLM may trigger some inhibitory signaling towards the AV3V region, thus failing to enhance the polydipsia induced by AngII infusion. This is conjecture and either way further studies need to be done to determine the differences in BP regulation and drinking behavior in our model.

The mouse RVLM is an extremely small nucleus that requires a good deal of skill to be localized. We feel confident that we carried out precise targeting and delivered the microinjections into mouse RVLM. However, there is some variability in targeting and in punching out tissue for biochemical analysis. Surrounding tissue is undoubtedly obtained outside of the area of interest. In hindsight laser capture microscopy would have been useful to better define tissue borders. We did however examine GFP expression outside of the RVLM and saw no expression.

To further examine effect of Nrf2 activation on BP, we used the widely used Nrf2 activator, SFN. Although this method compromised the RVLM specificity compared to viral

microinjection. In addition to activating Nrf2 nuclear translocation, SFN may possess some direct antioxidant properties via a Nrf2-independent mechanism [220, 221]. Nevertheless, the observation of effects in the RVLM and a consistent physiological outcome on BP in response to AngII made this method a good comparison to direct viral injection of cre in $Nrf2^{f/f}$ mice.

In conclusion, chronic cardiovascular diseases such as CHF and primary HTN are cardiovascular problems characterized by sustained sympathoexcitation and blunted baroreflex sensitivity. The central RAAS, especially the two functionally opposing components of ACE/AngII/AT1R and ACE2/Ang 1-7/Mas R, play a critical role in influencing SNA through modulating oxidative stress. Nrf2, an important antioxidant transcription factor, has been shown to reduce sympathetic tone in these two conditions. These studies indicate the likely relationship between ACE2 and Nrf2 in regulating SNA in HTN and that upregulation or activation of Nrf2 in CHF may be a beneficial therapeutic strategy in both CHF and HTN.

Chapter IX. References

1. Kong, X., et al., *Enhancing Nrf2 pathway by disruption of Keap1 in myeloid leukocytes protects against sepsis.* Am J Respir Crit Care Med, 2011. **184**(8): p. 928-38.

2. Coote, J.H., *Landmarks in understanding the central nervous control of the cardiovascular system.* Experimental Physiology, 2007. **92**(1): p. 3-18.

3. Dampney, R.A.L., *Central neural control of the cardiovascular system: current perspectives.* Advances in Physiology Education, 2016. **40**(3): p. 283-296.

4. Dampney, R.A., *Functional organization of central pathways regulating the cardiovascular system.* Physiological Reviews, 1994. **74**(2): p. 323-364.

5. Tanaka, J., H. Kaba, and H. Saito, *The A1 noradrenergic region enhances the responsivity of hypothalamic paraventricular neurohypophyseal neurons to inputs from the subfornical organ in the rat.* Experimental Brain Research, 1987. **68**(3): p. 586-592.

6. da Silva, E.F., et al., *A1 Noradrenergic Neurons Lesions Reduce Natriuresis and Hypertensive Responses to Hypernatremia in Rats.* PLOS ONE, 2013. **8**(9): p. e73187.

7. Hanna, B.D., F. Lioy, and C. Polosa, *Role of carotid and central chemoreceptors in the CO2 response of sympathetic preganglionic neurons.* J Auton Nerv Syst, 1981. **3**(2-4): p. 421-35.

8. Moreira, T.S., et al., *Central chemoreceptors and sympathetic vasomotor outflow.* J Physiol, 2006. **577**(Pt 1): p. 369-86.

9. Biaggioni, I. and D. Robertson, *Primer on the autonomic nervous system.* 2012.

10. Mai, J.r.K. and G. Paxinos, *The human nervous system.* 2012.

11. McKinley, M.J., et al., *Vasopressin Secretion: Osmotic and Hormonal Regulation by the Lamina Terminalis.* Journal of Neuroendocrinology, 2004. **16**(4): p. 340-347.

12. McKinley, M.J., et al., *The median preoptic nucleus: front and centre for the regulation of body fluid, sodium, temperature, sleep and cardiovascular homeostasis.* Acta Physiologica, 2015. **214**(1): p. 8-32.

13. Thomas, G.D., *Neural control of the circulation.* Advances in Physiology Education, 2011. **35**(1): p. 28-32.

14. Benjamin, E.J., et al., *Heart Disease and Stroke Statistics-2017 Update: A Report From the American Heart Association.* Circulation, 2017. **135**(10): p. e146-e603.

15. Heron, M., *Deaths: Leading Causes for 2015.* Natl Vital Stat Rep, 2017. **66**(5): p. 1-76.

16. Mosterd, A. and A.W. Hoes, *Clinical epidemiology of heart failure.* Heart, 2007. **93**(9): p. 1137-46.

17. Roger, V.L., *Epidemiology of heart failure.* Circ Res, 2013. **113**(6): p. 646-59.

18. McCullough, P.A., et al., *Confirmation of a heart failure epidemic: findings from the Resource Utilization Among Congestive Heart Failure (REACH) study.* J Am Coll Cardiol, 2002. **39**(1): p. 60-9.

19. King, M., J. Kingery, and B. Casey, *Diagnosis and evaluation of heart failure.* Am Fam Physician, 2012. **85**(12): p. 1161-8.

20. Cody, R.J., *Clinical trials of diuretic therapy in heart failure: Research directions and clinical considerations.* Journal of the American College of Cardiology, 1993. **22**(4 Supplement 1): p. A165-A171.

21. *The Effect of Digoxin on Mortality and Morbidity in Patients with Heart Failure.* New England Journal of Medicine, 1997. **336**(8): p. 525-533.

22. Muntner, P., et al., *Potential US Population Impact of the 2017 ACC/AHA High Blood Pressure Guideline.* Circulation, 2018. **137**(2): p. 109-118.

23. Nwankwo, T., et al., *Hypertension among adults in the United States: National Health and Nutrition Examination Survey, 2011-2012.* NCHS Data Brief, 2013(133): p. 1-8.

24. Cohen, J.D., *Hypertension epidemiology and economic burden: refining risk assessment to lower costs.* Manag Care, 2009. **18**(10): p. 51-8.

25. Carretero, O.A. and S. Oparil, *Essential Hypertension.* Circulation, 2000. **101**(3): p. 329-335.

26. Whelton, P.K., et al., *2017 ACC/AHA/AAPA/ABC/ACPM/AGS/APhA/ASH/ASPC/NMA/PCNA Guideline for the Prevention, Detection, Evaluation, and Management of High Blood Pressure in Adults: A Report of the American College of Cardiology/American Heart Association Task Force on Clinical Practice Guidelines.* Hypertension, 2018. **71**(6): p. e13-e115.

27. Egan, B.M., et al., *Prevalence of optimal treatment regimens in patients with apparent treatment-resistant hypertension based on office blood pressure in a community-based practice network.* Hypertension, 2013. **62**(4): p. 691-7.

28. Triposkiadis, F., et al., *The sympathetic nervous system in heart failure physiology, pathophysiology, and clinical implications.* J Am Coll Cardiol, 2009. **54**(19): p. 1747-62.

29. Verloop, W.L., et al., *A systematic review concerning the relation between the sympathetic nervous system and heart failure with preserved left ventricular ejection fraction.* PLoS One, 2015. **10**(2): p. e0117332.

30. Shah, A.M., et al., *Influence of Ejection Fraction on the Prognostic Value of Sympathetic Innervation Imaging With Iodine-123 MIBG in Heart Failure.* JACC: Cardiovascular Imaging, 2012. **5**(11): p. 1139-1146.

31. Floras, J.S., *Sympathetic Nervous System Activation in Human Heart Failure: Clinical Implications of an Updated Model.* Journal of the American College of Cardiology, 2009. **54**(5): p. 375-385.

32. Zucker, I.H., et al., *Chronic Baroreceptor Activation Enhances Survival in Dogs With Pacing-Induced Heart Failure.* Hypertension, 2007. **50**(5): p. 904-910.

33. Zucker, I.H., *Novel Mechanisms of Sympathetic Regulation in Chronic Heart Failure.* Hypertension, 2006. **48**(6): p. 1005-1011.

34. Zucker, I.H., et al., *Regulation of central angiotensin type 1 receptors and sympathetic outflow in heart failure.* American Journal of Physiology-Heart and Circulatory Physiology, 2009. **297**(5): p. H1557-H1566.

35. Gao, L., et al., *Sympathoexcitation by central ANG II: Roles for AT1 receptor upregulation and NAD(P)H oxidase in RVLM.* American Journal of Physiology-Heart and Circulatory Physiology, 2005. **288**(5): p. H2271-H2279.

36. Mancia, G. and G. Grassi, *The Autonomic Nervous System and Hypertension.* Circulation Research, 2014. **114**(11): p. 1804-1814.

37. Ferrier, C., H. Cox, and M. Esler, *Elevated total body noradrenaline spillover in normotensive members of hypertensive families.* Clin Sci (Lond), 1993. **84**(2): p. 225-30.

38. Bianchetti, M.G., et al., *Disturbed noradrenergic blood pressure control in normotensive members of hypertensive families.* Br Heart J, 1984. **51**(3): p. 306-11.

39. Piccirillo, G., et al., *Autonomic modulation of heart rate and blood pressure in normotensive offspring of hypertensive subjects.* Journal of Laboratory and Clinical Medicine, 2000. **135**(2): p. 145-152.

40. Klatt, E.C., V. Kumar, and S.L. Robbins, *Robbins and Cotran review of pathology*. 2010, Philadelphia: Saunders/Elsevier.

41. De Mello, W.C. and E.D. Frohlich, *On the local cardiac renin angiotensin system. Basic and clinical implications.* Peptides, 2011. **32**(8): p. 1774-1779.

42. Serneri, G.G.N., et al., *Cardiac Angiotensin II Formation in the Clinical Course of Heart Failure and Its Relationship With Left Ventricular Function.* Circulation Research, 2001. **88**(9): p. 961-968.

43. Mazzolai, L., et al., *Blood Pressure–Independent Cardiac Hypertrophy Induced by Locally Activated Renin-Angiotensin System.* Hypertension, 1998. **31**(6): p. 1324-1330.

44. Clausmeyer, S., et al., *Tissue-specific expression of a rat renin transcript lacking the coding sequence for the prefragment and its stimulation by myocardial infarction.* Endocrinology, 2000. **141**(8): p. 2963-70.

45. De Mello, W.C., *Chemical Communication between Heart Cells is Disrupted by Intracellular Renin and Angiotensin II: Implications for Heart Development and Disease.* Front Endocrinol (Lausanne), 2015. **6**: p. 72.

46. Dzau, V.J., *Vascular renin-angiotensin: a possible autocrine or paracrine system in control of vascular function.* Journal of cardiovascular pharmacology, 1984. **6 Suppl 2**: p. S377-82.

47. De Mello, W.C., *Intracellular angiotensin II increases the total potassium current and the resting potential of arterial myocytes from vascular resistance vessels of the rat. Physiological and pathological implications.* Journal of the American Society of Hypertension, 2013. **7**(3): p. 192-197.

48. Navar, L.G., *The intrarenal renin-angiotensin system in hypertension.* Kidney International, 2004. **65**(4): p. 1522-1532.

49. Bickerton, R.K. and J.P. Buckley, *Evidence for a Central Mechanism in Angiotensin Induced Hypertension.* Proceedings of the Society for Experimental Biology and Medicine, 1961. **106**(4): p. 834-836.

50. Ganten, D., et al., *Renin in dog brain.* American Journal of Physiology-Legacy Content, 1971. **221**(6): p. 1733-1737.

51. Farag, E., et al., *The renin angiotensin system and the brain: New developments.* Journal of Clinical Neuroscience, 2017. **46**: p. 1-8.

52. Paul, M., A. Poyan Mehr, and R. Kreutz, *Physiology of local renin-angiotensin systems.* Physiol Rev, 2006. **86**(3): p. 747-803.

53. Luoh, H.F. and S.H. Chan, *Participation of AT1 and AT2 receptor subtypes in the tonic inhibitory modulation of baroreceptor reflex response by endogenous angiotensins at the nucleus tractus solitarii in the rat.* Brain Res, 1998. **782**(1-2): p. 73-82.

54. Morimoto, S., et al., *Elevated blood pressure in transgenic mice with brain-specific expression of human angiotensinogen driven by the glial fibrillary acidic protein promoter.* Circ Res, 2001. **89**(4): p. 365-72.

55. Takahashi, H., et al., *The central mechanism underlying hypertension: a review of the roles of sodium ions, epithelial sodium channels, the renin-angiotensin-aldosterone system, oxidative stress and endogenous digitalis in the brain.* Hypertens Res, 2011. **34**(11): p. 1147-60.

56. Mancia, G., et al., *Control of circulation by arterial baroreceptors and cardiopulmonary receptors in hypertension.* J Cardiovasc Pharmacol, 1986. **8 Suppl 5**: p. S82-8.

57. Heesch, C.M., M.E. Crandall, and J.A. Turbek, *Converting enzyme inhibitors cause pressure-independent resetting of baroreflex control of sympathetic outflow.* Am J Physiol, 1996. **270**(4 Pt 2): p. R728-37.

58. Skeggs, L.T., Jr., J.R. Kahn, and N.P. Shumway, *The preparation and function of the hypertensin-converting enzyme.* J Exp Med, 1956. **103**(3): p. 295-9.

59. Fleming, I., *Signaling by the Angiotensin-Converting Enzyme.* Circulation Research, 2006. **98**(7): p. 887-896.

60. Ramchandran, R., et al., *Regulated cleavage-secretion of the membrane-bound angiotensin-converting enzyme.* J Biol Chem, 1994. **269**(3): p. 2125-30.

61. Coates, D., *The angiotensin converting enzyme (ACE).* Int J Biochem Cell Biol, 2003. **35**(6): p. 769-73.

62. Bicket, D.P., *Using ACE inhibitors appropriately.* Am Fam Physician, 2002. **66**(3): p. 461-8.

63. Tipnis, S.R., et al., *A human homolog of angiotensin-converting enzyme. Cloning and functional expression as a captopril-insensitive carboxypeptidase.* J Biol Chem, 2000. **275**(43): p. 33238-43.

64. Vickers, C., et al., *Hydrolysis of biological peptides by human angiotensin-converting enzyme-related carboxypeptidase.* J Biol Chem, 2002. **277**(17): p. 14838-43.

65. Xu, P., S. Sriramula, and E. Lazartigues, *ACE2/ANG-(1-7)/Mas pathway in the brain: the axis of good.* Am J Physiol Regul Integr Comp Physiol, 2011. **300**(4): p. R804-17.

66. Harmer, D., et al., *Quantitative mRNA expression profiling of ACE 2, a novel homologue of angiotensin converting enzyme.* FEBS Lett, 2002. **532**(1-2): p. 107-10.

67. Xia, H. and E. Lazartigues, *Angiotensin-converting enzyme 2: central regulator for cardiovascular function.* Curr Hypertens Rep, 2010. **12**(3): p. 170-5.

68. Xiao, L., et al., *Brain-selective overexpression of angiotensin-converting enzyme 2 attenuates sympathetic nerve activity and enhances baroreflex function in chronic heart failure.* Hypertension, 2011. **58**(6): p. 1057-65.

69. Potts, P.D., et al., *The cardiovascular effects of angiotensin-(1-7) in the rostral and caudal ventrolateral medulla of the rabbit.* Brain Res, 2000. **877**(1): p. 58-64.

70. Fontes, M.A., et al., *Evidence that angiotensin-(1-7) plays a role in the central control of blood pressure at the ventro-lateral medulla acting through specific receptors.* Brain Res, 1994. **665**(1): p. 175-80.

71. Silva, A.Q., R.A. Santos, and M.A. Fontes, *Blockade of endogenous angiotensin-(1-7) in the hypothalamic paraventricular nucleus reduces renal sympathetic tone.* Hypertension, 2005. **46**(2): p. 341-8.

72. Gironacci, M.M., et al., *Angiotensin-(1-7) inhibitory mechanism of norepinephrine release in hypertensive rats.* Hypertension, 2004. **44**(5): p. 783-7.

73. Byku, M., H. Macarthur, and T.C. Westfall, *Inhibitory effects of angiotensin-(1-7) on the nerve stimulation-induced release of norepinephrine and neuropeptide Y from the mesenteric arterial bed.* American journal of physiology. Heart and circulatory physiology, 2010. **298**(2): p. H457-H465.

74. Sriramula, S., et al., *ACE2 overexpression in the paraventricular nucleus attenuates angiotensin II-induced hypertension.* Cardiovasc Res, 2011. **92**(3): p. 401-8.

75. Xia, H., et al., *ACE2-mediated reduction of oxidative stress in the central nervous system is associated with improvement of autonomic function.* PLoS One, 2011. **6**(7): p. e22682.

76. Feng, Y., et al., *Angiotensin-converting enzyme 2 overexpression in the subfornical organ prevents the angiotensin II-mediated pressor and drinking responses and is associated with angiotensin II type 1 receptor downregulation.* Circ Res, 2008. **102**(6): p. 729-36.

77. Harman, D., *Aging: a theory based on free radical and radiation chemistry.* Journal of gerontology, 1956. **11**(3): p. 298-300.

78. Sies, H., *Oxidative stress.* 1985.

79. Fink, G. and Gale, *Encyclopedia of stress.* 2007.

80. Liguori, I., et al., *Oxidative stress, aging, and diseases.* Clin Interv Aging, 2018. **13**: p. 757-772.

81. Brown, G.C. and V. Borutaite, *There is no evidence that mitochondria are the main source of reactive oxygen species in mammalian cells.* Mitochondrion, 2012. **12**(1): p. 1-4.

82. Lushchak, V.I., *Free radicals, reactive oxygen species, oxidative stress and its classification.* Chem Biol Interact, 2014. **224**: p. 164-75.

83. Valko, M., et al., *Free radicals and antioxidants in normal physiological functions and human disease.* Int J Biochem Cell Biol, 2007. **39**(1): p. 44-84.

84. Sun, W., et al., *Monitoring structural modulation of redox-sensitive proteins in cells with MS-CETSA.* Redox Biol, 2019. **24**: p. 101168.

85. Tsutsui, H., S. Kinugawa, and S. Matsushima, *Oxidative stress and heart failure.* American Journal of Physiology-Heart and Circulatory Physiology, 2011. **301**(6): p. H2181-H2190.

86. Takimoto, E. and D.A. Kass, *Role of oxidative stress in cardiac hypertrophy and remodeling.* Hypertension, 2007. **49**(2): p. 241-8.

87. Lindley, T.E., et al., *Superoxide Is Involved in the Central Nervous System Activation and Sympathoexcitation of Myocardial Infarction–Induced Heart Failure.* Circulation Research, 2004. **94**(3): p. 402-409.

88. Gao, L., et al., *Superoxide Mediates Sympathoexcitation in Heart Failure.* Circulation Research, 2004. **95**(9): p. 937-944.

89. Vallance, P. and A. Hingorani, *Endothelial nitric oxide in humans in health and disease.* Int J Exp Pathol, 1999. **80**(6): p. 291-303.

90. Touyz, R.M., *Reactive oxygen species and angiotensin II signaling in vascular cells -- implications in cardiovascular disease.* Braz J Med Biol Res, 2004. **37**(8): p. 1263-73.

91. Touyz, R.M., *Reactive oxygen species, vascular oxidative stress, and redox signaling in hypertension: what is the clinical significance?* Hypertension, 2004. **44**(3): p. 248-52.

92. Gavazzi, G., et al., *Decreased blood pressure in NOX1-deficient mice.* FEBS Lett, 2006. **580**(2): p. 497-504.

93. Campos, R.R., *Oxidative stress in the brain and arterial hypertension.* Hypertension Research, 2009. **32**(12): p. 1047-1048.

94. Hirooka, Y., *Oxidative stress in the cardiovascular center has a pivotal role in the sympathetic activation in hypertension.* Hypertension Research, 2011. **34**(4): p. 407-412.

95. Huber, M.J., et al., *Activation of the (pro)renin receptor in the paraventricular nucleus increases sympathetic outflow in anesthetized rats.* Am J Physiol Heart Circ Physiol, 2015. **309**(5): p. H880-7.

96. Carmichael, C.Y. and R.D. Wainford, *Hypothalamic signaling mechanisms in hypertension.* Curr Hypertens Rep, 2015. **17**(5): p. 39.

97. Chan, S.H.H. and J. Chan, *Angiotensin-Generated Reactive Oxygen Species in Brain and Pathogenesis of Cardiovascular Diseases.* Antioxidants & redox signaling, 2012. **19**.

98. Wollert, K.C. and H. Drexler, *The renin–angiotensin system and experimental heart failure.* Cardiovascular Research, 1999. **43**(4): p. 838-849.

99. Leenen, F.H., et al., *Brain 'ouabain' mediates sympathetic hyperactivity in congestive heart failure.* Circ Res, 1995. **77**(5): p. 993-1000.

100. Tan, J., H. Wang, and F.H. Leenen, *Increases in brain and cardiac AT1 receptor and ACE densities after myocardial infarct in rats.* Am J Physiol Heart Circ Physiol, 2004. **286**(5): p. H1665-71.

101. Kar, S., L. Gao, and I.H. Zucker, *Exercise training normalizes ACE and ACE2 in the brain of rabbits with pacing-induced heart failure.* J Appl Physiol (1985), 2010. **108**(4): p. 923-32.

102. Ma, R., I.H. Zucker, and W. Wang, *Central gain of the cardiac sympathetic afferent reflex in dogs with heart failure.* American Journal of Physiology-Heart and Circulatory Physiology, 1997. **273**(6): p. H2664-H2671.

103. Wang, W. and R. Ma, *Cardiac Sympathetic Afferent Reflexes in Heart Failure.* Heart Failure Reviews, 2000. **5**(1): p. 57-71.

104. Zhu, G.-Q., et al., *AT1 receptor mRNA antisense normalizes enhanced cardiac sympathetic afferent reflex in rats with chronic heart failure.* American Journal of Physiology-Heart and Circulatory Physiology, 2004. **287**(4): p. H1828-H1835.

105. Liu, D., et al., *Neuronal Angiotensin II Type 1 Receptor Upregulation in Heart Failure.* Circulation Research, 2006. **99**(9): p. 1004-1011.

106. Zanzinger, J. and J. Czachurski, *Chronic oxidative stress in the RVLM modulates sympathetic control of circulation in pigs.* Pflugers Arch, 2000. **439**(4): p. 489-94.

107. Zimmerman, M.C., et al., *Superoxide Mediates the Actions of Angiotensin II in the Central Nervous System.* Circulation Research, 2002. **91**(11): p. 1038-1045.

108. Campese, V.M., Y. Shaohua, and Z. Huiquin, *Oxidative Stress Mediates Angiotensin II–Dependent Stimulation of Sympathetic Nerve Activity.* Hypertension, 2005. **46**(3): p. 533-539.

109. Sun, C., et al., *NAD(P)H Oxidase Inhibition Attenuates Neuronal Chronotropic Actions of Angiotensin II.* Circulation Research, 2005. **96**(6): p. 659-666.

110. Zimmerman, M.C., R.V. Sharma, and R.L. Davisson, *Superoxide Mediates Angiotensin II–Induced Influx of Extracellular Calcium in Neural Cells.* Hypertension, 2005. **45**(4): p. 717-723.

111. Grassi, G., G. Seravalle, and F. Quarti-Trevano, *The 'neuroadrenergic hypothesis' in hypertension: current evidence.* Experimental Physiology, 2010. **95**(5): p. 581-586.

112. Lochard, N., et al., *Brain-specific restoration of angiotensin II corrects renal defects seen in angiotensinogen-deficient mice.* J Biol Chem, 2003. **278**(4): p. 2184-9.

113. Morimoto, S., M.D. Cassell, and C.D. Sigmund, *Glia- and neuron-specific expression of the renin-angiotensin system in brain alters blood pressure, water intake, and salt preference.* J Biol Chem, 2002. **277**(36): p. 33235-41.

114. Jun, T., F. Ke-yan, and M. Catalano, *Increased superoxide anion production in humans: a possible mechanism for the pathogenesis of hypertension.* J Hum Hypertens, 1996. **10**(5): p. 305-9.

115. Sousa, T., et al., *Role of H(2)O(2) in hypertension, renin-angiotensin system activation and renal medullary disfunction caused by angiotensin II.* Br J Pharmacol, 2012. **166**(8): p. 2386-401.

116. Rodrigo, R., J. González, and F. Paoletto, *The role of oxidative stress in the pathophysiology of hypertension.* Hypertension Research, 2011. **34**(4): p. 431-440.

117. Dikalov, S.I. and Z. Ungvari, *Role of mitochondrial oxidative stress in hypertension.* Am J Physiol Heart Circ Physiol, 2013. **305**(10): p. H1417-27.

118. Wardyn, J.D., A.H. Ponsford, and C.M. Sanderson, *Dissecting molecular cross-talk between Nrf2 and NF-kappaB response pathways.* Biochem Soc Trans, 2015. **43**(4): p. 621-6.

119. Sun, Z., et al., *Keap1 controls postinduction repression of the Nrf2-mediated antioxidant response by escorting nuclear export of Nrf2.* Mol Cell Biol, 2007. **27**(18): p. 6334-49.

120. Gao, L., et al., *Selective Nrf2 Gene Deletion in the Rostral Ventrolateral Medulla Evokes Hypertension and Sympathoexcitation in Mice.* Hypertension, 2017. **69**(6): p. 1198-1206.

121. Gao, L., et al., *Superoxide mediates sympathoexcitation in heart failure: roles of angiotensin II and NAD(P)H oxidase.* Circ Res, 2004. **95**(9): p. 937-44.

122. Feng, Y., et al., *Brain-selective overexpression of human Angiotensin-converting enzyme type 2 attenuates neurogenic hypertension.* Circ Res, 2010. **106**(2): p. 373-82.

123. Jacquot, S., et al., *Optimizing PCR for Mouse Genotyping: Recommendations for Reliable, Rapid, Cost Effective, Robust and Adaptable to High-Throughput Genotyping Protocol for Any Type of Mutation.* Current Protocols in Mouse Biology, 2019. **9**(4): p. e65.

124. *ARRIVE Guidelines.* ANIMAL TECHNOLOGY AND WELFARE, 2014. **13**(1): p. 38-42.

125. Thireau, J., et al., *Heart rate variability in mice: a theoretical and practical guide.* Exp Physiol, 2008. **93**(1): p. 83-94.

126. Chen, J., et al., *Variability in coronary artery anatomy affects consistency of cardiac damage after myocardial infarction in mice.* American Journal of Physiology-Heart and Circulatory Physiology, 2017. **313**(2): p. H275-H282.

127. Gao, L., et al., *Selective Nrf2 Gene Deletion in the Rostral Ventrolateral Medulla Evokes Hypertension and Sympathoexcitation in Mice.* Hypertension, 2017. **69**(6): p. 1198-1206.

128. Hamelmann, E., et al., *Noninvasive measurement of airway responsiveness in allergic mice using barometric plethysmography.* Am J Respir Crit Care Med, 1997. **156**(3 Pt 1): p. 766-75.

129. Baudrie, V., D. Laude, and J.-L. Elghozi, *Optimal frequency ranges for extracting information on cardiovascular autonomic control from the blood pressure and pulse interval spectrograms in mice.* American Journal of Physiology-Regulatory, Integrative and Comparative Physiology, 2007. **292**(2): p. R904-R912.

130. Paxinos, G. and K.B.J. Franklin, *The mouse brain in stereotaxic coordinates*. 2019.

131. Berliner, D. and J. Bauersachs, *Current Drug Therapy in Chronic Heart Failure: the New Guidelines of the European Society of Cardiology (ESC).* Korean Circ J, 2017. **47**(5): p. 543-554.

132. Dampney, R.A.L., A.K. Goodchild, and E. Tan, *Identification of Cardiovascular Cell Groups in the Brain Stem.* Clinical and Experimental Hypertension. Part A: Theory and Practice, 1984. **6**(1-2): p. 205-220.

133. Gao, L., et al., *Simvastatin therapy normalizes sympathetic neural control in experimental heart failure: roles of angiotensin II type 1 receptors and NAD(P)H oxidase.* Circulation, 2005. **112**(12): p. 1763-70.

134. Gao, L., et al., *Exercise training normalizes sympathetic outflow by central antioxidant mechanisms in rabbits with pacing-induced chronic heart failure.* Circulation, 2007. **115**(24): p. 3095-102.

135. Angelova, P.R. and A.Y. Abramov, *Role of mitochondrial ROS in the brain: from physiology to neurodegeneration.* FEBS Letters, 2018. **592**(5): p. 692-702.

136. Tarafdar, A. and G. Pula, *The Role of NADPH Oxidases and Oxidative Stress in Neurodegenerative Disorders.* International Journal of Molecular Sciences, 2018. **19**(12): p. 3824.

137. Patel, M., *Targeting Oxidative Stress in Central Nervous System Disorders.* Trends Pharmacol Sci, 2016. **37**(9): p. 768-778.

138. *Transcriptional Regulation by Nrf2.* Antioxidants & Redox Signaling, 2018. **29**(17): p. 1727-1745.

139. Wang, H.-J., et al., *Exercise training prevents the exaggerated exercise pressor reflex in rats with chronic heart failure.* Journal of Applied Physiology, 2010. **108**(5): p. 1365-1375.

140. Riehle, C. and J. Bauersachs, *Small animal models of heart failure.* Cardiovascular research, 2019. **115**(13): p. 1838-1849.

141. Houser, S.R., et al., *Animal Models of Heart Failure.* Circulation Research, 2012. **111**(1): p. 131-150.

142. Gomes, A.C., et al., *Rodent models of heart failure: an updated review.* Heart Fail Rev, 2013. **18**(2): p. 219-49.

143. Zucker, I.H., *Novel mechanisms of sympathetic regulation in chronic heart failure.* Hypertension, 2006. **48**(6): p. 1005-11.

144. Guyenet, P.G., et al., *Rostral Ventrolateral Medulla and Hypertension.* 2018. **72**(3): p. 559-566.

145. Bai, J., et al., *Central administration of tert-butylhydroquinone attenuates hypertension via regulating Nrf2 signaling in the hypothalamic paraventricular nucleus of hypertensive rats.* Toxicol Appl Pharmacol, 2017. **333**: p. 100-109.

146. Guyenet, P.G., et al., *C1 neurons: the body's EMTs.* Am J Physiol Regul Integr Comp Physiol, 2013. **305**(3): p. R187-204.

147. Dash, K.E., et al., *Do Non-C1 Cells In The Rostral Ventrolateral Medulla Increase Blood Pressure?* 2017. **31**(1_supplement): p. 827.5-827.5.

148. Lassmann, H. and J. van Horssen, *Oxidative stress and its impact on neurons and glia in multiple sclerosis lesions.* Biochim Biophys Acta, 2016. **1862**(3): p. 506-10.

149. Frazzini, V., et al., *Altered Kv2.1 functioning promotes increased excitability in hippocampal neurons of an Alzheimer's disease mouse model.* Cell Death Dis, 2016. **7**: p. e2100.

150. Oyarce, M.P. and R. Iturriaga, *Contribution of Oxidative Stress and Inflammation to the Neurogenic Hypertension Induced by Intermittent Hypoxia.* Front Physiol, 2018. **9**: p. 893.

151. Kawasaki, Y., et al., *Clinicopathological significance of nuclear factor (erythroid-2)-related factor 2 (Nrf2) expression in gastric cancer.* BMC Cancer, 2015. **15**: p. 5.

152. Saxena, T., A.O. Ali, and M. Saxena, *Pathophysiology of essential hypertension: an update.* Expert Rev Cardiovasc Ther, 2018. **16**(12): p. 879-887.

153. Guyenet, P.G., *The sympathetic control of blood pressure.* Nature Reviews Neuroscience, 2006. **7**: p. 335.

154. Unger, T., et al., *Central blood pressure effects of substance P and angiotensin II: role of the sympathetic nervous system and vasopressin.* Eur J Pharmacol, 1981. **71**(1): p. 33-42.

155. Gao, L., et al., *Sympathoexcitation by central ANG II: roles for AT1 receptor upregulation and NAD(P)H oxidase in RVLM.* Am J Physiol Heart Circ Physiol, 2005. **288**(5): p. H2271-9.

156. Queiroz, T., M. Monteiro, and V. Braga, *Angiotensin-II-derived reactive oxygen species on baroreflex sensitivity during hypertension: new perspectives.* 2013. **4**(105).

157. Chappell, M.C., et al., *Identification of angiotensin-(1-7) in rat brain. Evidence for differential processing of angiotensin peptides.* J Biol Chem, 1989. **264**(28): p. 16518-23.

158. Yamazato, M., et al., *Overexpression of angiotensin-converting enzyme 2 in the rostral ventrolateral medulla causes long-term decrease in blood pressure in the spontaneously hypertensive rats.* Hypertension, 2007. **49**(4): p. 926-31.

159. Silva, R.A.P., et al., *Impact of ACE2 Deficiency and Oxidative Stress on Cerebrovascular Function With Aging.* Stroke, 2012. **43**(12): p. 3358-3363.

160. Santos Robson, A., *Angiotensin-(1–7).* Hypertension, 2014. **63**(6): p. 1138-1147.

161. Padda, R.S., et al., *Angiotensin-(1-7): A Novel Peptide to Treat Hypertension and Nephropathy in Diabetes?* J Diabetes Metab, 2015. **6**(10).

162. Diz, D.I., et al., *Angiotensin-(1-7) and baroreflex function in nucleus tractus solitarii of (mRen2)27 transgenic rats.* J Cardiovasc Pharmacol, 2008. **51**(6): p. 542-8.

163. Gomolak, J.R. and S.P. Didion, *Angiotensin II-induced endothelial dysfunction is temporally linked with increases in interleukin-6 and vascular macrophage accumulation.* Front Physiol, 2014. **5**: p. 396.

164. Dierschke, S.K., et al., *Angiotensin-(1–7) Attenuates Protein O-GlcNAcylation in the Retina by EPAC/Rap1-Dependent Inhibition of O-GlcNAc Transferase.* Investigative Ophthalmology & Visual Science, 2020. **61**(2): p. 24-24.

165. Fitzsimons, J.T., *Angiotensin, thirst, and sodium appetite.* Physiol Rev, 1998. **78**(3): p. 583-686.

166. Catt, K.J., et al., *Angiotensin II blood-levels in human hypertension.* Lancet, 1971. **1**(7697): p. 459-64.

167. Young, C.N. and R.L. Davisson, *Angiotensin-II, the Brain, and Hypertension: An Update.* Hypertension, 2015. **66**(5): p. 920-6.

168. Biancardi, V.C. and J.E. Stern, *Compromised blood-brain barrier permeability: novel mechanism by which circulating angiotensin II signals to sympathoexcitatory centres during hypertension.* J Physiol, 2016. **594**(6): p. 1591-600.

169. Biancardi, V.C., et al., *Circulating angiotensin II gains access to the hypothalamus and brain stem during hypertension via breakdown of the blood-brain barrier.* Hypertension, 2014. **63**(3): p. 572-9.

170. Jackson, L., et al., *Within the Brain: The Renin Angiotensin System.* Int J Mol Sci, 2018. **19**(3).

171. Wysocki, J., et al., *Targeting the degradation of angiotensin II with recombinant angiotensin-converting enzyme 2: prevention of angiotensin II-dependent hypertension.* Hypertension, 2010. **55**(1): p. 90-8.

172. Campagnole-Santos, M.J., et al., *Differential baroreceptor reflex modulation by centrally infused angiotensin peptides.* Am J Physiol, 1992. **263**(1 Pt 2): p. R89-94.

173. Maric-Bilkan, C. and M.B. Manigrasso, *Sex Differences in Hypertension: Contribution of the Renin–Angiotensin System.* Gender Medicine, 2012. **9**(4): p. 287-291.

174. White, M.C., R. Fleeman, and A.C. Arnold, *Sex differences in the metabolic effects of the renin-angiotensin system.* Biol Sex Differ, 2019. **10**(1): p. 31.

175. Liu, J., et al., *Sex differences in renal angiotensin converting enzyme 2 (ACE2) activity are 17beta-oestradiol-dependent and sex chromosome-independent.* Biol Sex Differ, 2010. **1**(1): p. 6.

176. Wang, C., et al., *NRF2 PREVENTS HYPERTENSION, INCREASED ADMA, MICROVASCULAR OXIDATIVE STRESS AND DYSFUNCTION IN MICE WITH TWO WEEKS OF ANGIOTENSIN II INFUSION.* American Journal of Physiology - Regulatory, Integrative and Comparative Physiology, 2017. **314**: p. ajpregu.00122.2017.

177. Grossman, E., *Does increased oxidative stress cause hypertension?* Diabetes Care, 2008. **31 Suppl 2**: p. S185-9.

178. Lopes, R.A., et al., *Downregulation of Nuclear Factor Erythroid 2–Related Factor and Associated Antioxidant Genes Contributes to Redox-Sensitive Vascular Dysfunction in Hypertension.* Hypertension, 2015. **66**(6): p. 1240-1250.

179. Senanayake, G.V., et al., *The dietary phase 2 protein inducer sulforaphane can normalize the kidney epigenome and improve blood pressure in hypertensive rats.* Am J Hypertens, 2012. **25**(2): p. 229-35.

180. Noyan-Ashraf, M.H., et al., *Dietary approaches to positively influence fetal determinants of adult health.* Faseb j, 2006. **20**(2): p. 371-3.

181. Chang, S.Y., et al., *Overexpression of angiotensinogen downregulates aquaporin 1 expression via modulation of Nrf2-HO-1 pathway in renal proximal tubular cells of transgenic mice.* J Renin Angiotensin Aldosterone Syst, 2016. **17**(3).

182. Zhao, S., et al., *Nrf2 Deficiency Upregulates Intrarenal Angiotensin-Converting Enzyme-2 and Angiotensin 1-7 Receptor Expression and Attenuates Hypertension and Nephropathy in Diabetic Mice.* Endocrinology, 2017. **159**(2): p. 836-852.

183. Kang, K.W., *Angiotensin II-mediated Nrf2 down-regulation: a potential causing factor for renal fibrosis?* Arch Pharm Res, 2011. **34**(5): p. 695-7.

184. Afonso, V., et al., *Reactive oxygen species and superoxide dismutases: role in joint diseases.* Joint Bone Spine, 2007. **74**(4): p. 324-9.

185. Zhu, H., et al., *Role of Nrf2 signaling in regulation of antioxidants and phase 2 enzymes in cardiac fibroblasts: protection against reactive oxygen and nitrogen species-induced cell injury.* FEBS Lett, 2005. **579**(14): p. 3029-36.

186. Pepe, G., et al., *beta-Lactoglobulin Heptapeptide Reduces Oxidative Stress in Intestinal Epithelial Cells and Angiotensin II-Induced Vasoconstriction on Mouse Mesenteric Arteries by Induction of Nuclear Factor Erythroid 2-Related Factor 2 (Nrf2) Translocation.* Oxid Med Cell Longev, 2019. **2019**: p. 1616239.

187. Tian, C., et al., *Myocardial infarction-induced microRNA-enriched exosomes contribute to cardiac Nrf2 dysregulation in chronic heart failure.* 2018. **314**(5): p. H928-H939.

188. Osburn, W.O. and T.W. Kensler, *Nrf2 signaling: an adaptive response pathway for protection against environmental toxic insults.* Mutat Res, 2008. **659**(1-2): p. 31-9.

189. Ruiz, S., et al., *Targeting the transcription factor Nrf2 to ameliorate oxidative stress and inflammation in chronic kidney disease.* Kidney Int, 2013. **83**(6): p. 1029-41.

190. Lim, J.L., et al., *Antioxidative defense mechanisms controlled by Nrf2: state-of-the-art and clinical perspectives in neurodegenerative diseases.* Arch Toxicol, 2014. **88**(10): p. 1773-86.

191. Wafi, A.M., et al., *Curcumin improves exercise performance of mice with coronary artery ligation-induced HFrEF: Nrf2 and antioxidant mechanisms in skeletal muscle.* J Appl Physiol (1985), 2019. **126**(2): p. 477-486.

192. Bai, Y., et al., *Sulforaphane Protects against Cardiovascular Disease via Nrf2 Activation.* Oxid Med Cell Longev, 2015. **2015**: p. 407580.

193. Deng, Y., et al., *[Expression of neprilysin gene is associated with methylation and histone modification on promoter in mouse neuroblastoma Neuro-2a cells].* Xi Bao Yu Fen Zi Mian Yi Xue Za Zhi, 2014. **30**(8): p. 810-3.

194. Deshotels, M.R., et al., *Angiotensin II Mediates Angiotensin Converting Enzyme Type 2 Internalization and Degradation Through an Angiotensin II Type I Receptor–Dependent Mechanism.* Hypertension, 2014. **64**(6): p. 1368-1375.

195. Balasubramanian, P., et al., *Obesity-induced sympathoexcitation is associated with Nrf2 dysfunction in the rostral ventrolateral medulla.* American Journal of Physiology-Regulatory, Integrative and Comparative Physiology, 2020. **318**(2): p. R435-R444.

196. Sita, G., et al., *Sulforaphane from Cruciferous Vegetables: Recent Advances to Improve Glioblastoma Treatment.* Nutrients, 2018. **10**(11).

197. O'Connell, T.D., et al., *Cardiac alpha1-adrenergic receptors: novel aspects of expression, signaling mechanisms, physiologic function, and clinical importance.* Pharmacol Rev, 2014. **66**(1): p. 308-33.

198. Zhong, J., et al., *Angiotensin-converting enzyme 2 suppresses pathological hypertrophy, myocardial fibrosis, and cardiac dysfunction.* Circulation, 2010. **122**(7): p. 717-28, 18 p following 728.

199. Lo, J., et al., *Angiotensin-converting enzyme 2 antagonizes angiotensin II-induced pressor response and NADPH oxidase activation in Wistar-Kyoto rats and spontaneously hypertensive rats.* Exp Physiol, 2013. **98**(1): p. 109-22.

200. Hernandez Prada, J.A., et al., *Structure-based identification of small-molecule angiotensin-converting enzyme 2 activators as novel antihypertensive agents.* Hypertension, 2008. **51**(5): p. 1312-7.

201. van Twist, D.J.L., A.A. Kroon, and P.W. de Leeuw, *Angiotensin-(1-7) as a strategy in the treatment of hypertension?* Current Opinion in Nephrology and Hypertension, 2014. **23**(5): p. 480-486.

202. Shi, Y., et al., *Ang 1-7 Prevents Systemic Hypertension, Attenuates Oxidative Stress and Tubulointerstitial Fibrosis, and Normalizes Renal Angiotensin-Converting Enzyme 2 and Mas Receptor Expression in Diabetic Mice.* Clinical science (London, England : 1979), 2014. **128**.

203. Tsuda, K., *Angiotensin 1–7 and the Sympathetic Nervous System in Hypertensive Kidney Disease.* American Journal of Hypertension, 2019. **32**(10): p. e3-e3.

204. de Macedo, S.M., et al., *Angiotensin converting enzyme 2 activator (DIZE) modulates metabolic profiles in mice, decreasing lipogenesis.* Protein and peptide letters, 2015. **22**(4): p. 332-340.

205. Sun, Y., et al., *Sulforaphane Protects against Brain Diseases: Roles of Cytoprotective Enzymes.* Austin J Cerebrovasc Dis Stroke, 2017. **4**(1).

206. Zhao, X., et al., *Dimethyl Fumarate Protects Brain From Damage Produced by Intracerebral Hemorrhage by Mechanism Involving Nrf2.* Stroke, 2015. **46**(7): p. 1923-8.

207. Jiang, T., et al., *ACE2-Ang-(1-7)-Mas Axis in Brain: A Potential Target for Prevention and Treatment of Ischemic Stroke.* Curr Neuropharmacol, 2013. **11**(2): p. 209-17.

208. Saraswathi, V., et al., *Nanoformulated copper/zinc superoxide dismutase attenuates vascular cell activation and aortic inflammation in obesity.* Biochem Biophys Res Commun, 2016. **469**(3): p. 495-500.

209. Savalia, K., et al., *Neuronal uptake of nanoformulated superoxide dismutase and attenuation of angiotensin II-dependent hypertension after central administration.* Free Radic Biol Med, 2014. **73**: p. 299-307.

210. Rosenbaugh, E.G., et al., *The attenuation of central angiotensin II-dependent pressor response and intra-neuronal signaling by intracarotid injection of nanoformulated copper/zinc superoxide dismutase.* Biomaterials, 2010. **31**(19): p. 5218-26.

211. Apostolova, N. and V.M. Victor, *Molecular strategies for targeting antioxidants to mitochondria: therapeutic implications.* Antioxid Redox Signal, 2015. **22**(8): p. 686-729.

212. Antimisiaris, S.G., S. Mourtas, and A. Marazioti, *Exosomes and Exosome-Inspired Vesicles for Targeted Drug Delivery.* Pharmaceutics, 2018. **10**(4).

213. Haack, K.K., et al., *Abstract 175: Activation of Nrf2 by Exercise Training and Curcumin Contributes to Sympatho-Inhibition in Heart Failure.* Hypertension, 2013. **62**(suppl_1): p. A175-A175.

214. Wafi, A.M., et al., *Exercise training upregulates Nrf2 protein in the rostral ventrolateral medulla of mice with heart failure.* Journal of Applied Physiology, 2019. **127**(5): p. 1349-1359.

215. Bryan, H.K., et al., *The Nrf2 cell defence pathway: Keap1-dependent and -independent mechanisms of regulation.* Biochemical Pharmacology, 2013. **85**(6): p. 705-717.

216. White, L.H., T.D. Bradley, and A.G. Logan, *Pathogenesis of obstructive sleep apnoea in hypertensive patients: role of fluid retention and nocturnal rostral fluid shift.* Journal of Human Hypertension, 2015. **29**(6): p. 342-350.

217. Tang, W.H.W., et al., *Fluid retention after initiation of thiazolidinedione therapy in diabetic patients with established chronic heart failure.* Journal of the American College of Cardiology, 2003. **41**(8): p. 1394-1398.

218. Buggy, J. and A.K. Johnson, *Angiotensin-induced thirst: effects of third ventricle obstruction and periventricular ablation.* Brain Res, 1978. **149**(1): p. 117-28.

219. Bichet, D.G., *Vasopressin and the Regulation of Thirst.* Ann Nutr Metab, 2018. **72 Suppl 2**: p. 3-7.

220. de Figueiredo, S.M., et al., *The antioxidant properties of organosulfur compounds (sulforaphane).* Recent Pat Endocr Metab Immune Drug Discov, 2015. **9**(1): p. 24-39.

221. O'Mealey, G.B., W.L. Berry, and S.M. Plafker, *Sulforaphane is a Nrf2-independent inhibitor of mitochondrial fission.* Redox Biol, 2017. **11**: p. 103-110.